The Dissertation Committee for David Wayne Hammers Certifies that this is the approved version of the following dissertation:

INFLUENCE OF INSULIN-LIKE GROWTH FACTOR-I ON SKELETAL MUSCLE REGENERATION

Committee:

Roger P Farrar, Supervisor

Laura J Suggs

Martin L Adamo

H. Lee Sweeney

Wesley J Thompson

John L Ivy

INFLUENCE OF INSULIN-LIKE GROWTH FACTOR-I ON SKELETAL MUSCLE REGENERATION

by

David Wayne Hammers B.S. Bioch.; M.A.

Dissertation

Presented to the Faculty of the Graduate School of

The University of Texas at Austin

in Partial Fulfillment

of the Requirements

for the Degree of

Doctor of Philosophy

The University of Texas at Austin

December 2012

Acknowledgements

I am very grateful for the excellent supervision and support of my advisor, Dr. Roger Farrar. None of this could have been done without his help and wisdom. I would also like to thank Dr. Laura Suggs for her invaluable role in my graduate education, and the rest of my dissertation committee, Dr. Martin Adamo, Dr. Lee Sweeney, Dr. Wesley Thompson, and Dr. John Ivy, for their guidance and support in this work. The included projects could not have been completed without the terrific help from my co-workers, Melissa Merscham-Banda, Dr. Ed Merritt, Apurva Sarathy, Chantal Pham, Viktoryia Rybalko, and Katie Hseih of the Farrar Lab, as well as Dr. Charles Drinnan, Julie Rytlewski, and Ryan Stowers of the Suggs Lab. My extended thanks also goes to Patty Coffman, Tan Thai, the entire Exercise Physiology department, and the great collaborators that took part in this work, Dr. RW Matheny, Dr. Thomas Walters, Dr. Holly VanRemmen, Dr. Christian Sell, and Dr. JS Estep.

INFLUENCE OF INSULIN-LIKE GROWTH FACTOR-I ON SKELETAL MUSCLE REGENERATION

David Wayne Hammers Ph.D.
The University of Texas at Austin, 2012

Supervisor: Roger P. Farrar

Skeletal muscle regeneration involves a tightly regulated coordination of cellular and signaling events to remodel and repair the site of injury. When this coordination is perturbed, the regenerative process is impaired. The expression of insulin-like growth factor-I (IGF-I) is robust in the typical muscle regenerative program, promoting cell survival and increasing myoblast activity. In this project, we found that severely depressed IGF-I expression and intracellular signaling in aged skeletal muscle coincided with impaired regeneration from ischemia/reperfusion (I/R). To hasten muscle regeneration, we developed the PEGylated fibrin gel (PEG-Fib) system as a means to intramuscularly deliver IGF-I in a controlled manner to injured muscle. This strategy resulted in greatly improved muscle function and histological assessment following 14 days of reperfusion, which are likely mediated by improved myofiber survival. Recent evidence suggests macrophages (MPs) are responsible for the upregulation of IGF-I following injury, therefore we developed a rapid, reproducible, and cost-effective model of investigating MP profiles in injured muscle via flow cytometry. Using information gathered from this model, we found that increasing the number of a non-inflammatory MP population improves the recovery of muscle from I/R. These data demonstrate that immunomodulatory therapies have the potential to greatly improve the recovery of skeletal muscle from injury.

Table of Contents

List of Tables

List of Figures

Chapter I: General Introduction

Skeletal muscle injury involves a complex program of degenerative and regenerative activities to repair the damaged tissue and restore contractile muscle function. Coordination of these processes is achieved by an orchestra of molecules, including intracellular components, cytokines/chemokines, growth factors, and protease byproducts, which create a milieu that directs the cellular constituents of the injury site to their proper state of activation in order to promote efficient skeletal muscle regeneration. Insulin-like growth factor-I (IGF-I), a peptide growth factor, is one of these post-injury components that has received considerable attention for its role in the muscle regenerative process, as it promotes myoblast activity [1], its activity is required for efficient regeneration [2], and its forced overexpression greatly facilitates regeneration [3, 4]. Thorough understanding of the biology of this fascinating molecule not only has the potential to lead to improved therapies of healthy individuals with muscle injuries, but also can be utilized to understand and treat individuals whose skeletal muscle injuries may resulting in disablement and/or mortality, such as the growing elderly population.

OBJECTIVES

The overall objective of this research project is to gather a broad understanding of IGF-I biology in muscle regeneration. Using tourniquet (TK)-induced ischemia/reperfusion (I/R) of the rodent hind limb as our injury model, we sought to accomplish the following aims:

1) Characterize the IGF-I response to I/R in young, healthy animals, and compare those results to aged animals, which serve as a population that exhibits regenerative impairments.
2) Develop an IGF-I based therapy using PEGylated fibrin gel as a delivery platform to improve functional recovery of muscle following I/R.
3) Generative a model to allow for investigation of inflammatory components in post-injury skeletal muscle, as they may be responsible for IGF-I regulation.

HYPOTHESES

1) Healthy muscle will display robust IGF-I upregulation in response to I/R.
2) Aged muscle will exhibit an attenuated IGF-I response in addition to regenerative impairments.
3) PEGylated fibrin gel-mediated delivery of IGF-I will improve functional recovery of skeletal muscle following I/R.
4) Post-injury macrophage profile modification can substantially affect skeletal muscle regeneration following I/R.

SIGNIFICANCE

The present work provides valuable insights into the biology of IGF-I in muscle regeneration, primarily in the context of therapeutic application. While the clinical utility of the approaches and results presented here may be questionable for healthy muscle, where the intrinsic regenerative drive is robust, they may provide incredible opportunities

for therapeutic development for individuals with compromised ability to undergo muscle regeneration, such as the elderly.

DELIMITATIONS AND LIMITATIONS

This work was completed on rodents using TK-induced I/R as an injury model, and therefore may not necessarily apply to other species or injury models. Experiments validating the broad applicability of the current findings would need to be performed. In addition, volumes utilized in this work would need to be optimized for larger species prior to testing true therapeutic benefit.

Chapter II: Review of the Literature

SKELETAL MUSCLE INJURY AND REPAIR

Inflammatory response

The injury-induced inflammatory response of skeletal muscle is a complex, temporally-orchestrated process that involves an initial infiltration of neutrophils, followed by subsequent infiltration of macrophages [Reviewed by 5]. The number of neutrophils increases substantially as early as 2 hours and peaks in ~6 hours in reloaded soleus muscles of previously hindlimb-suspended rats [6]. This early infiltration of neutrophils is responsible for additional muscle damage caused by the inflammatory response [6]. Additional damage is due to a superoxide-dependendent mechanism [7]. A population of macrophages characterized by positive immunostaining for the cell surface marker ED1 (rat specific) infiltrate the injured muscle and peak in prevalence at ~ 2 days after reloading [8]. These cells have been shown to invade and phagocytose injured/degenerating muscle cells [8, 9]. A second population of $ED2^{+}$ macrophages peak in prevalence ~4-7 days post-reloading [8]. These cells are often classified as resident macrophages that do not undergo phagocytosis of necrotic debris [9, 10], yet have a supportive role in muscle regeneration [11, 12].

Geissmann et al. [13] identified distinct inflammatory $CX3CR1^{low}/Ly6\text{-}C^{+}$ and non-inflammatory $CX3CR1^{high}/Ly6\text{-}C^{-}$ subsets of macrophages in the mouse, which correspond to $CD14^{+}/CD16^{-}$ and $CD14^{low}/CD16^{+}$ populations in humans. Arnold et al.

[14] demonstrated that CX3CR1^{low}/Ly-6C^{+} cells show high expression of the inflammatory cytokines TNF-α and IL-1β, and that exposure to and subsequent phagocytosis of necrotic tissue cause CX3CR1^{low}/Ly-6C^{+} cells to shift to the CX3CR1^{high}/Ly6C^{-} phenotype and express the anti-inflammatory cytokines TGF-β1 and IL-10 *in vitro*.

Myogenic Regeneration

The repair of injured myofibers is mediated by muscle-specific stem cells known as satellite cells. These cells are the primary source of myonuclei to repopulate injured skeletal muscle [Reviewed by 15]. Other types of cells, including circulating hematopoietic stem cells [16] and side-population cells [17], have been shown to have myogenic potential, but their involvement in muscle regeneration is small relative to that of satellite cells.

In uninjured muscle, satellite cells reside in a quiescent state between the sarcolemma and basal lamina [18]. In their quiescent state, satellite cells can be identified by their expression of Pax7 [19, 20]. Following an unknown stimulus induced by muscle injury, quiescent satellite cells are activated by a p38-dependent mechanism, induced to enter the cell cycle, and begin a stage of rapid proliferation [21]. Actively proliferating satellite cells are characterized by the expression of the myogenic regulatory factor MyoD [21-23].

Following the proliferative stage, the satellite cells begin to differentiate into myotubes, which then fuse into the injured myofiber. At this time, the cells reduce expression of MyoD and begin expression of myogenin [23]. The presence of central nuclei in a myofiber is evidence of a recently fused myotube. The central myonuclei typically move towards the periphery as the myofiber matures.

Decline in Regenerative Capacity with Age

The age-related decrement of skeletal muscle, termed sarcopenia, is largely characterized by the progressive loss of muscle mass, muscle strength, and reduced responsiveness to anabolic stimuli [24]. Skeletal muscle also exhibits a reduced regenerative capacity with age, characterized by loss of myoblast function, exacerbated loss of muscle mass, and reduced recovery of function [25, 26]. Strong evidence demonstrates this age-related impairment in regeneration is heavily influenced by diffusible factors, as evident by rejuvenation of aged muscle in both models of heterochronic muscle transplantation [27] and parabiosis of heterochronic mice [28].

IGF-I EFFECTS IN SKELETAL MUSCLE

General IGF-I Signaling and Skeletal Muscle Effects

IGF-I is an anabolic, liver-derived endocrine growth factor in the growth hormone axis that is also released in autocrine/paracrine fashion in many tissue types, including skeletal muscle [Reviewed by 29]. Activation of the IGF-I receptor, a tyrosine kinase, by

the binding of IGF-I induces a vast array of effects on skeletal muscle, including promotion of muscle hypertrophy [30-33], prevention of muscle atrophy [34-37], prevention of cell death by apoptosis [Reviewed by 38], and the potent stimulation of both myoblast proliferation and differentiation [1, 24, Reviewed by 29, 39]. Studies using pharmacological inhibitors to assay the activity of IGF-I on cultured myoblasts have shown that the proliferative activity of IGF-I is mediated by the MAPK/ERK pathway and the PI3K/Akt pathway is responsible for the differentiation-promoting activity [40].

IGF-I in Muscle Regeneration

IGF-I upregulation is induced in muscle by an injury stimulus. Following I/R, IGF-I mRNA increases within 24 hours of reperfusion, and peaks at 3 days [41]. This induction of IGF-I was observed in hypophysectomized rats, thus is independent of growth hormone actions [41]. The autocrine/paracrine actions of IGF-I on injured muscle is multi-faceted, as it promotes cell survival, stimulates myoblast proliferation, and induces myoblast differentiation [1]. Muscle-specific IGF-I over-expression causes muscle hypertrophy [32] and enhances muscle recovery following injury [4].

The cellular source of IGF-I expression in response to injury is a topic of controversy, as most reports of IGF-I upregulation, whether peptide or mRNA, is from whole muscle tissue. In histochemical studies, the localization of IGF-I is inconsistent, as well. IGF-I immunoreactivity following ischemia reperfusion injury of the EDL is said

to be localized to satellite cells, myoblasts, blood vessels, and nerves, with no IGF-I immunoreactivity in intact myofibers [42]. However, it is not clear how these investigators differentiated specific cell types among the mesh of IGF-I^{+} mononuclear cells. A similar result was reported in a subsequent study involving myotoxin induced injury [43], and by another research group using a cryo-injury model [44]. *In situ* hybridization for IGF-I mRNA expression following ischemia/reperfusion injury supports the same conclusion [41]. In contrast, Keller et al. [45] report IGF-I immunoreactivity only in regenerating myofibers of eccentrically damaged soleus muscle and not in the supporting mononuclear cells. However, due to the methodology of electrical stimulation-induced eccentric damage on soleus muscle, IGF-I expression within mature myofibers may be caused by mechanical stimulation alone [46] and not by substantial myofiber damage.

Decline in IGF-I Responsiveness with Age

IGF-I mRNA is decreased with age in human muscle [47]. Aged muscle demonstrates attenuated IGF-I induction following TK-induced I/R [26] and mechanical loading [48]. Muscle-specific IGF-I over-expression prevents the sarcopenic phenotype [3, 49], and enhances the recovery aged muscle following injury [3]. Our group has demonstrated the induction of IGF-I is reduced with age following I/R injury [26, 50].

Macrophages and IGF-I

There is evidence that macrophages are involved in the local induction of IGF-I following muscle injury. In addition to being necessary for normal muscle regeneration [14, 51-55], macrophages have been shown to express IGF-I [56, 57]. Furthermore, recent studies investigating muscle regeneration with clodronate liposome macrophage-depletion demonstrated that IGF-I gene expression is significantly reduced in the absence of invading macrophages [54, 58]. Lu et al. [59] recently demonstrated that post-injury IGF-I expression is largely dependent on the infiltration of $CCR2^{+}$ monocytes, and that Ly-$6C^{lo}$ $F4/80^{hi}$ macrophages isolated from injured muscle express relatively high levels of IGF-I.

Chapter III: Impairment of IGF-I Expression and Anabolic Signaling following Ischemia/Reperfusion in Skeletal Muscle of Old Mice

ABSTRACT

With the advancement of age, skeletal muscle undergoes a progressive decline in mass, function, and regenerative capacity. Previously, our laboratory has reported an age-reduction in recovery and local induction of IGF-I gene expression with age following tourniquet (TK)-induced skeletal muscle ischemia/reperfusion (I/R). In this study, young (6 mo) and old (24-28 mo) mice were subjected to 2 hours of TK-induced ischemia of the hindlimb followed by 1, 3, 5, or 7 days of reperfusion. Real time-PCR analysis revealed clear age-related reductions and temporal alterations in the induction of IGF-I. ELISA verified a reduction of IGF-I peptide with age following 7 days recovery from TK. Western blotting showed that the phosphorylation of Akt, mTOR, and FoxO3, all indicators of anabolic activity, were reduced in the muscles of old mice. These data indicate an age-related impairment of IGF-I expression and intracellular signaling does exist following injury, and potentially has a role in the impaired recovery of skeletal muscle with age.

INTRODUCTION

Sarcopenia is the progressive decline in skeletal muscle mass and function with advanced aging [See 24, 25 for review]. The skeletal muscle of aged individuals also demonstrates more susceptibility to injury [60, 61] and impaired regeneration following injury [26, 62, 63], suggesting that these characteristics are included in the sarcopenic phenotype. Investigations of muscle regeneration in heterochronic muscle transplantation [27] and parabiosis [28] models demonstrate that muscles of aged animals regenerate similarly as those of young when exposed to a young systemic environment. This indicates that diffusible, extrinsic factors have a substantial influence on intrinsic cellular processes in the age-related decline in muscle regenerative capacity, and suggests autocrine/paracrine growth factor(s), such as IGF-I, play a role in this phenomenon.

Surgical use of pneumatic tourniquets (TK) on the extremities occurs over 20,000 times a day worldwide in order to prevent excessive blood loss and provide a bloodless surgical field [64]. Their prolonged use results in a severe ischemia reperfusion (I/R) injury of the affected skeletal muscle [65], defining a very clinically-relevant problem. Considering the large proportion of orthopedic surgeries performed on elderly individuals, the extent of damage and subsequent recovery of aged skeletal muscle from TK-induced I/R is a topic of importance. Our laboratory has shown that skeletal muscles of aged rats have greater functional deficits than young following 7 and 14 days of recovery from TK-induced I/R injury, and an age-associated defect in the local induction of IGF-I is a potential mechanism contributing to this phenomenon [26].

Local induction of IGF-I in skeletal muscle occurs in various models of muscle injury [41-44, 66, 67]. The role IGF-I plays in injured muscle includes cell survival, satellite cell proliferation, and satellite cell differentiation [See 24, 39 for review, 68].

The specific aim of the present study was to compare the time course of IGF-I gene expression, protein levels, and signaling cascades in the skeletal muscle of young and old mice following TK-induced I/R. We found clear age-related alterations in the relative quantities and temporal patterns of IGF-I gene expression in our model of injury. In addition, TK-injured aged skeletal muscle exhibits deficits in IGF-I peptide levels and anabolic signaling downstream of the IGF-I receptor. These data further support our hypothesis that an age-associated decrease in IGF-I induction following injury is a potential cause of the impaired regeneration of aged skeletal muscle.

METHODS

Animals

Young (6 mo) and old (24-28 mo) male C57BL/6 mice were used for this study. Animals were housed individually with *ad libitum* access to food and water, and maintained on a 12-hour light/dark cycle. Age-separated mice were randomly assigned into 1, 3, 5, and 7-day recovery groups. All experimental procedures were approved and conducted in accordance with the guidelines set by The University of Texas at Austin IACUC.

Tourniquet Application

Mice were anesthetized with 2% isoflurane gas prior to and for the duration of tourniquet application. A single, randomly selected hind limb was elevated, and a pneumatic tourniquet (D.E. Hokanson, Inc.) was wrapped snuggly against the proximal portion of the limb and inflated to 250 mm Hg by the Portable Tourniquet System (Delfi Medical Innovations Inc.) to ensure complete occlusion of blood flow to the limb for a duration of 2 hours [69]. Body temperature was maintained at 37±1º C with the use of a heat lamp during this procedure. After 2 hours, the pneumatic tourniquet was removed, and the mouse was returned to its cage for recovery. For all measures, muscles from the uninjured contralateral limb served as internal controls, as performed in other studies [26, 70, 71].

Force Measurements

Gastrocnemius muscles were surgically isolated from all other muscles and connective tissue, and subjected to functional measurements. The Achilles tendon was secured to the muscle lever arm of a servomotor (model 305B, Cambridge Technologies) interfaced with a computer equipped with an A/D board (National Instruments). The muscle was stimulated to contract using an Isolated Pulse Stimulator (Model 2100; A-M Systems) with leads applied to the sciatic nerve. Muscle temperature was kept constant at 37º C with warm mineral oil and a radiant heat lamp throughout the procedure. Optimal length of the muscle was determined by measuring maximal twitch tension at a stimulation of 0.5 Hz. At optimal length, the muscle was stimulated at 150 Hz to elicit

the peak tetanic tension (P_o), and was allowed 2 minutes of rest between each contraction. Data were stored and analyzed using LabView software (National Instruments).

Tissue Harvesting

The hind limb muscles were quickly harvested from both the TK and contralateral leg, and frozen in liquid nitrogen-cooled isopentane and stored at -80° C until later analysis. Plantaris muscles were fixed in 10% formalin for histological evaluation. Mice were euthanized with an overdose of sodium pentobarbital (100mg/kg).

Histological Analysis

Formalin-fixed muscles were embedded in paraffin wax, cut into 5 μm thick cross sections, and stained with hematoxylin & eosin (H&E). Slides were evaluated using an Olympus BX41 microscope at 4, 10 and 40 X magnification. Images were captured at 40 X magnification using an Olympus BX41 microscope and an Olympus DP71 digital camera.

F_2-Isoprostane levels

Levels of F_2-isoprostanes (IsP), byproducts of lipid peroxidation and an indicator of oxidative stress, were measured, as previously described [72], in the gastrocnemius of 2 hour, 24 hour, and 5 day recovery groups of young mice (n = 6), and in 24 hour and 5 day recovery groups of old mice (n = 6) using gas chromatography. The levels are indicated as nanograms of IsPs per gram of muscle tissue.

RT-PCR

Real-time PCR experiments were performed as previously described [26]. RNA was extracted from EDL muscles using RNA-STAT (Tel-Test, Friendswood, TX). Samples underwent chloroform extraction and centrifugation, followed by precipitation in isopropanol at -20º C. Precipitated RNA was centrifuged, the supernatant removed, and the pellet dissolved in nuclease-free water. RNA was quantified on a spectrophotometer at a wavelength of 260 nm. Conversion of total RNA to single-strand cDNA was accomplished using the High-Capacity cDNA Archive Kit (P/N 4322171; Applied Biosystems; Foster City, CA). Briefly, 5 – 10 μg total RNA were reverse transcribed using random primers for the following incubation times: 25º C for 10-minutes, then 37º C for 2 hours. cDNA samples were stored at -80º C until use.

RT-PCR was performed on cDNA using commercially available (mouse 18S, ABI P/N Hs99999901_s1 and IGF-I, ABI P/N Mm00439561_m1, exon boundary 3-4) hydrolysis primers and probes. The PCR reaction was performed in an ABI 7500 thermal cycler with the fluorescence of 3 to 15 cycles was set as background. Data was collected at the annealing step of each cycle, and the threshold cycle (Ct) for each sample calculated by determining the point at which the fluorescence exceeded the threshold limit. Standard curves for each probe/primer pair were established by serial 10-fold dilutions of cDNA of known concentrations, and the Ct values from samples were plotted along the curves to obtain relative values. All samples were then normalized to 18S

rRNA**.** Data points represent the average of two to three runs, each in duplicate, and each performed on separate cDNA synthesis reactions.

ELISA

Tissue levels of IGF-I were measured by a method similar to that described by D'Ercole et al. [73], with minor modifications. Briefly, ~100 mg of frozen muscle tissue (tibialis anterior + EDL muscles) were powdered under liquid nitrogen and suspended in 5 mL of acetic acid per gram of tissue. Tissue suspensions were incubated on ice for 30 minutes and insoluble material was removed by centrifugation (10 minutes @ 5,000 g, 4º C). Extracts were lyophilized and resuspended in 0.1 M Tris (pH 8.0) at 2 mL/g of tissue. Samples were cleared by centrifugation (10 minutes @ 10,000 g, 4º C). Protein concentrations of cleared lysates were determined by the method described by Bradford [74]. An equal amount of protein was used to determine the IGF-I content using an IGF-I ELISA kit (Immuno Diagnostic Systems; Fountain Hills, AZ). Input volumes of the samples were increased to 25 µl, and the volume of diluent was decreased to 0.25 mL. The remainder of the assay was performed according to the manufacturer's instructions.

SDS-PAGE

Samples from control and TK gastrocnemius muscles were homogenized at 4º C in a buffer containing 50 mM HEPES (pH 7.6), 150 mM NaCl, 1% Triton-X 100, 20 mM β-glycerol phosphate, 10 mM NaF, 1 mM Na_3VO_4, 10 ng/mL each of leupeptin and aprotinin, 1 mM PMSF, and 1:100 dilutions of phosphatase inhibitor cocktails 1 & 2

(Sigma-Aldrich). The resulting homogenate was centrifuged at 12,000g for 30 minutes, and the supernatant was kept for analysis. Protein concentrations of all samples were determined as described by Bradford [74]. Samples were boiled in 4X Laemmli's sample buffer at a ratio of 3:1, and equal amounts of total protein were loaded into each well of a 5% stacking/15% separating polyacrylamide gel. Gels were run at constant current until necessary protein separation was achieved.

To verify equal loading of protein content among lanes, Coomassie blue staining of randomly selected gels was performed following SDS-PAGE separation. Gels were washed in dH_2O for 30 minutes, incubated in Bio-Safe Coomassie blue solution (Bio-Rad) for 1 hour, and washed again in dH_2O overnight. Gel images were taken using the Chemidoc XRS system (Bio-Rad). Volumetric analysis of all bands of each lane was performed using Quantity One software to verify that there were no substantial differences in total protein content despite differences in distribution of protein content between groups.

Western Blotting

Following SDS-PAGE separation, proteins were transferred to a PVDF membrane (Millipore) and blocked with 5% milk in 0.1% Tween 20 in TBS (TBST) for 1 hour. Ponceau-S staining was performed to ensure equal transfer prior to blocking. Membranes were incubated in 1:1000 dilutions of primary antibody in either 1% milk-TBST or 5% BSA-TBST overnight at 4° C, then in 1:2000 dilutions of goat anti-rabbit HRP

conjugated secondary antibody (Pierce) in either 1% milk-TBST or 5% milk-TBST for 2 hours. Blots were visualized by ECL detection (Perkin-Elmer) using the Chemidoc XRS system (Bio-Rad). Band volumetric analysis was performed using Quantity One software. Following ECL detection of phospho-proteins, membranes were stripped and re-probed for total protein. Anti-phospho-mTOR (Ser 2448; 2971), anti-phospho-FoxO3a (Ser 253; 9466), anti-Akt (9272), anti-mTOR (2972), and anti-FoxO3a (9467) primary antibodies were purchased from Cell Signaling Technology. Anti-phospo-Akt 1/2/3 (Ser 473; sc-7985-R) primary antibody was purchased from Santa Cruz Biotechnology. All experiments were repeated in triplicate to verify results.

Data Analysis

All values are expressed as mean ± SEM. Statistical analysis involved two-factor ANOVA (age and TK treatments; Tukey post-hoc tests) or Student's *t*-tests, where appropriate, using SPSS 16.0 software ($\alpha = 0.05$).

RESULTS

Functional Evaluations

Previously, we have reported that rats exhibit age-related increases in functional deficits of the plantar flexor muscles following 7 and 14 days recovery from 2 hour TK-induced I/R injury [26]. To verify that a similar phenomenon occurs in a mouse model, young and old mice were evaluated for maximum force production of the gastrocnemius *in situ* after 7 days of reperfusion (**Figure 3.1**). At 7 days post-TK, young and old

animals demonstrated functional deficits of 67 and 78%, respectively ($p \leq 0.05$ between the age groups).

Muscle Mass

Figure 3.2 depicts the wet masses of all GAS muscles obtained in this study. In general, TK-injured muscles increased in mass 1 day post-TK, and this increase remained elevated through 3 days. Histological evidence confirmed this early post-TK increase coincides with edema and swelling of the myofibers. Following day 3, muscle masses of both age groups demonstrated progressive declines until day 7, when young and old muscles demonstrated significant decreases of 13 and 22% decreases in mass, respectively. At this time, the muscle mass of old mice was 27% lower than that of young. This decrease in old represents a 38% greater loss of mass, relative to day and age-matched controls, than the loss observed in young.

Histology

H&E-stained plantaris muscle cross-sections from young and old 1, 3, 5, and 7-day recovery mice were evaluated (**Figure 3.3**). Control muscles from both young and old animals demonstrated no pathology, exhibiting angular fibers with peripheral nuclei. Following 1 day of recovery from I/R, old muscle demonstrated a higher degree of swelling (rounding of the myofibers), edema, neutrophil infiltration, and internalization of nuclei than young. Both age groups demonstrated a comparable degree of multifocal degeneration and necrosis. Similarly at day 3, old muscles demonstrated more myofiber

swelling, edema, and infiltration of macrophages. Young muscles exhibited similar neutrophil infiltration as that observed in old, following injury, but revealed higher degrees of multifocal degeneration, necrosis, and internalized nuclei; neutrophil infiltration was similar to that of old. Old muscles in the 5-day recovery group exhibited similar degrees of degeneration/necrosis as those of young, yet had more severe instances of edema, infiltration of neutrophils and macrophages, and internalization of nuclei. Old muscles demonstrated a higher incidence of centrally located nuclei (i.e. regeneration) at this time, suggesting more damage had incurred. At 7 days, young and old muscles had similar degrees of edema, degeneration, and infiltration of neutrophils and macrophages; old muscles demonstrated higher amounts of swelling and regeneration than young at this time.

Lipid peroxidation

I/R injury has traditionally been largely attributed to oxidative stress caused by the generation of reactive oxygen species (ROS). To test the prevalence of oxidative stress in our 2 hour TK model, we measured IsPs, by-products of the lipid peroxidation reaction and a good indicator of oxidative stress *in vivo* [75], in the gastrocnemius muscles of young and old mice **(Figure 4.4**). In young mice, IsPs were elevated as soon as 2 hours post-TK, and remained elevated through the 5-day recovery mark ($p \leq 0.05$ for all times). IsP levels were also elevated in the muscles of old mice, as seen at 1 and 5 days post-TK ($p \leq 0.05$ for both times). This demonstrates that oxidative stress occurs quickly and is persistent in our model of TK-induced I/R.

IGF-I gene expression

The local induction of IGF-I mRNA in skeletal muscle following an injury stimulus is well documented [26, 41, 66, 67]. Using our model of muscle injury, IGF-I mRNA in control and TK EDL muscles were measured by RT-PCR and were quantified relative to young 1 day control values (**Figure 3.5A**), revealing both a quantitative and temporal shift with age in the first 7 days of reperfusion. TK-induced injury resulted in significant increases in IGF-I gene expression at days 1, 3, and 7 post-TK in both young, and at days 3, 5, and 7 in old compared to their respective controls. In young, IGF-I mRNA displayed a robust peak 3 days post-TK, while the old showed a delayed and quantitatively diminished peak at day 5. Old mice demonstrated significantly less TK-induced IGF-I gene expression than young at days 1 and 3, and was higher in expression at its peak on day 5. These data demonstrate temporal and quantitative impairment of IGF-I expression occurs with age following TK-induced injury.

IGF-I peptide levels

Having observed that IGF-I mRNA decreased with age, we next sought to determine whether intramuscular immunoreactive IGF-I levels are also reduced. A significant increase in IGF-I peptide following 7 days of recovery occurs in young, and not in old **(Figure 3.5B**). These data indicate IGF-I peptide levels, in addition to mRNA, are reduced with age following TK-induced I/R.

Akt, mTOR, and FoxO3 signaling

To investigate the time-course of anabolic activity in young and old skeletal muscle following I/R, the phosphorylation of key proteins of the phosphoinositide 3-kinase (PI3K)/Akt pathway were analyzed (**Figure 3.6**). Early in recovery, levels of p-Akt and total Akt diminished to almost undetectable levels in both young and old, with no difference between the ages. At day 5, p-Akt content rose in the young mice, while old muscles still demonstrated no return of p-Akt signal. Similarly, p-Akt levels were higher in the young than old at day 7 ($p \leq 0.05$). These data indicate an age-related delay in Akt activation following I/R injury.

Mammalian target of rapamycin (mTOR) is a crucial mediator of anabolic activity in skeletal muscle [See 76 for review]. There were no age-related differences in p-mTOR among age groups until day 7. At this time, there were large increases in p-mTOR values in the young mice relative to day-matched control levels, which were higher than those of old mice ($p \leq 0.05$), suggesting phosphorylation of mTOR is impaired/delayed in aged muscle recovering from I/R.

The FoxO class transcription factors (FoxOs) are targets of active Akt kinase activity. In their active, unphosphorylated state, these proteins reside in the nucleus and promote gene expression of atrophy-stimulating genes, such as the E3 ubiquitin ligase, atrogin-1 [37]. Phosphorylation of FoxOs by Akt induces translocation from the nucleus and degradation in the cytosol [See 77 for review]. Content of p-FoxO3 followed the same pattern as p-mTOR. After 7 days of recovery, p-FoxO3 content in young was substantially higher than old ($p \leq 0.05$). The physiological relevance of these signaling

deficits are strengthened by the exacerbated loss of mass in the muscles of old following TK application (**Figure 3.2, Day 7**).

DISCUSSION

The substantial loss of muscle mass and function that result from TK use are a concern given the high proportion of elderly individuals who undergo orthopedic surgery, as muscle mass and strength are negatively associated with disability and mortality rates [See 78 for review]. The data presented in this study demonstrate clear age-related alterations in local IGF-I gene expression, IGF-I peptide levels, and anabolic signaling in skeletal muscle following I/R in mice. In this study we present several novel findings including a correlation between IGF-I mRNA levels and protein levels in aged muscle and a reduction in intracellular signals generated by the IGF-I receptor. In addition, we find an elevation in potentially active FoxO in the muscle of aged animals. These novel findings extend our previous observations and provide important information regarding the potential mechanisms that underlie the reduced capacity for aged muscle to recover from injury.

Due to its pleiotrophic effects, IGF-I is an important molecule in the study of skeletal muscle response to injury. IGF-I stimulates both the proliferation and differentiation of myoblasts via activation of the MAP kinase and PI3K/Akt pathways, respectively [40]. In differentiated muscle, IGF-I is hypertrophic and anti-atrophic, with both actions largely attributed to PI3K/Akt activation [30, 32-34, 36, 79]. IGF-I

overexpression also increases the recruitment of circulating bone marrow-derived stem cells [80, 81] and hastens the resolution of inflammation [4] following muscle injury. Additional benefits of IGF-I may include protection of cells from oxidative stress [82, 83], mitochondrial dysfunction [84], and apoptosis [See 38 for review], as seen in non-muscle tissues.

Due to the positive effects of IGF-I, we hypothesize that the age-related impairment of IGF-I expression is a contributing factor to the general decrement of aged muscle following injury. This is supported by evidence that the forced overexpression of IGF-I in the skeletal muscles of aged mice prevents the sarcopenic phenotype [3, 49] and protects injured muscles from the exacerbated decrement caused by aging [3]. In addition, the administration of IGF-I has the ability to restore the proliferative potential of satellite cells in atrophied aged muscles [85]. Despite these effects of IGF-I on sarcopenia, it was only recently shown that the injury-induced upregulation of IGF-I is impaired with age [26]. The present study verifies this age-related reduction in the injury-induced IGF-I expression exists in the mouse model of TK-induced I/R with the distinctive finding that a delay in peak expression also occurs, as young peak in expression at 3 days post-TK and old at 5 days post-TK. We also verify that IGF-I peptide levels are reduced with age. The merits of these findings are further strengthened by recent evidence that functional IGF-I receptors are required for the efficient regeneration of injured skeletal muscle, thereby highlighting the importance of IGF-I to

muscle regeneration [2]. This current line of evidence suggests that non-genetic, IGF-I-based intervention may be an effective method of therapeutic intervention.

The skeletal muscle of aged mice also demonstrate significant deficits in phosphorylation of Akt, mTOR, and FoxO3, all indicators of positive anabolic activity, compared to their young counterparts after 7 days of recovery from TK-induced I/R. Activation of the PI3K/Akt pathway leads to an increase in protein synthesis through a mTOR-dependent process [33, 86], and prevents atrophy through a mostly FoxO-dependent process [37]. Indirect activation of mTOR by Akt initiates the activation of pro-translational signaling by the activation p70 S6 Kinase ($p70^{S6K}$) and the deactivation of 4E-Binding Protein (4E-BP) through phosphorylation [86, 87]. The reduction of pAkt and pmTOR in old muscle suggests protein synthetic pathways are attenuated with age following I/R. A similar delayed response of Akt activation in old rats was recently found to coincide with impaired hypertrophy using the functional overload model [88]. The present data indicates that the mechanism responsible for the age-related decrease in signaling is prior to the activation of Akt, perhaps due to changes in IGF-I ligand levels. We are, however, limited by the fact that different muscles were used for mRNA/peptide and signaling assays. We also cannot, at this time, discount the possibility of age-related alterations in the expression and/or activation of upstream mediators of Akt activation, such as the IGF-I receptor, IRS-1, and/or PI3K, or proteins downstream of mTOR, including mTORC1, $p70^{S6K}$, 4E-BP, and/or ribosomal protein S 6.

Another important finding of the current study is the substantially reduced pFoxO3 levels in the TK muscles of old mice. In differentiated muscle, active FoxO proteins are localized in the nucleus and activate transcription of the muscle-specific E3 ubiquitin ligases Atrogin-1 and MuRF-1 [34, 37, 89] and many genes associated with autophagy [90-92], causing substantial atrophy. In addition, FoxOs are responsible for the upregulation of the cell cycle inhibitor $p27^{kip1}$, thereby preventing satellite cell proliferation [93, 94]. FoxOs have also been shown to induce apoptosis *in vitro* [95, 96]. IGF-I mediated phosphorylation of FoxOs by Akt causes their exclusion from the nucleus, thereby preventing their transcriptional activity [34, 37]. These data suggest FoxO activity is elevated in TK-injured aged muscle, leading to an age-related increase in atrophy stimulation and/or reduced proliferative potential of satellite cells.

In summary, the present data demonstrate that the local induction of IGF-I gene expression, IGF-I peptide levels, and signaling of the PI3K/Akt pathway in skeletal muscle are attenuated with age following I/R. This result is clinically significant due to the growing elderly population and the large proportion of orthopedic surgeries within this demographic. However, further investigation needs to address the mechanisms behind the age-related reduction in IGF-I response, i.e. whether it is due to extrinsic factors, intrinsic phenomena, or an interaction thereof. Despite this, the results of this study strengthen the use of IGF-I based therapy as a potential treatment to promote normal regeneration in the injured skeletal muscle of aged individuals.

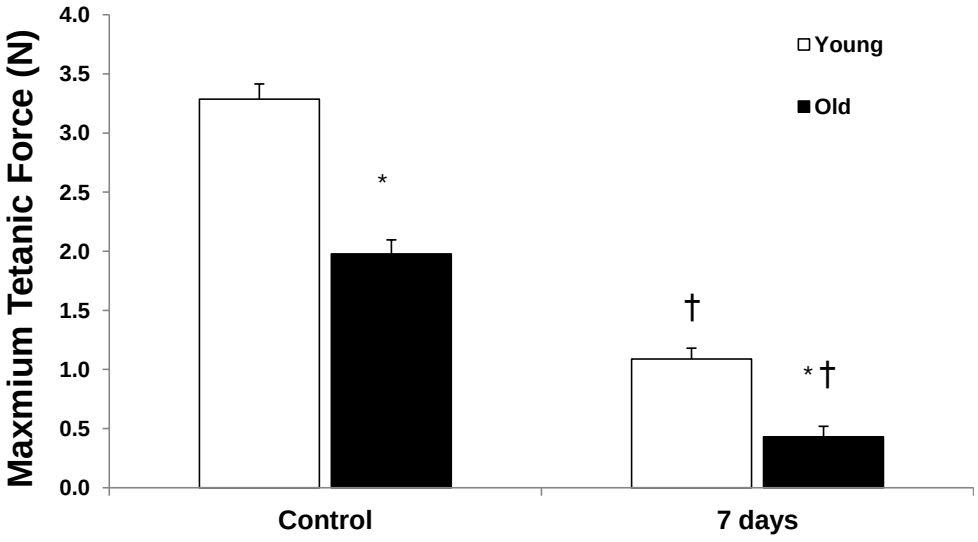

Figure 3.1. Maximum force production of gastrocnemius muscles from 6 mo (young) and 24-27 mo (old) C57BL/6 mice was evaluated *in situ* following 7 days of recovery from I/R. Values are represented as mean ± SEM; *p ≤ 0.05 vs. treatment-matched young; †p≤ 0.05 vs. age-matched controls.

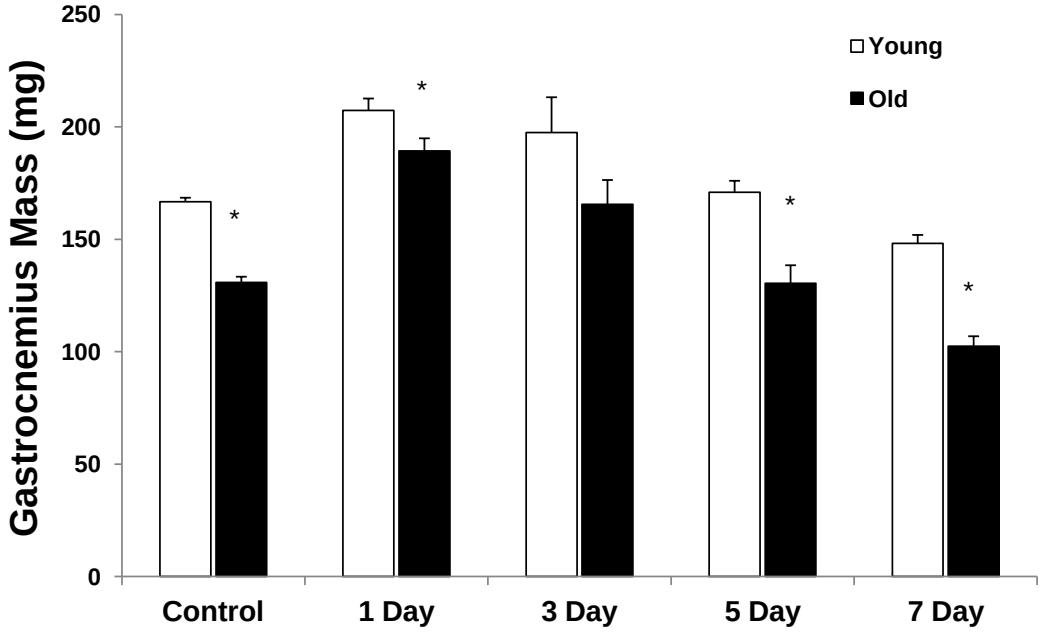

Figure 3.2. Wet masses of gastrocnemius muscles (**A**) were measured from 6 mo (young) and 24-27 mo (old) C57BL/6 mice following 1, 3, 5, 7 days of recovery from 2 hour TK-induced I/R. Values are represented as mean ± SEM; *$p \leq 0.05$ vs. day-matched young.

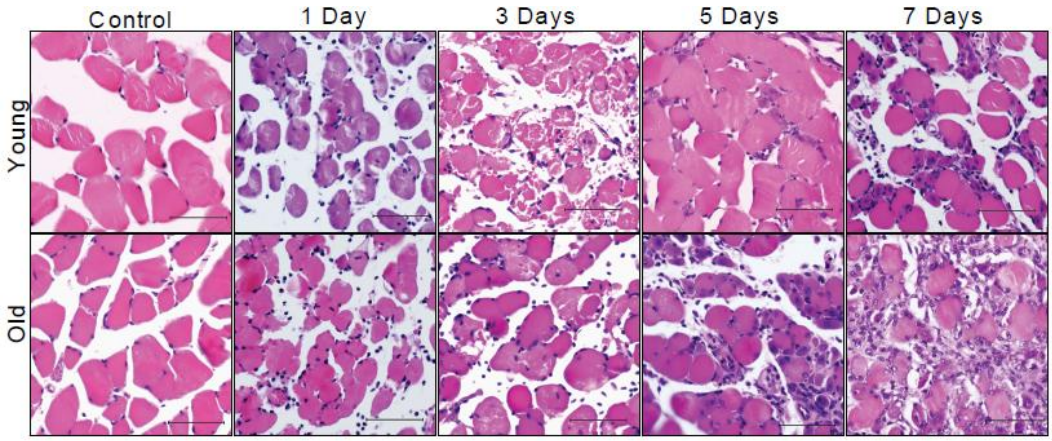

Figure 3.3. Plantaris muscles from 6 mo (young) and 24-27 mo (old) C57BL/6 mice were paraffin-embedded and stained with hematoxylin & eosin following 1, 3, 5, and 7 days of recovery from 2 hour TK-induced I/R. Inset bar represents 100 μm.

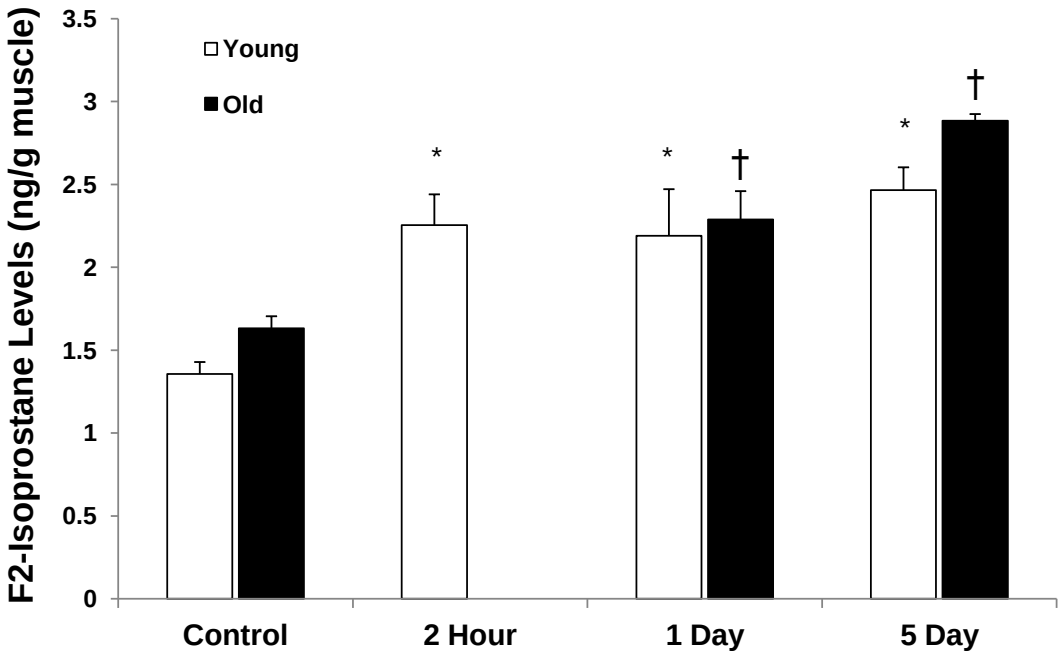

Figure 3.4. F_2-isoprostanes were measured in the gastrocnemius muscles of 6 mo (young) C57/BL6 mice following 2 hours, 1 day, and 5 days of reperfusion and of 24-28 mo (old) mice following 1 day and 5 days of reperfusion. Values are represented as mean ± SEM; * $p \leq 0.05$ vs. young control; † $p \leq 0.05$ vs. old control.

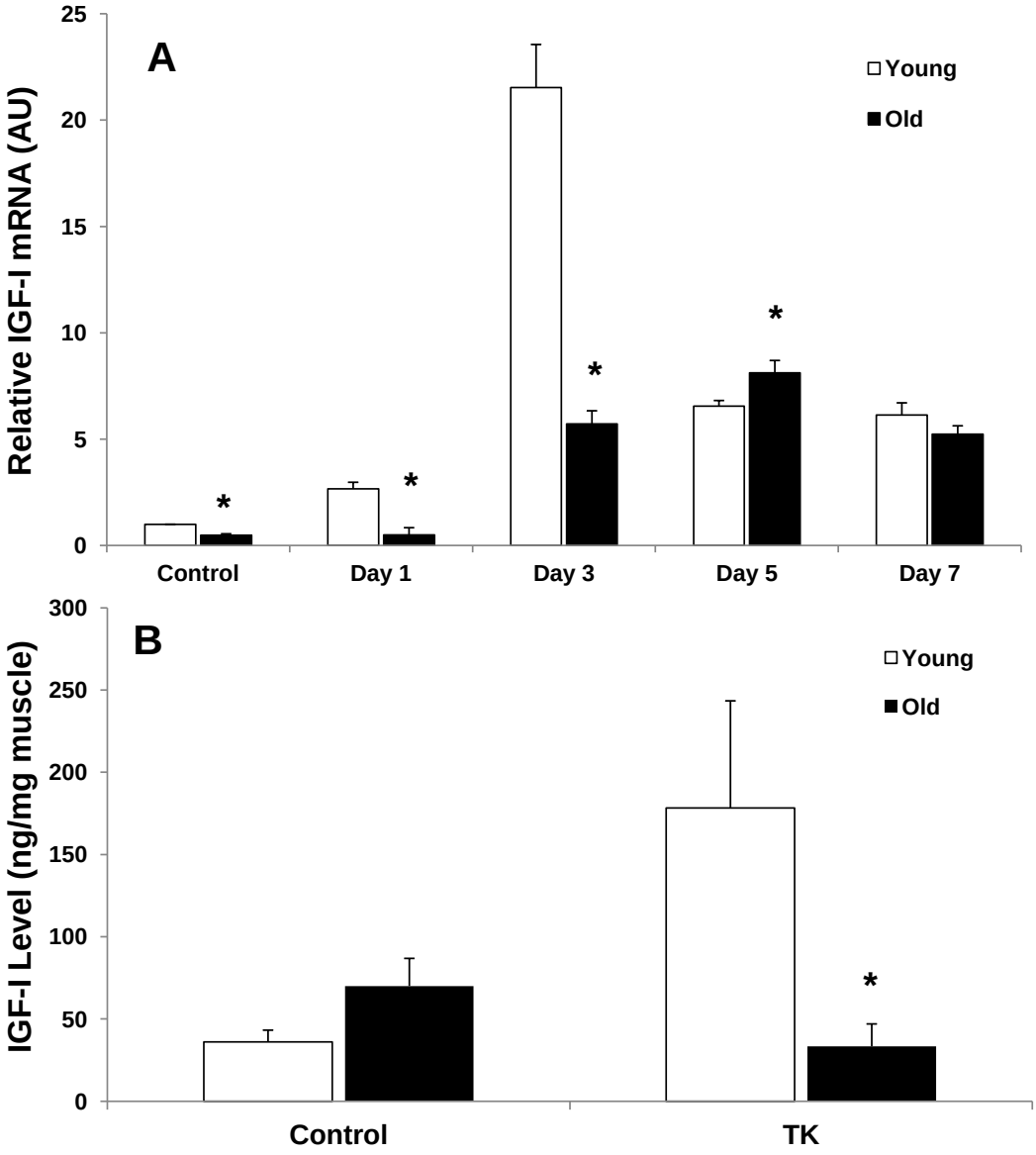

Figure 3.5. Real time-PCR was performed to measure relative expression of IGF-I mRNA in the extensor digitorum longus muscle of 6 mo (young) and 24-27 mo (old) C57BL/6 mice following 1, 3, 5, and 7 days of recovery from 2 hour TK-induced I/R (**A**). Whole tissue IGF-I peptide levels were measured by ELISA in the tibialis anterior and extensor digitorum longus muscles following 7 days recovery from TK-induced I/R (**B**). Values are represented as mean ± SEM; *$p \leq 0.05$ vs. treatment-matched young.

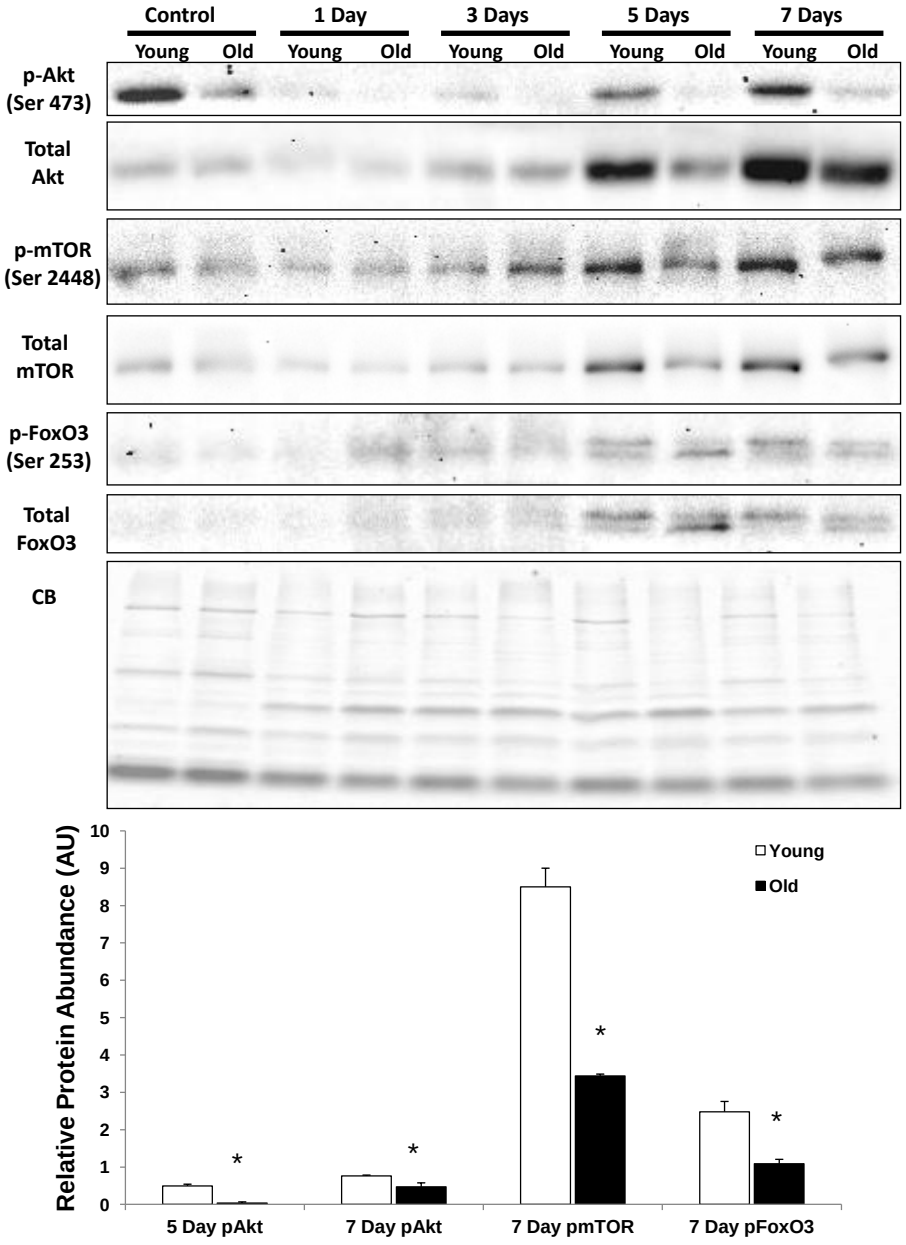

Figure 3.6. Representative Western blots and quantitative values of Akt, mTOR, and FoxO3 phosphorylation in the gastrocnemius muscle of 6 mo (young) and 24-27 mo (old) C57BL/6 mice following 1, 3, 5, and 7 days of recovery from 2 hour TK-induced I/R. Coomassie blue (CB)-stained polyacrylamide gel demonstrates that equal loading occurred in all lanes. Values are represented as mean ± SEM; *p ≤ 0.05 vs. young.

Chapter IV: Controlled Release of IGF-I from a Biodegradable Matrix Improves Functional Recovery of Skeletal Muscle from Ischemia/Reperfusion

ABSTRACT

Ischemia/reperfusion (I/R) injury is a considerable insult to skeletal muscle, often resulting in prolonged functional deficits. In the current study we evaluated the controlled release of insulin-like growth factor-I (IGF-I), from a biodegradable PEGylated fibrin gel matrix and the subsequent recovery of skeletal muscle from I/R. The hind limbs of male Sprague-Dawley rats were subjected to 2 hour tourniquet (TK)-induced I/R then treated with saline, bolus IGF-I (bIGF), PEGylated fibrin gel (PEG-Fib), or IGF-I conjugated PEGylated fibrin gel (PEG-Fib-IGF). Functional and histological evaluations were performed at 14 days of reperfusion, and muscles from 4-day animals were analyzed by Western blotting and histological assessments. There was no difference in functional recovery between saline, bIGF, or PEG-Fib groups. However, PEG-Fib-IGF treatment resulted in significant improvement of muscle function and structure. Activation of the PI3K/Akt pathway was significantly elevated in PEG-Fib-IGF muscles, compared to PEG-Fib treatment, at 4 days of reperfusion, suggesting involvement of this pathway as a mediator of improvement. Increases in myoblast activity was not evident as a result of PEG-Fib-IGF treatment. Taken together, these data give evidence for a protective role for the delivered IGF. These results indicate PEG-Fib-IGF is a viable therapeutic technique in the treatment of skeletal muscle I/R injury.

INTRODUCTION

Ischemia/reperfusion (I/R) injury is a considerable perturbation to the extremities, often occurring in instances of vascular surgeries, orthopedic surgeries, or tourniquet (TK) use [65, 97]. The ischemic phase of I/R includes the accumulation of metabolites and depletion of ATP, while the more detrimental reperfusion phase is characterized largely by a burst of free radicals, causing severe damage to affected cell membranes, that can ultimately lead to apoptosis and/or necrosis [65, 98].

Histopathology and large functional deficits persist in the skeletal muscle of rodents following TK-induced I/R [26, 69]. In response to I/R, local upregulation of the pro-regenerative growth factor, insulin-like growth factor-I (IGF-I) occurs [26, 41, 50]. The actions of IGF-I following muscle injury include the stimulation of myoblast proliferation, promotion of myoblast differentiation, and improved survival of affected cells [1, 38]. Over-expression of IGF-I does facilitate skeletal muscle recovery following cardiotoxin-induced injury [4], therefore we hypothesized that increasing the local concentration of IGF-I would be a potential therapeutic method for the treatment of skeletal muscle I/R. Since the beneficial effects of IGF-I are mediated largely by the Ras/Raf-1/ERK MAP kinase and PI3K/Akt pathways [1], we also hypothesized that one or both of these pathways must be involved in any measurable IGF-I mediated improvements in muscle recovery.

The controlled release of growth factors from an intramuscular (IM), biodegradable matrix over time is an attractive alternative to multiple bolus injections of growth factor, and is more clinically feasible than genetic over-expression treatments. In previous experiments, a polyethylene glycol (PEG)-ylated fibrin gel (PEG-Fib) matrix containing covalently-bound growth factor has effectively improved left ventricular function following myocardial infarction [99, 100]. Following injection and subsequent polymerization, the covalently-bound growth factor is released from the PEG-Fib matrix into the local environment as degradation occurs, thereby allowing for the controlled release of growth factor from a single injection. This property makes PEG-Fib an attractive tool for growth factor therapy following muscular injuries.

In the present study, we tested our hypothesis that PEG-Fib-mediated delivery of IGF-I will improve the functional recovery of skeletal muscle following I/R. A bi-functional succinimidylglutarate PEG (SG-PEG-SG) was used to successfully conjugate fibrinogen and IGF-I, leading to a matrix that releases supra-physiological amounts (>10 ng/mL) of IGF-I out to at least 4 days, *in vitro*. The PEG-Fib-IGF matrix was utilized as an IM-delivered treatment for TK-induced I/R of skeletal muscle. Functional and histological evaluations were performed following 14 days of reperfusion. Four day reperfusion groups were used to assess signaling and histology.

METHODS

Animals

Male Sprague-Dawley rats (6-9 mo; Charles River) were used for this study. Rats were housed individually, maintained on a 12-hour light/dark cycle, and were allowed *ad libitum* access to food and water. All experimental procedures were approved and conducted in accordance with guidelines set by the University of Texas at Austin Institutional Animal Care and Use Committee.

Tourniquet Application

The 2 hour TK-induced I/R reperfusion model of muscle injury was performed as previously described [26]. Briefly, a single, randomly-selected hind limb was elevated, and a pneumatic TK (Hokanson) was placed proximal to the knee. The TK was inflated to 250 mm Hg using the Portable Tourniquet System (Delfi Medical Innovations) for a 2-hour duration. During the course of this procedure, rats were anaesthetized with 2% isoflurane, and body heat was maintained with the use of a heat lamp.

PEGylated Fibrin Gel Delivery of IGF-I

Growth factor conjugated PEGylated fibrin gel was prepared essentially as previously described [99-101]. Briefly, bifunctional SG-PEG-SG (NOF America Corp) was reacted with reconstituted porcine fibrinogen (Sigma; 5:1 PEG:fibrinogen molar ratio; pH 7.8) and hIGF-I (Peprotech). Polymerization was induced by the addition of 25 U/mL hThrombin (Sigma). The final concentrations of fibrinogen and IGF-I were 10 mg/mL and 25 μg/mL, respectively.

Twenty-four hours following release of the TK, 0.25 mL of either sterile PBS (saline; n = 8), bolus IGF-I (bIGF; 25 μg/mL; n = 4) empty PEGylated fibrin gel (PEG-Fib; n = 6), or IGF-I conjugated PEGylated fibrin gel (PEG-Fib-IGF; n = 6) was injected into the lateral gastrocnemius (LGAS) muscle of the TK-injured limb. PEG-Fib and PEG-Fib-IGF treatments were injected as a fluid and polymerized *in situ*. Functional assessments were performed at 14 days of reperfusion.

In a subsequent experiment aimed at investigating potential mechanisms behind PEG-Fib-IGF-mediated improvements, 0.25 mL of PEG-Fib (n = 4) or PEG-Fib-IGF (n = 4) was injected in the same manner, while animals were allowed 4 days of reperfusion. LGAS muscles were harvested from euthanized animals, embedded in OCT compound, frozen in liquid nitrogen-cooled isopentane, and stored at -80 ºC until further analysis.

Functional Assessment

Following 14 days of reperfusion, evaluation of LGAS force production *in situ* was performed as previously described [102]. Briefly, the GAS muscle was isolated from all other muscles in anaesthetized rats, innervation to the medial GAS was removed, and the Achilles tendon was secured to the lever arm of a dual-mode servomotor (Aurora Scientific Model 310B). The muscle was activated using a stimulator (A-M Systems Model 2100) with electrodes applied to the tibial nerve. Optimal length (Lo) was determined by finding the length producing the maximal twitch force. Maximal peak tetanic tension (Po) was measured at Lo at a frequency of 150 Hz and the minimal

voltage required to elicit a maximal response. Each contraction was followed by 2 minutes of rest. Muscle temperature was maintained with a heat lamp and mineral oil. Data were stored and analyzed using LabView software. After the completion of contractile measurements, the muscles were dissected free, weighed, embedded in OCT compound, frozen in liquid nitrogen-cooled isopentane, and stored at -80 ºC until further analysis. LGAS measurements of non-injured limbs were used for a non-TK control values (n = 14).

Histology and Immunohistochemistry

Frozen, OCT-embedded muscle samples from 4 and 14 reperfusion groups were sectioned on a cryostat (Leica CM1900), and prepared on a slide. Hematoxylin & eosin (H&E) staining was performed, as previously described [102], and slides were observed with a light microscope (Nikon Diaphot) with the 20X objective lens. Images were taken using a mounted digital camera (Optronix Microfire). Myofiber cross-sectional area (CSA) was measured by outlining using ImageJ software (250-600 fibers/group).

Immunohistochemistry (IHC) was performed as previously described [102]. Slides were blocked with 5% normal donkey serum and 1% BSA in PBS, and stained with anti-desmin (1:200; Santa Cruz), anti-neonatal myosin heavy chain (1:200; Santa Cruz), anti-myogenin (1:200; Santa Cruz), or anti-MyoD (1:200; Santa Cruz) antibodies. Sections were detected with donkey anti-goat IgG-FITC fluorescein (1:100; Santa Cruz), donkey anti-rabbit-FITC fluorescein (1:100; Santa Cruz) or a donkey anti-mouse IgG-

TRITC fluorescein (1:100; Santa Cruz) and counter-stained with DAPI. Immunofluorescence was visualized with a Leica DM LB2 fluorescence microscope with the 20X objective lens and photographed with a Leica DFC340FX digital camera. For quantification, the total number of nuclei co-expressing DAPI and either MyoD or myogenin were counted using ImageJ and expressed as a percentage of total nuclei present in the image area. The number of intact myofibers expressing desmin or neonatal myosin heavy chain was counted using ImageJ and expressed as a percentage of the total number of myofibers in the image area. For each measure, 3 fields of view were evaluated from 3 muscles per group.

Western Blotting

Western blotting was performed as previously described [26] using anti-IGF-I (Peprotech), anti-pAkt1/2/3 (Ser 473; Santa Cruz Biotechnology), anti-Akt (Cell Signaling), anti-pmTOR (Ser 2448; Cell Signaling), anti-mTOR (Cell Signaling), anti-p-$p70^{S6K}$ (Thr 389; Santa Cruz Biotechnology), anti-$p70^{S6K}$ (Cell Signaling), and anti-MuRF-1 (ECM Biosciences) antibodies. The membrane was stripped of phosphorylation-specific antibodies and was re-probed with total protein antibodies. Values were quantified relative to those of the PEG-Fib control group. Coomassie blue staining (Bio-Rad) was performed to verify equal loading.

ELISA

IGF-I release kinetics were performed similar to that previously described [100] using the hIGF-I Quantikine ELISA kit (R&D Systems). Procedures were followed as directed by the manufacturer's instructions. Release kinetics were quantified as percent of total IGF-I released from the matrix.

Statistical Analysis

Functional assessments and IHC values were analyzed using an appropriate form of ANOVA (Tukey post-hoc test; $\alpha = 0.05$), and Western blotting data were analyzed using Student's T-test ($\alpha = 0.05$). All values are represented as the mean ± SEM, unless noted otherwise.

RESULTS AND DISCUSSION

Genetic over-expression studies have demonstrated that IGF-I does facilitate muscle regeneration following traumatic injury [4], thus making it a promising molecule to be utilized therapeutically for the treatment of muscle injuries. However, its short half-life (10 – 30 min) and potentially negative systemic effects has limited the molecule's therapeutic application. The purpose of this study was to evaluate the therapeutic potential of delivering IGF-I in a controlled manner, using an intramuscular PEG-Fib platform, in the treatment of skeletal muscle I/R.

Conjugation and release of IGF-I from PEGylated fibrin gel

Because covalent bonding of PEG to both fibrinogen and growth factor is essential to achieve controlled release when using the PEG-Fib delivery system (**Figure 4.1**), we first had to verify the formation of fibrinogen-PEG-IGF-I complexes. Simultaneous incubation of fibrinogen, SG-PEG-SG, and IGF-I resulted in the formation of large IGF-I immunoreactive complexes, as determined by Western blotting (**Figure 4.2A**). This covalent bonding occurs when each SG functional group on the PEG molecule reacts with a free amine on a neighboring protein. Release kinetics of IGF-I from the PEG-Fib matrix was measured in sequential release samples using ELISA. Though the majority of IGF-I is released from the matrix with the first 24 hours (**Figure 4.2B**), a physiologically relevant dose of ~12 ng/mL [103, 104] was measured at 96 hours (**Table 4.1**). This early release is likely due to the low molecular weight of IGF-I (~7.5 kDa), which limits the number of free amine groups required for reaction with SG-PEG-SG. For example, the slightly larger SDF-1α (~11 kDa) is progressively released across 7 days from PEG-Fib [100]. IGF-I immunoreactivity in the release samples was also analyzed by Western blotting to demonstrate that IGF-I was mostly released as free peptides, rather than large complexes that may have impaired bioactivity (**Figure 4.2B bottom**).

PEGylated fibrin gel delivery of IGF-I improves recovery of muscle

The specific aim of the current study was to determine the efficacy of PEG-Fib-IGF treatment in improving the functional recovery of skeletal muscle from I/R. To accomplish this, an IM injection of saline, bIGF, PEG-Fib, or PEG-Fib-IGF treatment

was administered to the LGAS 24 hours after TK release. Functional evaluations of the LGAS were performed after 14 days of reperfusion. We observed no difference in functional recovery with saline, bIGF, or PEG-Fib treatments (**Figure 4.3**). PEG-Fib-IGF treatment, however, resulted in substantial recovery of force, compared to saline treatment (19.2±1.0 N vs. 12.4±0.6 N; $p < 0.05$). This improvement is dependent on an improvement in specific tension of the muscle, rather than just changes in muscle mass (**Table 4.2**). Interestingly, there were no significant differences in muscle mass or cross-sectional area between the groups, however both control and PEG-Fib-IGF groups strongly trended towards higher values in both parameters than other groups. This lack of statistical difference is likely due to large variations from persisting inflammation and/or edema in groups demonstrating more histological pathology (saline, bIGF, and PEG-Fib) [26, 105]. These results indicate the PEG-Fib-IGF treatment has therapeutic potential for skeletal muscle I/R, achieving comparable results to recovery in muscle-specific IGF-I overexpression models [4]. The lack of benefit from a single bolus injection of IGF-I agrees with the results of previous studies [106], and highlights the importance of covalent bonding of IGF-I to the matrix in order to prolong release and protect the IGF-I molecule from rapid degradation.

Histological evaluations of H&E stained LGAS cross-sections were also performed at the 14-day reperfusion time point (**Figure 4.4**). Saline-treated muscle displayed the typical abundance of small myofibers containing central nuclei seen in skeletal muscle following I/R, which is evidence of substantial degeneration/regeneration

cycling of injured myofibers. The presence of large myofibers of round morphology in these samples is indicative of focal edema and/or myofiber hypercontraction, which are both hallmarks of muscle pathology. Bolus IGF-I treated muscle displayed similar characteristics as saline treatment in terms of histological pathology and left-skewing of distribution of myofiber size. Treating I/R-affected muscles with PEG-Fib alone resulted in modest improvements in the histological morphology and myofiber distribution of the LGAS. This superficial improvement is not surprising, as PEG-Fib strongly binds many important growth factors, including transforming growth factor-β (TGFβ) [107-109], fibroblast growth factors (FGFs) [110, 111], and vascular endothelial growth factor (VEGF) [112]. Muscles treated with PEG-Fib-IGF displayed almost no signs of pathology and demonstrated a myofiber size distribution comparable to that of control muscle. In addition, the distribution of muscle fibers < 2000 μm^2 in size was quantified (**Figure 4.5**), revealing that PEG-Fib-IGF treatment resulted in significantly less small fibers than other treatment groups and was no different than control muscle. These data indicate improvements in histological morphology accompany the improved functional recovery of skeletal muscle from I/R using PEG-Fib-IGF as a treatment strategy.

To accompany our data depicting improved recovery following PEG-Fib-IGF treatment, IHC staining for desmin, neonatal myosin heavy chain (nMHC), and myogenin was performed in saline, PEG-Fib, and PEG-Fib-IGF groups (**Figure 4.6**). Desmin is a sarcomere-associated protein whose immunoreactivity is rapidly lost in perturbed myofibers [105]. We found a significantly higher incidence of desmin-positive

myofibers in PEG-Fib-IGF treated muscles than in saline or PEG-Fib groups, which is in agreement with our H&E depiction of healthier muscle following PEG-Fib-IGF treatment. In addition, we looked at immunoreactivity of nMHC, an immature myosin heavy chain isoform that is found in actively regenerating muscle [113], and nuclear expression of myogenin, a muscle regulatory factor (MRF; muscle specific transcription factor) expressed in the later stages of myogenesis [39], as indicators of active muscle regeneration. PEG-Fib-IGF treatment resulted in significantly less nMHC-positive fibers than both saline and PEG-Fib groups, and significantly less myogenin-positive nuclei than saline treatment. These results suggest that the myogenic/regenerative program is near completion in PEG-Fib-IGF treated muscles following 14 days of reperfusion, yet is still prominent in saline and PEG-Fib treatment groups. Taken together, our data indicate that PEG-Fib-IGF mediated therapy hastens both the histological and functional recovery of skeletal muscle from I/R injury, compared to all other tested groups.

Hyperactivation of the PI3K/Akt pathway may mediate therapeutic effect

From the data demonstrating PEG-Fib-IGF-mediated improvement in muscle recovery from I/R, we gathered that 2 potential mechanisms are responsible for our results: 1) PEG-Fib-IGF is facilitating the regenerative actions of myoblasts, thereby speeding up the regenerative time frame, or 2) PEG-Fib-IGF exerts a protective effect on the existing myofibers, thus resulting in less damage from the I/R insult. We therefore repeated PEG-Fib (control) and PEG-Fib-IGF treatment groups with only 4 days of reperfusion to discern which mechanism is likely behind the beneficial effect of PEG-

Fib-IGF treatment. The 4-day reperfusion period was chosen because an appreciable amount of IGF-I is still being released from PEG-Fib-IGF (**Table 4.1**) and it is a time point of maximum myoblast proliferation [23, 114].

The canonical intracellular signaling induced by activation of the IGF-IR in skeletal muscle includes the Ras/Raf-1/ERK MAP kinase and PI3K/Akt pathways [1]. Activation of the ERK pathway is generally associated with induction of myoblast proliferation [103], while activation of the PI3K/Akt pathway results in diverse effects, including activation of protein synthesis, abrogation of catabolism, promotion of cell survival, and stimulation of myoblast differentiation [103, 115]. To investigate if either of these pathways are differentially expressed between PEG-Fib and PEG-Fib-IGF treated muscles, LGAS muscles were harvested after 4 days of reperfusion and analyzed by Western blotting for phosphorylation of ERK and Akt. Phosphorylation of ERK was not different between the 2 treatments, however, p-Akt of the PEG-Fib-IGF treatment demonstrated an ~2-fold increase in content over PEG-Fib treated muscles (**Figure 4.7**). IGF-I-induced activation of Akt promotes protein synthesis, which is regulated through the activation of mTOR and $p70^{S6K}$ [116], and negatively regulates muscle atrophy by preventing the expression muscle-specific E3 ubiquitin ligases (components of the ubiquitin-proteasome system) through inactivation of FoxO transcription factors [117, 118]. PEG-Fib-IGF treatment also resulted in similar increases in mTOR and $p70^{S6K}$ phosphorylation as those found for Akt, as well as vastly reduced levels of MuRF-1, a cytosolic E3 ubiquitin ligase implicated with sarcomere degradation [119, 120],

demonstrating hyper-activation of the PI3K/Akt pathway is a feature of PEG-Fib-IGF treatment.

Activation of Akt has been shown to protect cells from apoptotic and/or necrotic fates in a number of models and tissues [95, 121-123]. In agreement with this, H&E staining revealed dramatically reduced signs of muscle pathology following PEG-Fib-IGF treatment (**Figure 4.8 top**), compared to PEG-Fib treatment, suggesting a lower magnitude of initial muscle injury corresponds with the increased Akt activation. Unexpectedly, we could not detect any difference in frequency of MyoD (**Figure 4.8 bottom**), an early expressed MRF, or myogenin (data not shown) positive nuclei, therefore enhanced activation of myoblasts does not appear to be a mechanism of the improved recovery with PEG-Fib-IGF treatment. These results in conjunction with the signaling data suggest PEG-Fib-IGF treatment improves muscle recovery from I/R by promoting hyper-activation of the PI3K/Akt pathway, thereby limiting the extent of cell death and degeneration that typically accompanies the I/R perturbation. In agreement with this, previous studies in our research group have demonstrated reduced activation of this pathway correlates with a reduction in functional recovery in aged rats from TK-induced I/R [26]. To verify this conclusion, however, future investigations to thoroughly quantify differential cellular damage between the two groups would need to be performed.

CONCLUSION

I/R injury is a considerable perturbation to skeletal muscle, often resulting in substantial and prolonged functional deficits. In the current report, we have demonstrated that the sustained release of IGF-I from an IM, biodegradable PEGylated fibrin gel matrix significantly improves the functional recovery of skeletal muscle from TK-induced I/R. We also identify activation of the PI3K/Akt pathway, and not enhanced myoblast activity, as a potential mechanism mediating this beneficial effect. The results of this study may lead to future investigations to test the effectiveness of PEG-Fib-IGF treatment in other models of muscle injury, including crush injuries and lacerations.

This particular form of growth factor is distinct from purely synthetic polymer delivery systems in the form of monolith devices, foams, or particles in that the material is both injectable and can retain the delivered agent to the site of injury [124]. Since both fibrin-based and PEG-containing products are currently FDA approved, the translation of this form of therapy into the clinical realm is realistic. Additional directions may include the delivery of growth factor combinations to optimize tissue and/or incorporation of stem cells to facilitate the regenerative process of damaged tissue. For example, vasculogenic factors, such as VEGF or HGF, can possibly be used in this system to improve vascular regeneration following injury or other conditions where perfusion is compromised.

Table 4.1. IGF-I release from PEGylated fibrin matrix

Time (h)	[IGF-I] (ng/mL)
2	1297±198
6	725±240
24	784±327
48	210±57
72	58.5±0.3
96	12.3±2.2
144	3.5±0.1

Values indicated are mean±SD; n = 3 trials

Table 4.2. Muscle parameters following 14 days of reperfusion

	LGAS mass (mg)	CSA (cm^2)	SPo (N/cm^2)
Uninjured	1689±47	1.35±0.04	19.6±0.5
Saline	1461±55	1.20±0.04	10.5±0.8*
Bolus IGF-I	1491±112	1.18±0.10	10.5±0.7*
PEG-Fib	1522±93	1.12±0.07	11.7±1.0*
PEG-Fib-IGF	1643±75	1.30±0.06	14.8±0.6*,#

LGAS = lateral gastrocnemius; CSA = cross-sectional area; SPo = specific tension. Values indicated are mean±SEM. * $p < 0.05$ vs. Uninjured, # $p < 0.05$ vs. Saline, bolus IGF-I, and PEG-Fib groups.

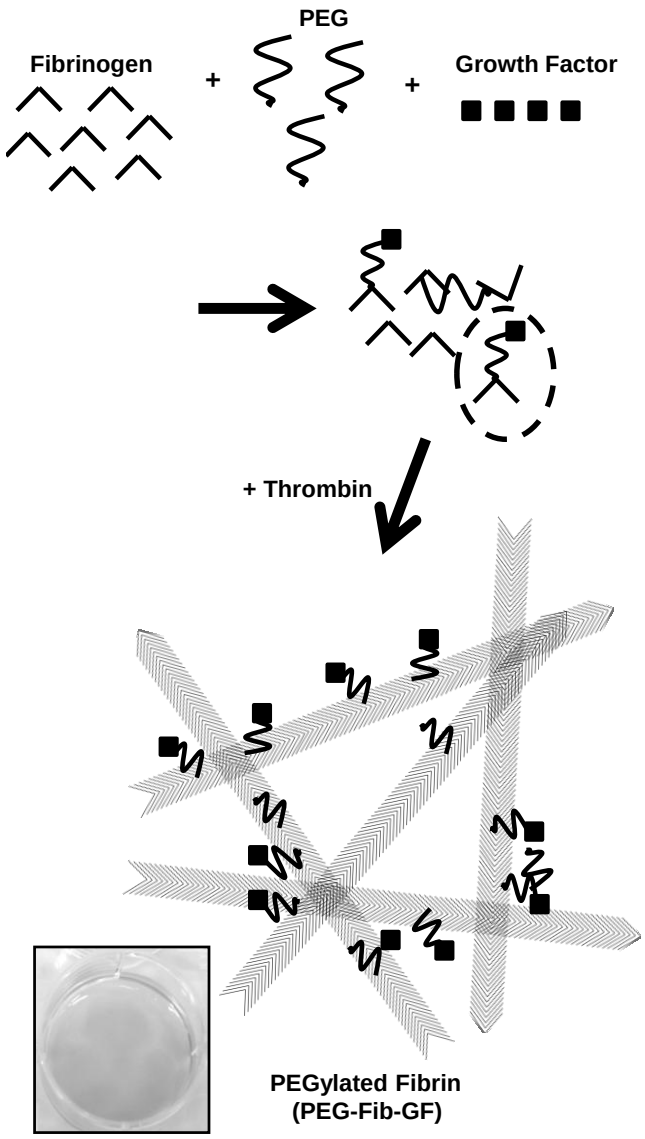

Figure 4.1. Generation of growth factor-conjugated PEGylated fibrin gel (PEG-Fib-GF) is achieved by the co-incubation of fibrinogen, bi-functional polyethylene glycol (PEG), and growth factor. The result is a mixture of various covalently linked products composed of the original components. This mixture is polymerized by the addition of thrombin to generate PEG-Fib-GF.

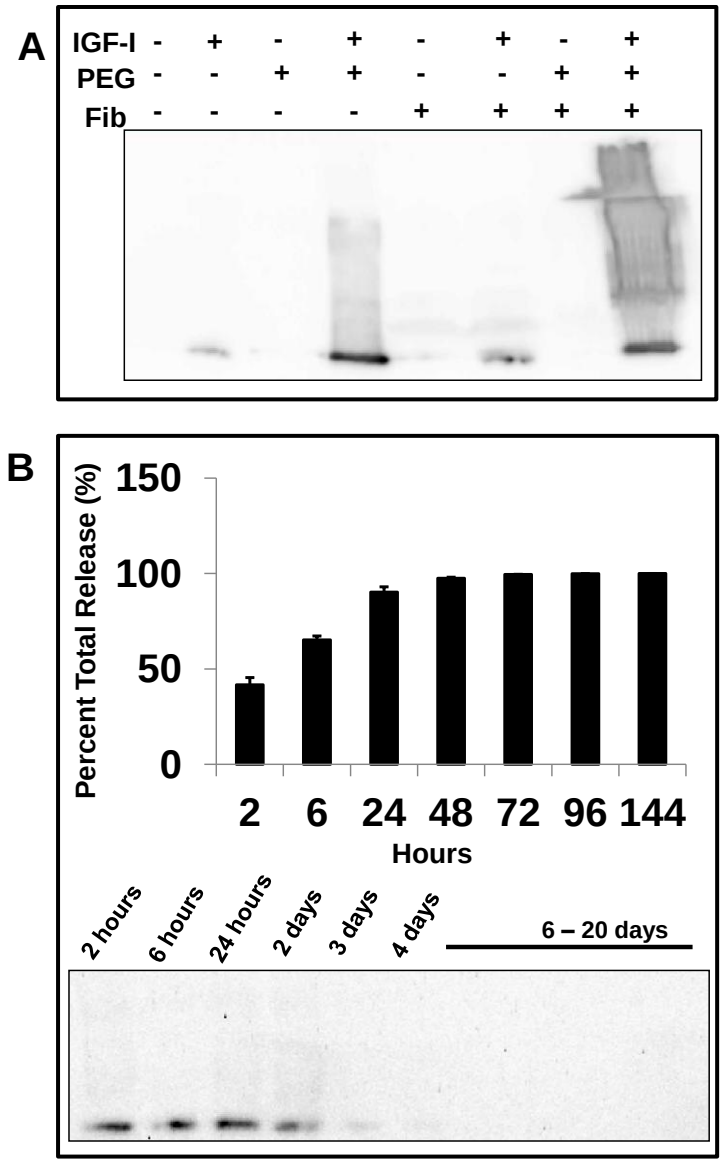

Figure 4.2. Covalent conjugation of IGF-I to PEGylated fibrinogen is verified by Western blotting using an anti-IGF-I antibody (**A**). Release kinetics of IGF-I from the PEGylated fibrin gel delivery system (**B top**) was determined by ELISA. Western blotting confirms that the majority of immunoreactive IGF-I released from PEGylated fibrin gel is consistent that with of IGF-I peptide (**B bottom**), rather than large complexes. Values represented are the mean ± SD of 3 separate trials.

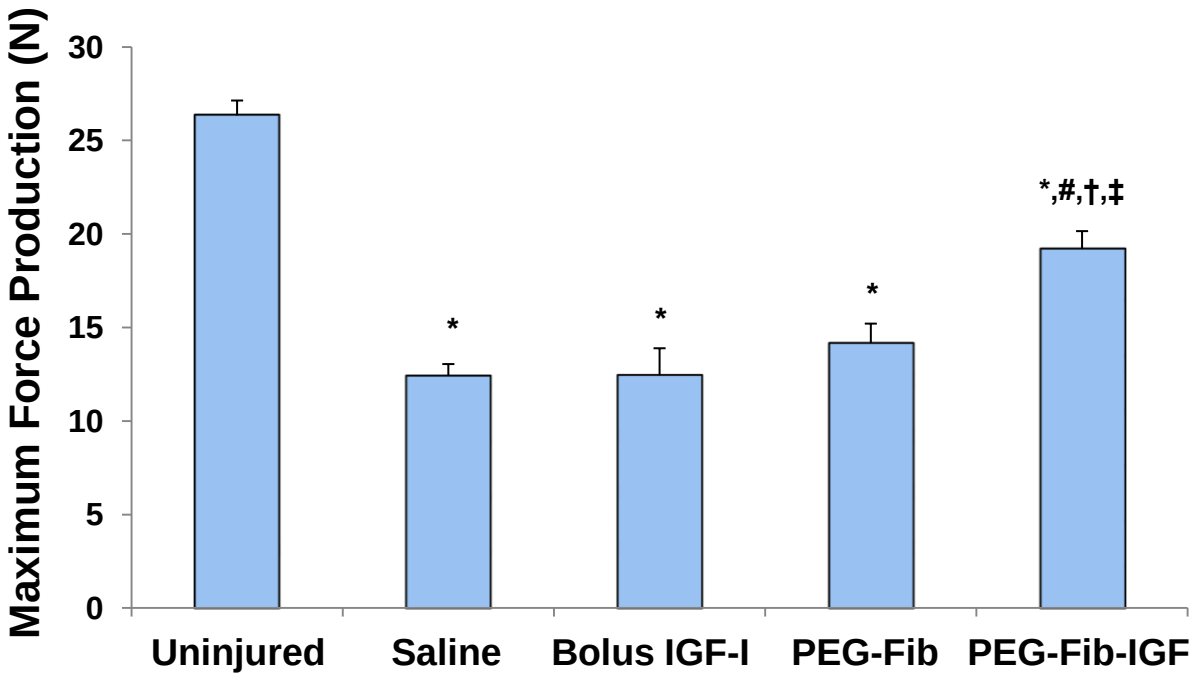

Figure 4.3. After 14 days of reperfusion, maximum force production of the lateral gastrocnemius (LGAS) was measured *in situ* from the following treatment groups: saline, bolus IGF-I, PEGylated fibrin gel (PEG-Fib), and IGF-I conjugated PEG-Fib (PEG-Fib-IGF). Values represented are the mean ± SEM; *$p < 0.05$ vs. uninjured, #$p < 0.05$ vs. saline, † $p < 0.05$ vs. bolus IGF-I, ‡ $p < 0.05$ vs. PEG-Fib.

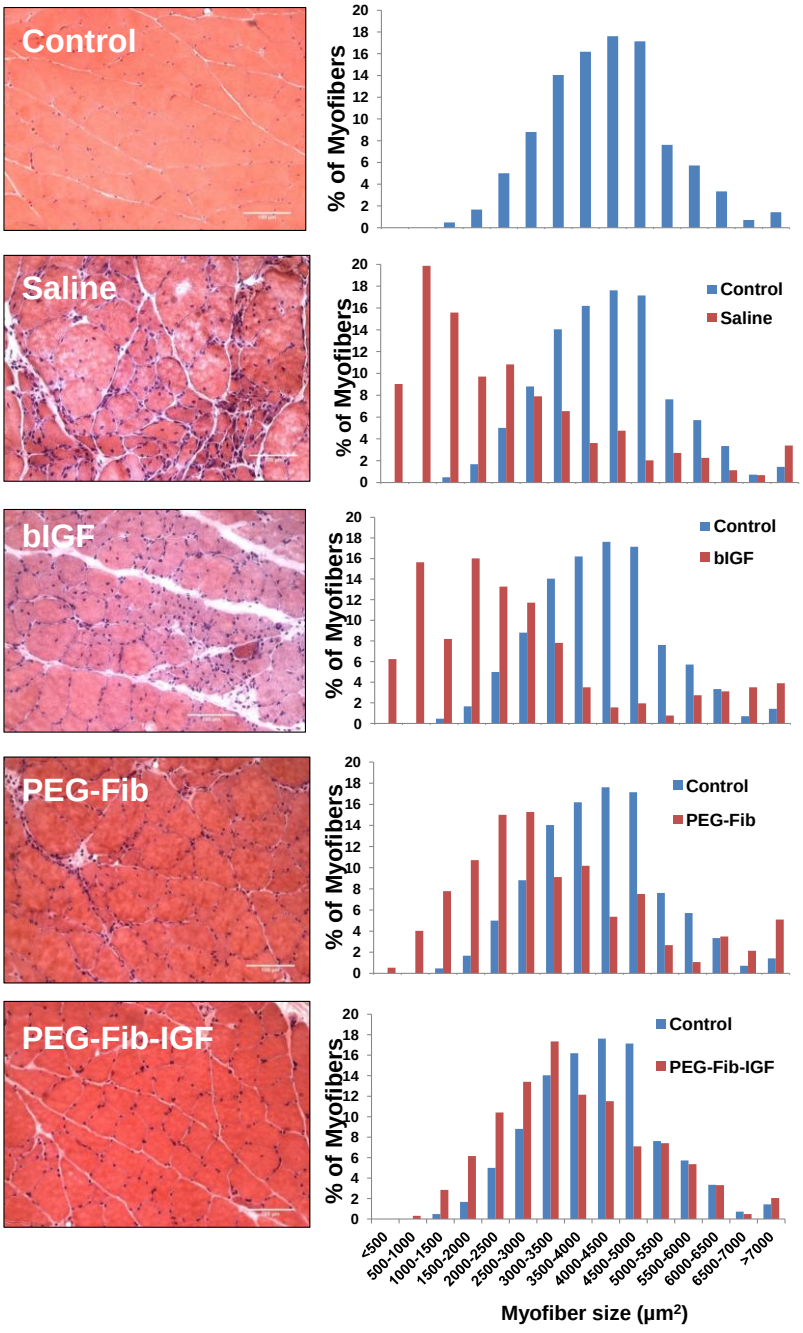

Figure 4.4. H&E stained sections were prepared (left) and evaluated for fiber size composition (right; 250-600 fibers evaluated per group).

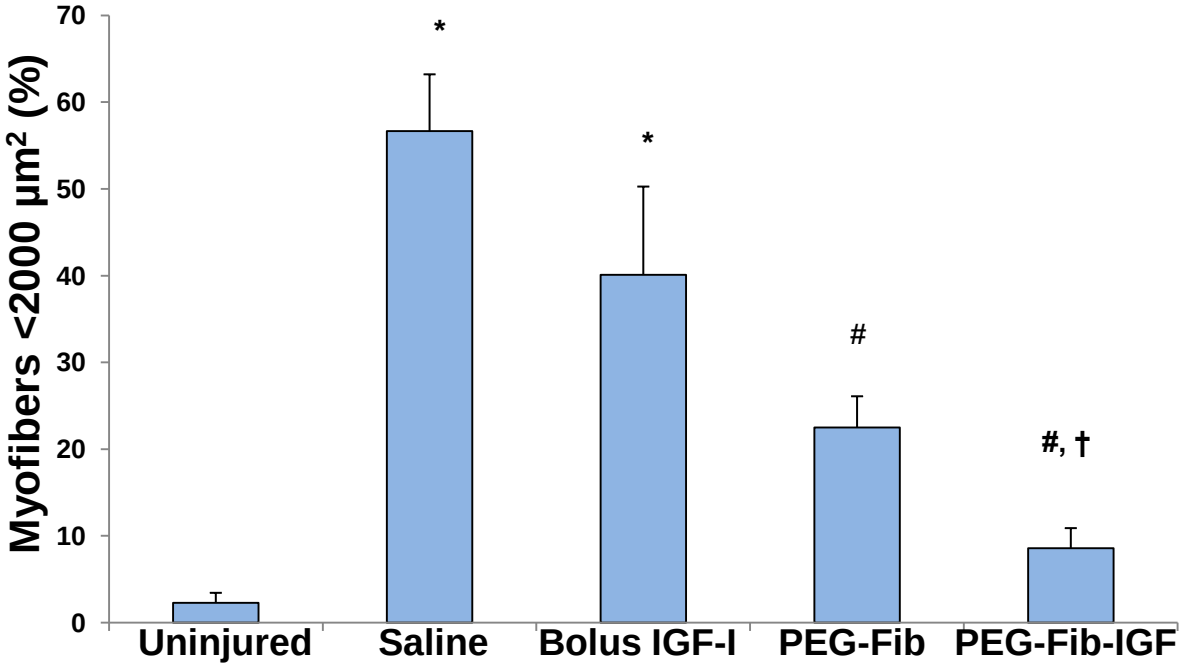

Figure 4.5. Proportions of small muscle fibers (< 2000 μm^2) were compared among the different treatment groups. Values represented are the mean ± SEM; *p < 0.05 vs. uninjured, #p < 0.05 vs. saline, † p < 0.05 vs. bolus IGF-I, ‡ p < 0.05 vs. PEG-Fib.

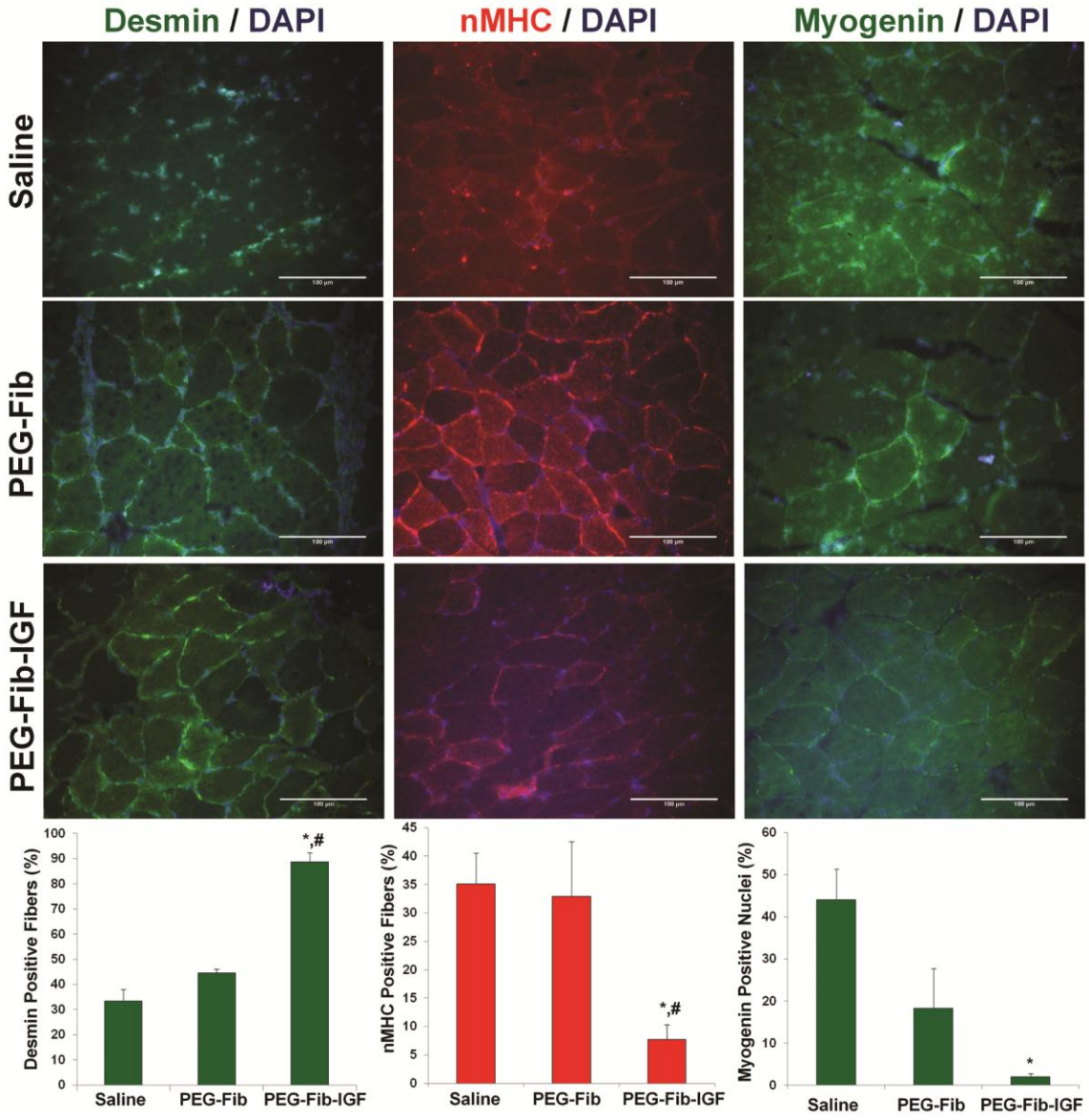

Figure 4.6. Immunohistochemistry for desmin, neonatal myosin heavy chain (nMHC), and myogenin was performed on the lateral gastrocnemius muscles from saline, PEGylated fibrin gel (PEG-Fib), and IGF-I conjugated PEG-Fib (PEG-Fib-IGF) groups following 14 days of reperfusion. Representative slides and marker-specific quantifications are provided. Values represented are the mean ± SEM; *$p < 0.05$ vs. saline, #$p < 0.05$ vs. PEG-Fib.

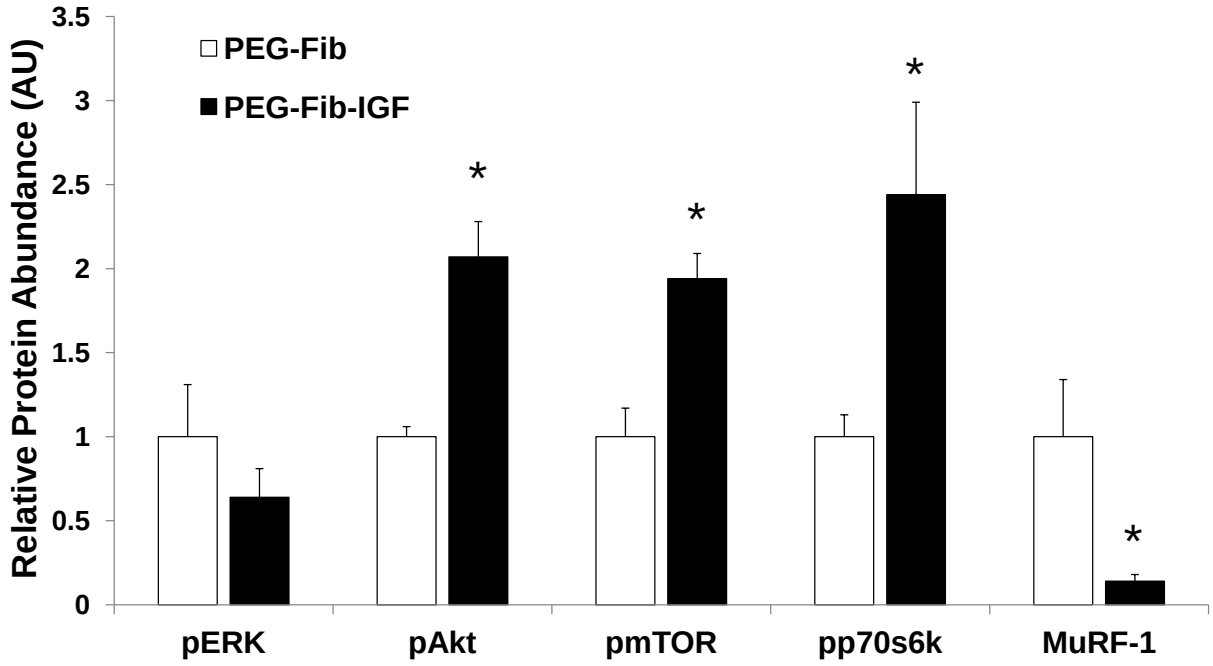

Figure 4.7. Western blotting was performed on PEGylated fibrin gel (PEG-Fib) and IGF-I conjugated PEG-Fib (PEG-Fib-IGF) treated lateral gastrocnemius muscles following 4 days of reperfusion. Proteins assessed include the phosphorylated and total protein forms of ERK, Akt, mTOR, and $p70^{S6K}$, as well as the E3 ubiquitin ligase MuRF-1. Values represented are the mean ± SEM; *$p < 0.05$ vs. PEG-Fib.

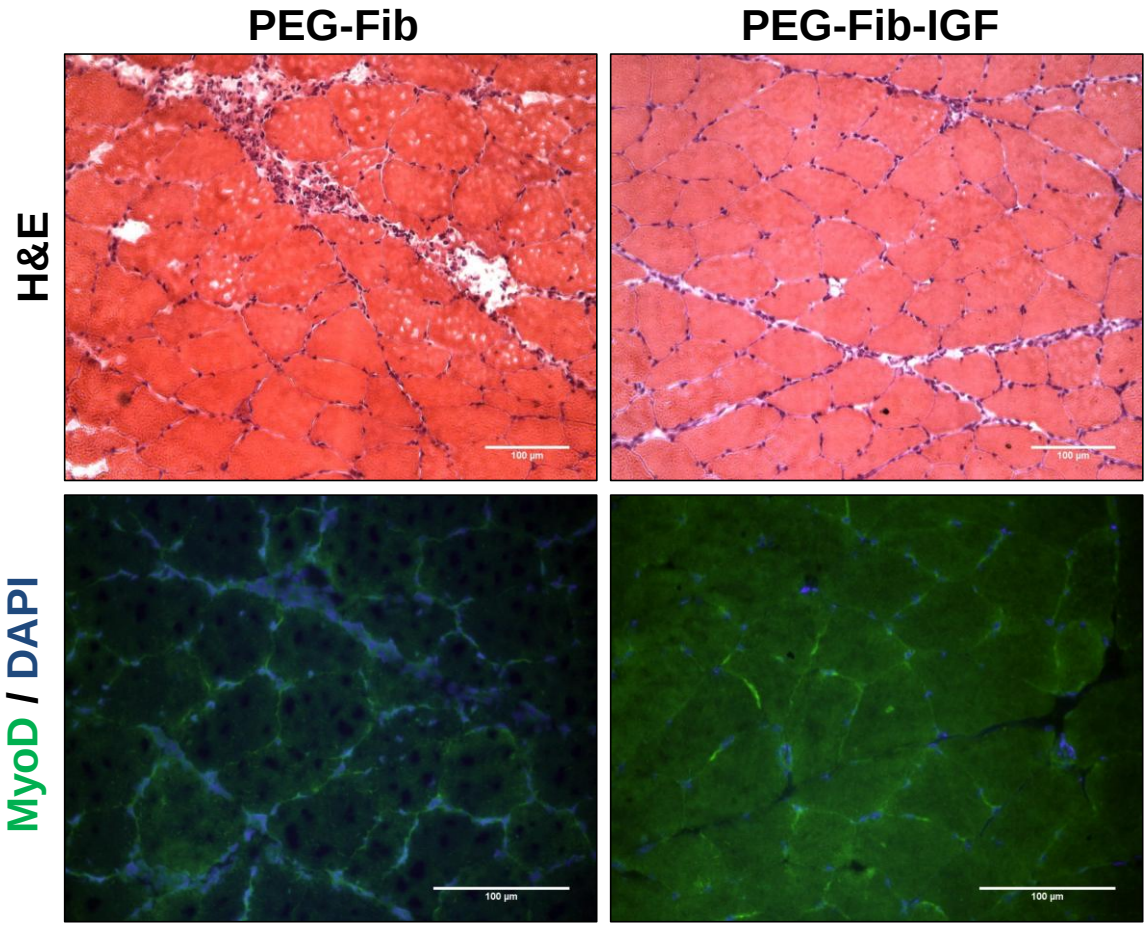

Figure 4.8. H&E staining and immunohistochemistry for the myoblast marker MyoD were performed on PEGylated fibrin gel (PEG-Fib) and IGF-I conjugated PEG-Fib (PEG-Fib-IGF) treated lateral gastrocnemius muscles following 4 days of reperfusion.

Chapter V: Evaluation of Ischemia/Reperfusion induced Macrophage Profiles in Skeletal Muscle

ABSTRACT

The presence of macrophages (MPs) is essential for skeletal muscle to properly regenerate following injury. The purpose of this study was to develop simple model for the evaluation of MP profiles in injured muscle to facilitate the understanding of the complex post-injury environment. Using flow cytometry, we identified 3 distinct $CD11b^+$ cell populations that differ in expression of Ly-6C and F4/80. This model was utilized for the analysis of muscle-specific MP patterns and evaluation of immunomodulation by fibrin-based treatments following hind limb ischemia/reperfusion (I/R) injury. Furthermore, we demonstrate that the $Ly\text{-}6C^{lo}$ $F4/80^+$ population of MPs can be isolated via FACS and be utilized as an effective therapeutic treatment for I/R of skeletal muscle.

INTRODUCTION

Macrophages (MPs) are an essential part of the muscle regenerative process, as demonstrated through numerous studies where their post-injury infiltration has been perturbed [14, 54-56, 59, 125]. The recently emerging paradigm of MP infiltration of entails immature monocytes expressing high levels of Ly-6C migrating into damaged tissue [13]. These cells differentiate into inflammatory MPs that partake in phagocytosis of necrotic debris, then switch to an anti-inflammatory phenotype to aid in the myogenic repair process [14]. This phagocytosis-induced phenotype shift appears to be a CREB-dependent process [126], and is likely due to phosphatidylserine ingestion [127].

Of particular interest to our research group, much evidence suggests that MPs are required for the robust post-injury upregulation of IGF-I, as severely reduced IGF-I expression has been reported with chlodronate-depletion [56] and CCR2/CCL2 disruption [59, 125]. Frenette et al [128] revealed that MPs are required for IGF-I expression in myoblast co-cultures. In addition, Lu et al [59] demonstrate that IGF-I is highly expressed in both the Ly-6C^{hi} and Ly-6C^{lo} subsets of F4/80^{+} cells, with more being expressed in the latter. This evidence strongly suggests that MPs are the primary cellular source of IGF-I in regenerating skeletal muscle. Therefore, conditions resulting in impaired IGF-I expression following injury, such as aging [26, 50], may very well be caused by a MP impairment. In agreement with this, elderly humans exhibit altered post-exercise MP profiles [129], and aged rodents have lower leukocyte mobilization and infiltration following myocardial ischemia/reperfusion [130, 131]. Furthermore, a mouse

diabetic model, the db/db mouse, shows reduced regeneration and lower MP numbers following cardiotoxin injury [132].

The purpose of the present study was to develop a simple method for the evaluation of inflammatory cells in injured skeletal muscle. With a tri-color flow cytometric analysis, we identified 2 distinct mouse CD11b MP populations that differ in relative expression of F4/80 and Ly-6C in I/R affected hind limb muscles. Using this analysis, we revealed that intramuscular fibrinogen-based therapies increase macrophage prevalence in injured muscle, which may account for notable histological improvements our group has reported [133]. In agreement with this, FACS isolation and subsequent intramuscular injection of the Ly-6C^{lo} F4/80^{+} population improved functional recovery of muscle from I/R.

METHODS AND MATERIALS

Animals

Male C57BL/6 mice (~6 mo) were used for this study. Animals were housed individually with *ad libitum* access to food and water, and maintained on a 12-hour light/dark cycle. All experimental procedures were approved and conducted in accordance with the guidelines set by The University of Texas at Austin IACUC.

Tourniquet Application

Mice were anesthetized with 2% isoflurane gas prior to and for the duration of tourniquet application. A single, randomly selected hind limb was elevated, and a pneumatic tourniquet (D.E. Hokanson, Inc.) was wrapped snuggly against the proximal portion of the limb and inflated to 250 mm Hg by the Portable Tourniquet System (Delfi Medical Innovations Inc.) to ensure complete occlusion of blood flow to the limb for a duration of 2 hours [69]. Body temperature was maintained at 37±1º C with the use of a heat lamp during this procedure. After 2 hours, the pneumatic tourniquet was removed, and the mouse was returned to its cage for recovery.

PEGylated fibrin gel injection

Following 24 hours of reperfusion, 100 uL of saline, empty PEGylated fibrin gel (PEG-Fib), or IGF-I conjugated PEG-Fib (PEG-Fib-IGF), described previously [133], was injected into the gastrocnemius muscles of the TK-affected limb (50 uL into each head). Briefly, human fibrinogen (Sigma) was allowed to react with SG-PEG-SG (NOF America) and human IGF-I (Peprotech) to generate covalently-linked products. Gel polymerization was initiated by the addition of human thrombin (Sigma; 25 U/ml). The final concentration of components was 10 mg/mL fibrinogen, 0.5 mg/mL SG-PEG-SG, and 25 ug/mL IGF-I.

Macrophage Isolation and Flow Cytometry

Tibialis anterior (TA) and lateral gastrocnemius (LG) muscles were harvested from euthanized mice, finely minced with scissors, and incubated for 40 minutes in 10

volumes/muscle weight of 1% collagenase II (Invitrogen) dissolved in DMEM at 37 C. Samples were filtered through 40 um nylon cell strainers (BD), and prepared for flow cytometry using PE-conjugated anti-CD11b (BD), FITC-conjugated anti-Ly6C (Biolegend), and APC-conjugated anti-F4/80 (Biolegend). Appropriate isotype controls were also used to verify specificity of staining. Samples were run on the BD Fortessa Flow Cytometer at the University of Texas Institute of Cell and Molecular Biology core facility. Fluorescence activated cell sorting (FACS) was performed using the BD FACSAria. Data were analyzed using Flowing Software 2.

Force Measurements

Gastrocnemius muscles were surgically isolated from all other muscles and connective tissue, and subjected to functional measurements. The Achilles tendon was secured to the muscle lever arm of a servomotor (model 305B, Cambridge Technologies) interfaced with a computer equipped with an A/D board (National Instruments). The muscle was stimulated to contract using an Isolated Pulse Stimulator (Model 2100; A-M Systems) with leads applied to the sciatic nerve. Muscle temperature was kept constant at 37º C with warm mineral oil and a radiant heat lamp throughout the procedure. Optimal length of the muscle was determined by measuring maximal twitch tension at a stimulation of 0.5 Hz. At optimal length, the muscle was stimulated at 150 Hz for 350 ms to elicit the peak tetanic tension (P_o), and was allowed 2 minutes of rest between each contraction. Data were stored and analyzed using LabView software (National Instruments).

Histology

Slides of paraffin-embedded gastrocnemius muscles were prepared. Hematoxylin & eosin (H&E) staining was performed, as previously described [102], and slides were observed with a light microscope (Nikon Diaphot) with the 20X objective lens. Images were taken using a mounted digital camera (Optronix Microfire).

Statistical Analysis

Data were analyzed using Student's T-tests or ANOVA, where appropriate ($\alpha = 0.05$). Values are represented as mean ± SEM.

RESULTS

Macrophage profile characterization

The investigation of inflammatory cell profiles in injured skeletal muscle by flow cytometric techniques varies by lab, and often involves costly purification techniques, a large array of labeling antibodies, and/or the use of novel transgenic animals to label/modify specific cell populations. To provide a rapid and cost-effective, yet reliable, method of inflammatory profile analysis, freshly isolated cells from I/R-injured muscles were labeled with fluorochrome-conjugated anti-CD11b, expressed by monocyte lineage cells and neutrophils, anti-Ly6C, a surface marker highly expressed on inflammatory monocytes/MPs and neutrophils, and anti-F4/80, a marker associated with mature MPs. Analysis of $CD11b^+$ cells reveals 3 distinct subpopulations of cells that vary in

expression of Ly-6C and F4/80 (**Figure 5.1A**). This includes a population of F4/80$^-$ Ly-6C^{mid} cells [quadrant 1 (Q1)] , which are likely neutrophils, a F4/80$^+$ Ly6C^{hi} population (Q4), which appear to be early infiltrating, inflammatory MPs, and F4/80$^+$ Ly-6C^{lo} cells (Q2) representing mature, pro-regenerative MPs [14]. In agreement, each population demonstrates appropriate profiles in side-scatter (SSC) vs. forward-scatter (FSC) plots (**Figure 5.1B**).

Muscle-specific MP profiles following I/R

First experimental utility of this technique was to investigate differential immune profiles of lateral gastrocnemius (LG) and tibialis anterior (TA) muscles following I/R. Following reperfusion, both muscles have roughly equivalent proportions of Q1, Q2, and Q4 cells (**Figure 5.2A**). CD11b$^+$ cells were barely detectable in control muscle, and resided mostly in Q2 (**Figure 5.2B**). Cell populations were quantified relative to 3 day LG CD11b+ cells ($3.28x10^4$ cells/mg muscle), revealing that TA muscles contain a significantly higher number of CD11b+, Q2, and Q4 cells at 3 days of reperfusion (**Figure 5.2C**). This difference was gone by day 5. These results indicate that muscle-specific immune profiles occur following I/R injury, which may reflect differential susceptibility to damage or post-injury monocyte migration between the muscles.

Immunomodulatory effects of PEGylated fibrin gel

In a previous study, our laboratory group reported that an intramuscular injection of IGF-I-conjugated PEGylated fibrin gel (PEG-Fib-IGF) drastically improved the recovery of skeletal muscle from I/R [133]. To investigate whether immunomodulation

occurs in PEG-based therapy, saline, PEG-Fib, or PEG-Fib-IGF was injected into the LG of mice following 24 hours of reperfusion, followed by MP profile evaluation for both the LG and TA in 3 and 5-day reperfusion groups (**Figure 5.3**). At 3 days, there is a clear PEG-Fib effect on $CD11b^+$ and Q2 cell numbers (52 and 65% increase, respectively), compared to saline, in the LG, though IGF-I appears to have no effect beyond PEG-Fib at this time. Day 5, however, shows a clear IGF-I effect, as PEG-Fib-IGF treated LGs show a substantial 47 and 43% reduction in $CD11b^+$ and Q2 cells, respectively compared to saline treatment. In addition to revealing novel effects of PEG-based treatments, these data also demonstrate a clear disconnect between the MP accumulation (day 3) and persistence (day 5). Interestingly, the non-treated TA muscles appear to mirror the relative MP composition of the treated LGs, suggesting PEG-Fib based treatments may have a whole limb effect in regards to MP prevalence.

Increasing intramuscular MPs improves functional muscle recovery

The above-mentioned results suggest that increasing the number of MPs in a regenerating muscle may facilitate the recovery process. To directly test this hypothesis, $CD11b^+$ Ly-$6C^{lo}$ $F4/80^+$ cells were isolated from 3 day reperfusion muscles using FACS, then injected (~$1.5x10^6$ cells) into day-matched gastrocnemius muscles. Functional assessment at 14 days of reperfusion revealed significant improvements in maximum tetanic force production (2.2 N vs. 1.4 N), muscle mass (142 mg vs. 111 mg), and mass-normalized force production (15.7 N/g vs. 12.4 N/g) in the MP treated group, compared to saline treated muscle. This also translated to significantly improved recovery (in terms

of % of contralateral limb) of maximum force and muscle mass, while mass-normalized force demonstrated an obvious effect (**Figure 5.4**). In agreement, MP-treated muscles display an improved histological appearance over saline treatment (**Figure 5.5**). These data clearly show that increasing MP prevalence substantially improves skeletal muscle functional recovery from I/R, and suggests MP-based treatments may have therapeutic promise.

DISCUSSION

The present study depicts a simple, reliable method for the investigation of MP profiles in injured skeletal muscle. Given the absolute importance of MPs in the regenerative process, this provides a great tool in the investigations of conditions where skeletal muscle regeneration is impaired, such as aging [26, 50] and metabolic disorders [132]. In addition, we demonstrate that increasing MP prevalence by intramuscular injection of isolated MPs enhances muscle regeneration from I/R, suggesting novel, MP-based therapies have potential for treatment of muscle injuries.

To investigate MP profiles in muscle injures, we analyzed $CD11b^{+}$ subpopulations that differ in degree of Ly-6C and F4/80 expression. Using this method of analysis, we observed differences in MP abundance in the LG and TA following 3 days of reperfusion, suggesting that these 2 muscles may exhibit either different amounts of initial damage or different efficiencies of monocytes chemotaxis to the muscle.

We also identified that PEG-Fib (with or without IGF-I) increases MP accumulation at 3 days of reperfusion. Interestingly, fibrinogen is a direct ligand for CD11b (an integrin receptor), resulting in migratory, phagocytotic, and cytokine expression changes [134]. This observation of PEG-Fib-induced increases in MPs could either be a result of increased infiltration, increased MP proliferation, or better MP survival. These mechanistic details can be evaluated *in vitro*. The substantial decrease in MP numbers with PEG-Fib-IGF at day 5 strongly suggests that MP persistence is independent of MP accumulation. Since PEG-Fib-IGF appears to improve myofiber survival [133], a resulting sharp decline in intracellular leakage and/or amount of necrotic material is likely a major factor in MP persistence. This IGF-I mediated effect on $CD11b^+$ cell prevalence agrees well with those reported from muscle-specific IGF-I overexpressing mice following cardiotoxin injury [4].

An incredibly interesting find detailed in this report is that FACS-isolated Ly-$6C^{lo}$ $F4/80^+$ MPs greatly enhance functional muscle recovery from I/R upon intramuscular injection, indicating MP-mediated approaches represent a potential therapies for muscle injuries. This MP-mediated improvement in recover could occur through a number of possible mechanisms, including an increase of local IGF-I [59], improved survival and/or activity of myoblasts [14, 135, 136], or facilitation of muscle remodeling [56, 58]. While our data is unique to skeletal muscle, similar therapies have been utilized to improve outcomes of myocardial infarction [137], sternal wounds [138], and skin ulcers [139-142]. In fact, heterochronic MP transfer demonstrates that MPs from young donors can

hasten wound healing of old mice [143], suggesting MPs are perhaps the mediating factor in improved muscle regeneration of heterochronic muscle transplantation [27] and parabiosis [28] models. This would be an exciting avenue to explore in future investigations.

The current report provides a simple method for the analysis of MP profiles in injured muscle, providing a great tool for the investigation of novel, immunological mechanisms involved in muscle regeneration. In conjunction with immunomodulatory tactics, such as PEG-Fib, it is possible to investigate whether impaired regenerative situations, such as aging and metabolic disorders, are possibly a result of defective cellular infiltration or intrinsic deficits associated with MPs. In doing so, it would also be possible to identify whether MP-derived IGF-I is the main effector responsible for regenerative defects found in such conditions, or if IGF-I expression is simply a surrogate that indicates MP levels. We also provide strong evidence the MP-based therapies are effective for the treatment of muscle injuries, which may be more favorable than stem cell based therapy in situations where aberrant differentiation or long-term cellular persistence may be a concern.

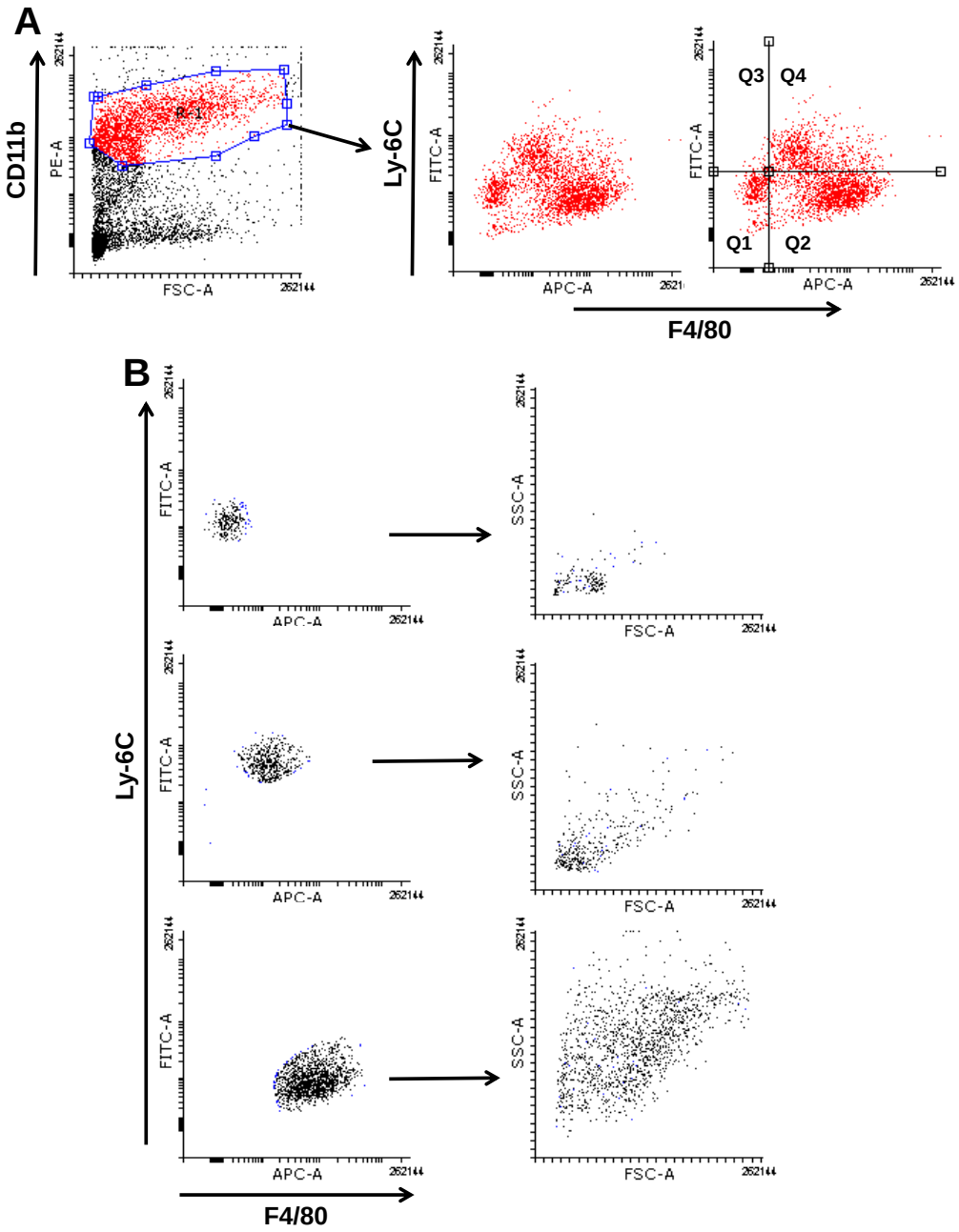

Figure 5.1. Cells isolated from muscle following 3 days of reperfusion were labeled with PE-anti-CD11b, FITC-anti-Ly-6C, and APC-anti-F4/80 and subjected to flow cytometry. The $CD11b^{+}$ population was further characterized by differential expression of Ly-6C and F4/80 (**A**), demonstrating 3 distinct subpopulations (Q1, Q2, Q4)**.** These subpopulations exhibit distinct side-scatter and forward-scatter characteristics (**B**).

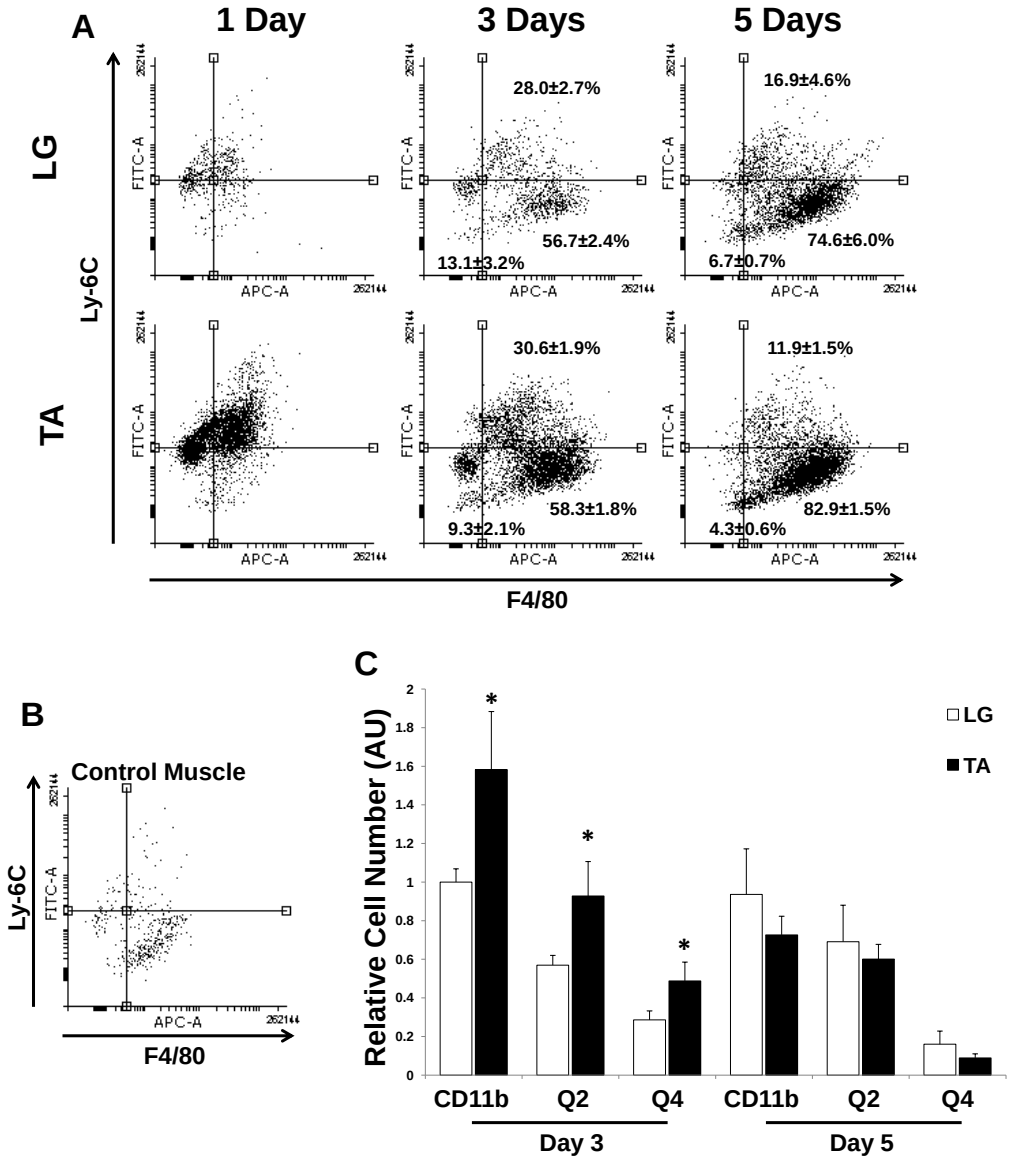

Figure 5.2. Comparison of flow CD11b$^+$ cell profiles in lateral gastrocnemius (LG) and tibialis antierior (TA) muscles following 1 (n = 1), 3 (n = 5), and 5 days (n = 4) of reperfusion (**A**). Control muscles demonstrate a very low number CD11b$^+$ cells (**B**). Cell population quantification (**C**) demonstrates muscle-specific numbers of CD11b$^+$, Q2, and Q3 exist between the LG and TA. Values are normalized to absolute number of CD11b$^+$ cells of the LG, and are represented as mean ± SEM; *$p < 0.05$ vs. LG.

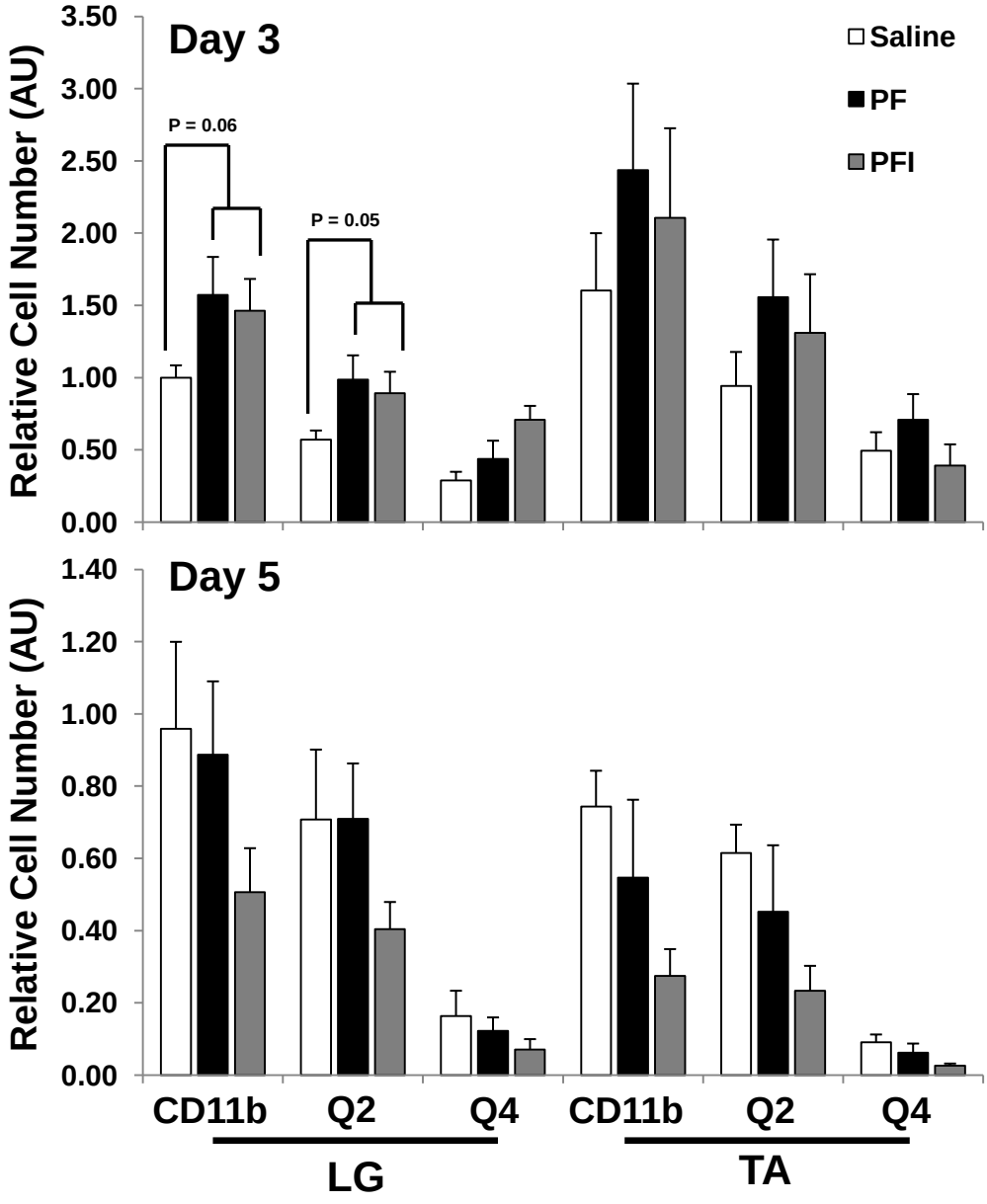

Figure 5.3. Relative cell quantification of 3 and 5-day reperfusion lateral gastrocnemius (LG) and tibialis anterior (TA) muscles treated with saline (n = 4), PEGylated fibrin gel (PF; n = 4), or IGF-I conjugated PF (PFI; n = 3-4). Values are relative to 3-day saline LG $CD11b^{+}$ numbers, and are represented as mean ± SEM.

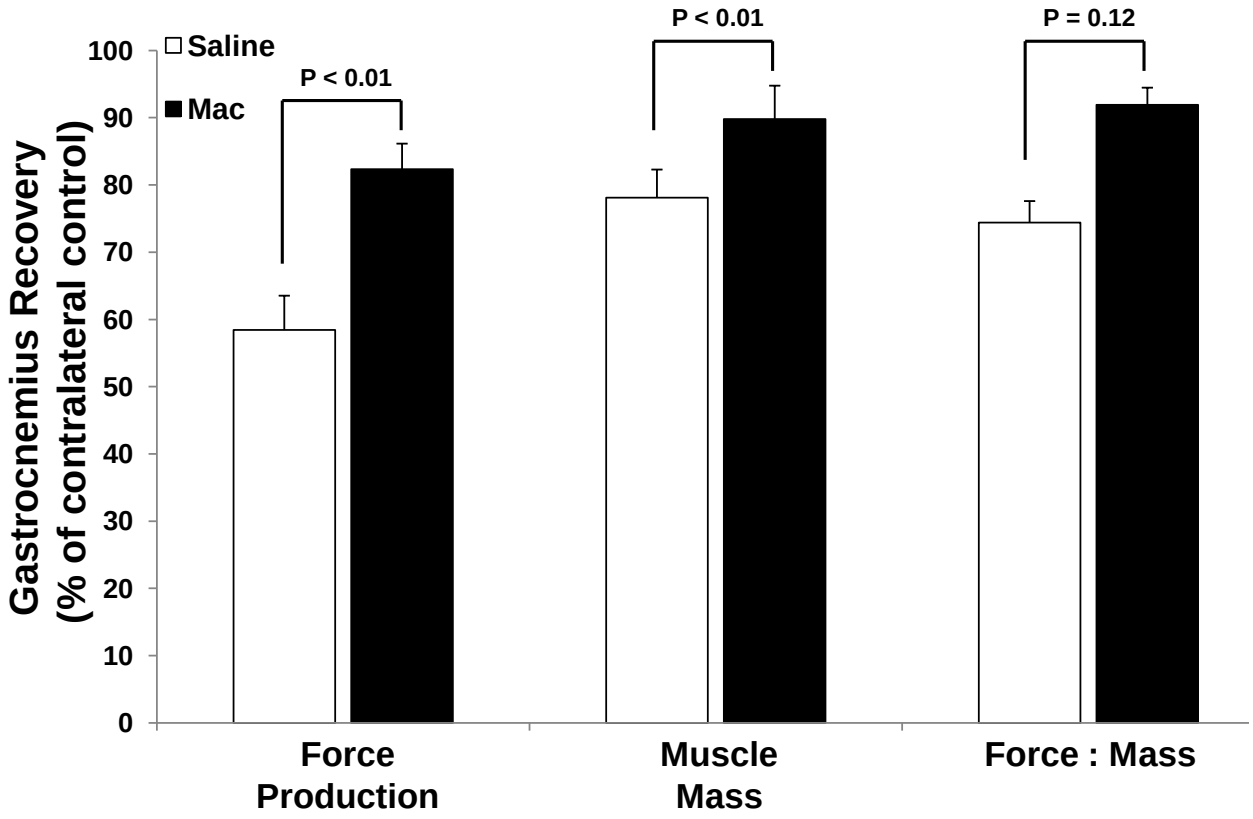

Figure 5.4. Maximum tetanic force production, muscle mass, and mass-normalized force production of the mouse gastrocnemius at 14 days of reperfusion following saline or macrophage (Mac) treatment (n = 4).

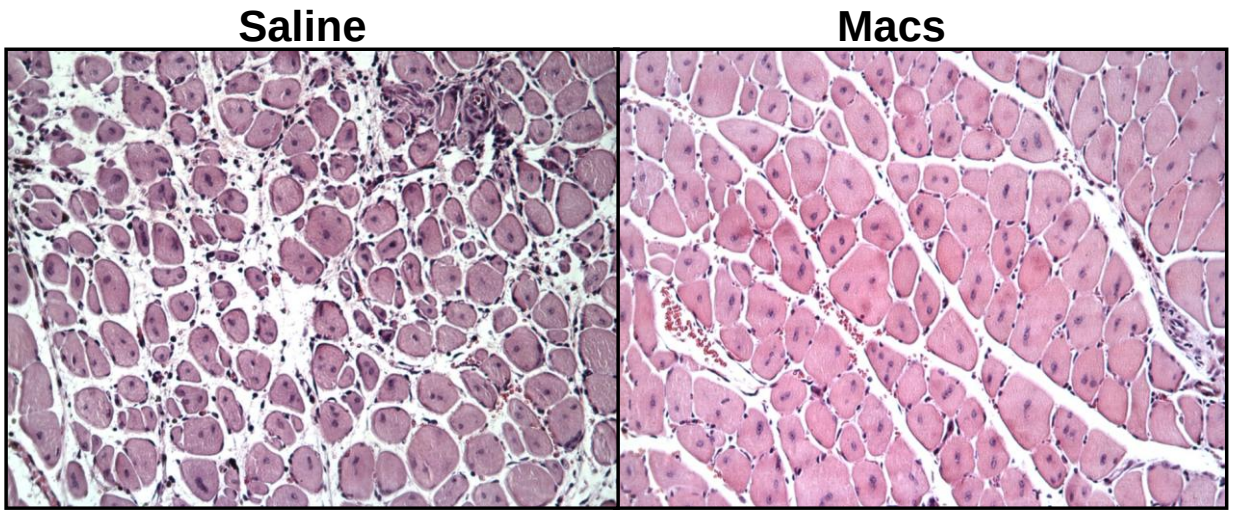

Figure 5.5. Representative H&E slides of saline and macrophage-treated (Macs) gastrocnemius muscles following 14 days of reperfusion. 20X magnification.

Chapter VI: General Discussion

SUMMARY OF RESULTS

1) Ischemia/reperfusion (I/R) injury of skeletal muscle results in robust upregulation of the IGF-I system. This upregulation is greatly attenuated in aged skeletal muscle, and coincides with substantial regenerative defects.
2) Sustained release of IGF-I from an intramuscular injection of PEGylated fibrin gel greatly improves functional recovery of skeletal muscle following I/R. This therapeutic benefit is likely attributed to improved survival of affected myofibers.
3) Flow cytometric analysis demonstrates 3 distinct subsets of $CD11b^{+}$ cells are present in I/R-injured skeletal muscle. These subpopulations differ in relative expression of Ly-6C and F4/80. Isolation and intramuscular injection of the Ly-$6C^{lo}$ $F4/80^{+}$ population improves functional recovery of I/R-affected muscle, demonstrating that increases in MP prevalence can improve functional recovery of skeletal muscle.

CONCLUSIONS

In summary, the present body of work demonstrates that extrinsic factors in post-injury intramuscular environment substantially affect the regeneration of the muscle. Specifically, we show that aging is characterized by impaired skeletal muscle regenerative capacity and exhibits attenuated post-injury IGF-I activity, sustained release

of IGF-I from a biodegradable matrix greatly improves functional recovery of muscle from injury, and that macrophage prevalence in a damaged muscle can affect the functional recovery. When put together in cohesive context with a specific condition in focus, such as sarcopenia, the approaches reported in this work provide the means to conduct insightful mechanistic work at the cellular and molecular levels, with at least two promising therapeutic modalities, IGF-I delivery via PEGylated fibrin gel and macrophage-based therapy, for the treatment of skeletal muscle injuries in individuals with regenerative impairments.

FUTURE DIRECTIONS

This report provides the foundation for many different directions of future research. Logically, it would be important to investigate whether an age-related decline in macrophage infiltration occurs, and whether this is the mechanism responsible for the attenuated IGF-I response. Utilization of IGF-I delivery via PEGylated fibrin gel and/or macrophage-based therapies to treat injuries to sarcopenic muscle is also an avenue that should be pursued. Indeed, similar approaches to characterize other conditions of impaired regeneration, such as metabolic disorders, would be incredibly fruitful. Further refinement of macrophage-based therapies, such as differentiation of monocytes or hematopoietic stem cells, to provide adequate cell numbers would be necessary to enhance translational feasibility of this treatment modality.

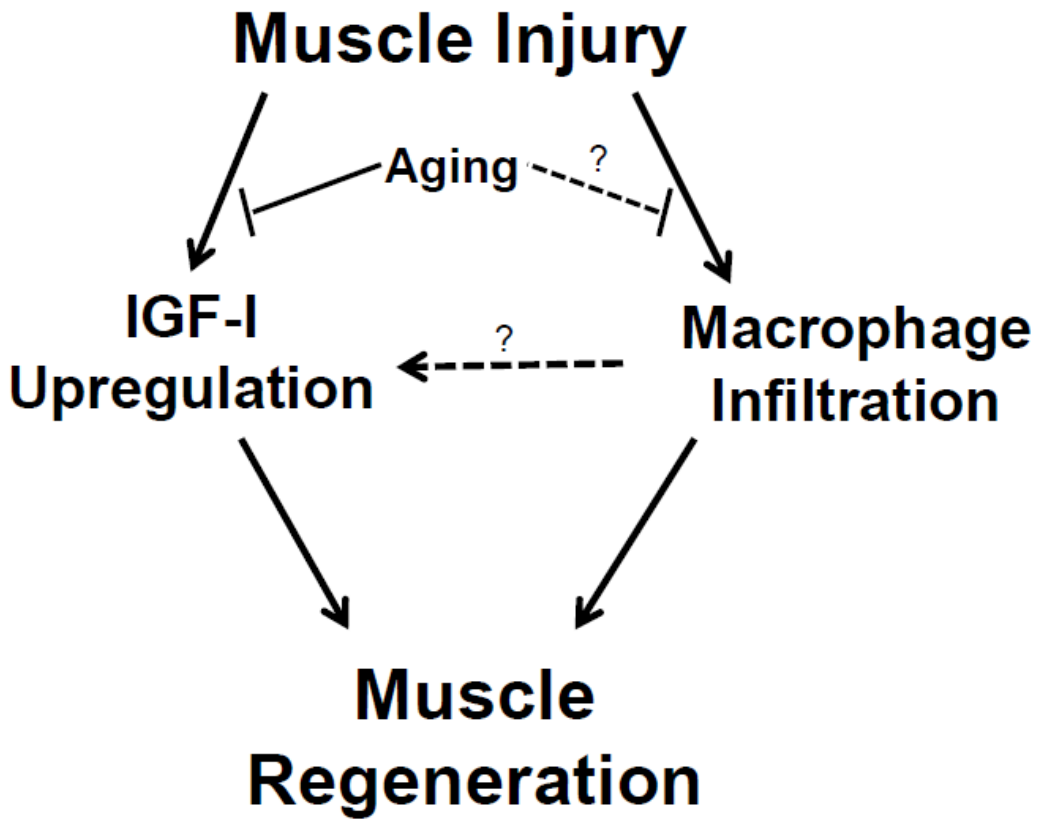

Figure 6.1. This schematic summarizes the results presented in the current work. Skeletal muscle injury results in both the upregulation of IGF-I and the infiltration of macrophages. Both of these events positively affects muscle regeneration, while a decrease in IGF-I response, as shown with age, reduces muscle recovery. It remains to be tested whether aging negatively affects macrophage infiltration and whether macrophages are the cellular source of IGF-I in regenerating muscle.

Appendix A: Expanded Methods

I. Tourniquet Application

1.) Fill vaporizer with isoflurane (ISO).
2.) Turn on oxygen tank to 1.5 L/min.
3.) Pre-charge induction chamber for 5 min by turning ISO vaporizer up to 5%.
4.) After precharging induction chamber, turn vaporizer down to 2 or 2.5%, and place rat in chamber. Monitor rat in chamber for 5 minutes.
5.) Quickly remove rat and move to bed with nose cone. Make sure rat is under heat lamp, but at least 18 inches away from it.
6.) Turn down vaporizer to 1.5 or 2%.
7.) Shave one leg of rat on bed while in nose cone.
8.) Wrap tape around foot of shaved leg. Hang the shaved leg with tape from clamp and leave for 5 minutes to drain excess blood from leg.
9.) Place tourniquet (TK) tightly around leg as close to body as possible.
10.) Once TK is tightly in place. Turn on PTS and set to 250 mmHg. Hold the TK's into position on leg and inflate.
11.) While rat is undergoing TK-induced ischemia, monitor respiration and maintain proper level of anesthetic.
12.) At appropriate time point deflate TK and place rat back in its home cage.

II. Muscle Removal and Storage

Solutions

0.9% NaCl solution (in dH2O)

Procedure

1.) Prepare workstations for tissue harvest: Pre-cut foil into appropriate number of ~2.5 inch squares and label appropriately; Suspend ~25 mL of isopentane in hanging freeze dish over a pool of liquid nitrogen; Add an appropriate amount of 0.9% NaCl solution to a weigh-boat.
2.) Quickly excise muscles from animal and place in weigh-boat containing 0.9% NaCl. If not dead already, sacrifice animal either by cutting femoral arteries or lethal injection of sodium pentabarbitol into heart.
3.) Tare balance with a new weigh-boat, remove a single muscle from saline with forceps, blot off excess liquid on Kim wipes, and weigh muscle. Record the weight into lab notebook.
4.) Remove muscle from balance, place in cassette, and submerge it in liquid nitrogen-cooled isopentane. Remove from isopentane, quickly remove muscle from cassette, wrap in appropriately labeled foil, and submerge in pool of liquid nitrogen.
5.) Weigh and freeze remaining muscles similarly. If balance does not return to zero following the removal of a muscle, re-tare the balance before weighing next muscle.
6.) When finished with all samples, remove from liquid nitrogen pool, place in properly labeled box, and store at -80º C until further processing.
7.) Dispose of weigh-boats, turn-off balance, pour isopentane back into original container (can be reused many times), pour liquid nitrogen back into original container, and prepare animal for proper disposal.

III. Muscle Homogenization

Solutions

1 M HEPES (pH 7.6; NaOH)

5 M NaCl

10% Triton X-100

1 M β-glycerol phosphate

1 M NaF

100 mM PMSF

(Store these at 4º C; may be made on prior date; check viability of chemical storage prior to use)

Procedure

1.) Prepare all stock solutions and store at 4º C. Gather all materials needed; label all microcentrifuge tubes (you will need at least 5 for each sample) properly. Begin icing dH2O, 50 mL conical tube, microcentrifuge tubes, homogenation tubes, Teflon pestals (or polytron rotor). It is essential that all materials are kept as cold as possible throughout entire homogenization process.

2.) Mix the pre-lysis buffer as indicated below:

Pre-Lysis Buffer [Final]	**[Stock]**	**For 50 mL**
50 mM HEPES (pH 7.6; NaOH)	1 M	2.5 mL
150 mM NaCl	5 M	1.5 mL
1% Triton X-100	10%	5.0 mL
20 mM β-glycerol phosphate	0.5 M	1 mL
10 mM NaF	1 M	0.5 mL
dH20		32.5 mL

*this solution can be mixed prior to day of homogenization

Immediately before beginning homogenization, add the following ingredients:

Protease Inhibitors (add fresh)	**[Stock]**	**For 50 mL**
1 mM Na3VO4	10 mM	5 mL
10 ng/mL Leupeptin	1 mg/mL	500 uL
10 ng/mL Aprotinin	2 mg/mL	250 uL
1:100 Phosphatase Inhibitor Cocktail 1		500 uL
1:100 Phosphatase Inhibitor Cocktail 2		500 uL
1 mM PMSF	100 mM	500 uL

*Leupeptin must be mixed from powder form prior to addition

This homogenization buffer is specific for determining phosphorylated states of proteins other goals may require alternative buffers. Before homogenization procedure, calculate an estimated volume of buffer to be required. If more than 50 mL is required, prepare only 50 mL at a time. Keep buffer on ice for duration of homogenization procedure.

3.) Intstall either Teflon pestal in drill press or rotor to polytron; surround with ice. Make sure all equipment is working.
4.) Remove 3-4 muscle samples at a time from -80º C freezer and place in ice.
5.) Remove 1 sample from ice, carefully remove foil, and excise ~200 mg of connective tissue-free muscle tissue sample. Rewrap remaining muscle sample in foil and refreeze in liquid nitrogen.
6.) Record weight of excised muscle in laboratory notebook, mince muscle with scissors, and transfer to cold homogenization tube. Add homogenization buffer to muscle in a 15:1 volume to mass ratio (i.e. 0.2 g x 15 mL/g = 3 mL of buffer).

7.) Remove ice surrounding Teflon pestal or polytron rotor. Keep homogenization tube surrounded by ice and carry to drill press or polytron.

8.) For Teflon pestal: Turn-on drill press, slowly raise homogenization tube until pestal reaches bottom of tube, then pull back down until suction is breached. After 5 passes, place tube back in ice to cool, then perform 5 more passes. Repeat this until all major portions of muscle are absent from homogenate. For polytron: Raise homogenization tube until rotor is in contact with bottom of tube. Turn-on polytron and set at desired speed for 10 seconds. After 10 seconds, turn-off polytron and place tube in ice. Repeat if necessary.

9.) Allow homogenate to sit in ice to let foam settle. During this time wipe Teflon pestal with Kim wipe, or manually remove connective tissue from polytron rotor and run at high speed in clean, cold dH2O, then replace ice until next run.

10.) Distribute homogenate evenly between 2 (more may be necessary) pre-chilled, properly-labeled microcentrifuge tubes. Aliquot 100 uL into a 3rd tube. This portion will be used to determine total protein content of muscle, therefore can be stored at -80º C at this point. Place all other tubes on ice.

11.) Repeat starting at step 5 until all samples are homogenized, then repeat starting at step 4 until no more than 32 microcentrifuge tubes are prepared.

12.) Make sure centrifuge is working properly, place samples into F-20/MICRO centrifuge rotor head in a manner that keeps balance across the head, and secure the lid. Set the rotor speed to 9650 rpm (12000g; RCF = 0.00001118r N^2) and run for 30 minutes. Make sure the temperature is at 4º C.

13.) Remove centrifuged samples from head and return to ice. Remove lipid layer with micropipette and dispose. Carefully transfer supernatant into a clean, chilled, properly-labeled microcentrifuge tube, without disturbing the pellet.

14.) Store homogenates in a properly labeled container in -80º C freezer until further needed.

IV. Protein Concentration Determination

Solutions

20% solution of Bio-Rad Protein Assay dye reagent (can be stored at 4º C for 2 weeks)

10 mg/mL BSA

Procedure

1.) Remove samples from -80º C freezer and place in ice to allow a slow thaw.
2.) Properly label all tissue culture tubes that will be needed for entire procedure (one for each sample + 4 for BSA standards + 1 for blank) Turn on spectrophotometer and set wavelength to 595 nm.
3.) Make serial dilutions of 10 mg/mL BSA such that you end with dilutions of 1.25, 2.5, 5, and 10 mg/mL. Aliquot 2.5 mL of diluted protein assay solution into 5 tissue culture tubes (one will be your blank the other 4 will be for your BSA standards). Add 5 uL of each BSA standard into its respective tissue culture tube; add nothing to the tube designated as the blank. Vortex each tube after protein addition; solution should turn from dark red to blue; intensity of blue should increase with increasing protein concentration. Let sit for 5 minutes before reading absorbance. Signal will deteriorate after 30 minutes.
4.) Vortex blank briefly and carefully transfer to an empty, clean cuvette. Wipe the sides of the cuvette carefully with a Kim wipe, place blank into spectrophotometer in the correct orientation, and “Blank” the system. Repeat

to take sequential measurements of BSA standards and record the absorbance. Dispose of BSA standards and retain blank in curvette, as it will be used for the duration of this procedure. Dispose of used cuvettes and tissue culture tubes properly when finished.

5.) Open an Excel spreadsheet and plot your BSA standard data as absorbance vs. [BSA]. Generate a scatter plot and run a linear regression analysis to obtain the equation and R^2 value. If your R^2 is above 0.98, continue to next step; if not, repeat starting at step 3. BSA standard solutions may be stored in freezer for up to 1 year.

6.) Check homogenized samples on ice. If fully thawed, prepare tissue culture tubes with 2.5 mL protein assay solution. If not fully thawed, do not agitate samples; this will cause proteins to fractionate. Take thawed sample from ice, vortex briefly, and aliquot 5 uL into proper tube containing protein assay solution. Quickly return sample to ice and vortex tube. Repeat for each sample. Prepare no more than 10-15 samples at a given time to prevent possible deterioration of signal. Return homogenates to -80 ºC freezer as soon as possible.

7.) "Blank" spectrophotometer with blank, and begin taking absorbance measurements on homogenate samples. Record the measurement for each sample in your lab notebook. Dispose of all waste properly.

8.) With the recorded absorbance data, return to the Excel spreadsheet with the BSA standard curve to calculate protein concentration of each homogenate. The equation for the standard curve will be in the form $y = mx + b$, where y is the absorbance (Abs; AU) and x is the protein concentration ([P]; mg/mL). Rearrange equation to read $[P] = (Abs - b)/ m$. Plug in absorbance values to determine respective protein concentrations. Record in lab notebook and create a table detailing this data.

9.) Manipulate [P] data to determine proper loading amounts of sample for a given protein content using either 2X or 4X Laemmli's buffer.

V. Sample Preparation

1.) Obtain ice, properly label microcentrifuge tubes, and begin to heat beaker of H2O. Remove protein samples from -80 ºC freezer and place on ice to slow thaw.
2.) Transfer appropriate amount of 4X Laemmli's sample buffer to each tube. When protein samples are completely thawed, vortex protein sample, and transfer sample to tube in a 3:1 ratio (i.e. 25 uL of 4X sample buffer + 75 uL of protein sample = 100 uL of prepared sample). Quickly return original samples to freezer.
3.) Make sure H2O bath is boiling. Place samples in sample floater and put in boiling water for 5 minutes.
4.) Remove from H2O after 5 minutes. Sample can be loaded into a gel when cooled to room temperature, or can be frozen for future use.

VI. SDS-Polyacrylamide Gel Electrophoresis (SDS-PAGE)

Solutions

1.5 M Tris pH 6.8

10% APS (make fresh or store at -20 ºC)

20% SDS

10X Running buffer

1X Running buffer

10X Running Buffer		**1X Running Buffer**	
30.28 g	Trizma base	100 mL	10X running buffer
144.2 g	Gycine	5 mL	20% SDS
Bring to 1 L with dH2O		Bring to 1 L with dH2O	

Procedure

1.) Gather 15 mL conical tubes, glass slides, and all gel casting equipment. Label tubes to be either the "Stacking Gel" or the "Separating Gel". Wipe both sides of all glass slide with methanol, and assemble gel casting apparatus.
2.) Mix both separating and stacking gels simultaneously in their respective tubes following the recipes below (DO NOT add APS or TEMED yet):

5% Stacking Gel	**8% Separating Gel**	**10% Separating Gel**
1.25 mL 40% Acrylamide	2.0 mL 40% Acrylamide	2.50 mL 40% Acrylamide
0.65 mL 2% Bis	0.22 mL 2% Bis	0.27 mL 2% Bis
1 mL 1.5 M Tris pH 6.8	2.50 mL 1.5 M Tris pH 6.8	2.50 mL 1.5 M Tris pH 6.8
50.0 Ul 20% SDS	50.0 uL 20% SDS	50.0 uL 20% SDS
6.99 mL dH2O	5.22 mL dH2O	4.65 mL dH20
50 uL 10% APS	20.7 uL 10% APS	25.89 uL 10% APS
10 uL TEMED	3.99 uL TEMED	4.99 uL TEMED

12.5% Separating Gel	**15% Separating Gel**	**18% Separating Gel**
3.13 mL 40% Acrylamide	3.76 mL 40% Acrylamide	4.51 mL 40% Acrylamide
0.35 mL 2% Bis	0.41 mL 2% Bis	0.49 mL 2% Bis
2.50 mL 1.5 M Tris pH 6.8	2.50 mL 1.5M Tris pH 6.8	2.50 mL 1.5M Tris pH 6.8
50 uL 20% SDS	50 uL 20% SDS	50 uL 20% SDS
3.93 mL dH2O	3.23 mL dH2O	2.39 mL dH2O
32.5 uL 10% APS	38.94 uL 10% APS	46.71 uL 10% APS
6.25 uL TEMED	7.50 uL TEMED	8.99 uL TEMED

3.) Add APS and TEMED (in that order) to separating gel. Vortex briefly, and pipette into gel casting plates until it is ~2 inches from top of short plate. Carefully add butanol over poured separating gel to ensure a smooth surface. Allow separating gel to polymerize.

4.) Once separating gel has polymerized, pour out butanol and rinse thoroughly with dH2O. Absorb excess H2O with KimWipe.

5.) Add APS and TEMED to stacking gel, and pour over separating gel. Carefully place comb over top and make sure no air bubbles are trapped. Allow stacking gel to polymerize.

6.) Once polymerized, remove from casting stand and place in electrophoresis module with short plates facing inward. Fill inner space with 1X Running buffer. Remove combs.

7.) Place the sample loading guide over inner space. Load 5 uL of protein marker to either outside lane (1 or 10). Load appropriate amounts of prepared sample into correct lanes. Record this arrangement in lab notebook.

8.) Remove sample loading guide, fill outer space with 1X Running buffer until 1/3 to ½ the height of the gel. Cover with electrophoresis module cover.

9.) Turn ON power supply and set to constant current (50 mA for every module connected), 200 V, and 200 W. Run for appropriate time (i.e. when desired separation is achieved).

VII. Electro-transfer to PDVF Membrane

Solutions

1 M Tris stock un-pHed

20% SDS

Anode I solution

Component	**Reagent and Amount**
300 mM Tris	300 mL of 1 M Tris Stock
0.05% SDS	2.5 mL of 20% SDS
10% methanol	100 mL
10mM β-mercaptoethanol	0.78 mL

**Bring to 1 L*

Anode II solution

Component	**Reagent and Amount**
25mM Tris	25 mL of 1 M Tris Stock
0.05% SDS	2.5 mL of 20% SDS
10% methanol	100 mL
10mM β-mercaptoethanol	0.78 mL

** Bring to 1 L*

Cathode solution

Component	**Reagent and Amount**
25mM Tris	25 mL of 1 M Tris Stock
40 mM α-amino hexanoic acid	5.248 g
0.05% SDS	2.5 mL of 20% SDS
10% methanol	100 mL
10mM β-mercaptoethanol	0.78 mL

** Bring to 1 L*

Procedure

1.) Pour an appropriate amount of Anode I solution into a weigh boat.
2.) Remove gel from electrophoresis module and carefully remove short plate. Slowly cut gel at desired molecular weights. Notch the top corner of lane 1 and place in Anode I solution filled weigh boat.

3.) Cut a piece of PDVF membrane the size of the gel just prepared. Mark the upper right-hand corner with a pencil. Place this into pure methanol, then move to another weigh boat containing Anode I solution. Allow to equilibrate for at least 5 minutes.
4.) Cut 2 pieces of extra-thick blotting paper that corresponds in size to the membrane (2 pieces for every membrane). Soak 1 of these in Anode II solution.
5.) Open transfer cell and gently place Anode II solution-soaked blotting paper to electrode. Roll over with test tube to remove all air bubbles.
6.) Remove membrane from Anode I solution and place on top of blotting paper. Roll test tube over.
7.) Gently place soaked gel over membrane and make sure notched corner lines up with marked membrane corner. Check to see if any air bubbles.
8.) Soak other piece of blotting paper in Cathode solution. Remove and place over gel. Roll over with test tube.
9.) Replace transfer cell cover. Turn ON power supply and set to 300 mA constant current, 25 V, and 200 W. Time of transfer will depend on size and abundance of protein of interest.

VIII. Immunoblotting

Solutions

5 M NaCl

1 M Tris pH 7.5

0.1% TBST

Component	Reagent and Amount
20 mM Tris	20 mL 1 M Tris pH 7.5
500 mM NaCl	100 mL 5 M NaCl
0.1% Tween-20	1 mL

**Bring to 1 L*

Procedure:

1.) Prepare 25 mL of 5% milk in TBST for every membrane being transferred. Pour milk into plastic shaking dish.
2.) Remove membrane from transfer cell and place in milk. Rotate at room temperature for at least 1 hour.
3.) Depending on primary antibody to be used, prepare 5 mL of either 1% milk-TBST (Santa Cruz antibodies) or 5% BSA-TBST (Cell Signaling antibodies). Transfer to a properly labeled 15 mL conical tube. Add appropriate amount of primary antibody to achieve desired dilution (usually 1:1000 works).
4.) Pour milk out of shaker and add a small amount of TBST to rinse milk off of membrane. Using gloves and forceps, remove membrane from shaker and curve to fit into the tube containing the prepared primary antibody solution. Make sure protein covered side is facing inward (i.e. is exposed to the primary antibody). Place in 4 ºC rotator overnight.
5.) Add ~15 mL of TBST to a plastic shaker, and remove membrane from 15 mL conical tube to place in shaker. Rotate at room temperature for 15 minutes. Perform 3 washes total. Return primary antibody solution to 4 ºC.
6.) Prepare 10 mL of either 1% milk-TBST (Santa Cruz antibodies) or 5% milk-TBST (Cell Signaling antibodies). Add appropriate amount of correct secondary antibody to achieve a 1:2000 dilution (may need to adjust, depending on antibody used). Rotate at room temperature for at least 1 hour (2 hours for better results).

7.) Dump out secondary antibody solution, rinse with TBST, and perform 5 5-minute washes with TBST.

IX. Membrane Stripping and Re-probing

Solutions

1 M Tris pH 6.7

20% SDS

Stripping buffer

Component	**Reagent and Amount**
62.5 mM Tris	32.5 mL 1 M Tris pH 6.7
2% SDS	50 mL 20% SDS
100 mM ß-mercaptoethanol	3.9 mL

**Bring to 500 mL*

1 M Tris pH 7.5

5 M NaCl

0.1% TBST

Component	**Reagent and Amount**
20 mM Tris	20 mL 1 M Tris pH 7.5
500 mM NaCl	100 mL 5 M NaCl
0.1% Tween-20	1 mL

**Bring to 1 L*

Procedure:

1.) Remove membrane cassette and place back in dH2O filled shaking dish. Turn oven on and let warm to 50 ºC.
2.) Pour out dH2O, pour in ~10 mL of stripping buffer, and place dish lid securely. Place in oven for 30 minutes, agitating occasionally.
3.) Prepare 25 mL 5% milk-TBST for every membrane, and pour into a clean shaking dish. Have another clean dish with ~50 mL TBST.
4.) After 30 minutes, remove dish from oven, remove membrane, and rinse in fresh TBST. Then transfer membrane to 5% milk and begin immunoblotting procedure.

X. PEGylated Fibrin gel

1) Reconstitute fibrinogen at a concentration of 80 mg/mL in PBS (pH 7.8) at 37 C until it is completely dissolved.
2) Reconstitute SG-PEG-SG at 4 mg/mL in PBS (pH 7.8). Vortex briefly.
3) Add equal volumes of Fibrinogen and PEG solutions, then filter sterilize. Add equal volumes of fibrinogen/PEG mix and 100 ug/mL IGF-I (sterile). Incubate mixture at 37 C for 45 minutes.
4) Induce polymerization of the resulting mix by adding an equal volume of 25 U/mL thrombin dissolved in 40 mM $CaCl_2$ (pH 7.8).

XI. *In situ* Force Measurements

1.) Make an incision on the skin down the midline of the posterior portion of the lower limb from the popliteal area t othe calcaneus.

2.) Carefully expose the biceps femoris, then cut it to expose the gastrocnemius muscles.
3.) Carefully isolate the gactrocnemius from the biceps femoris. Cut the calcaneus. Then isolate the gastrocnemius from the soleus and and plantaris.
4.) Severe the tibial nerve as it enters the medial head of the gastrocnemius.
5.) Using the calcaneus as an anchor, attach the Achilles tendon to the lever arm of the dual-mode servomotor (Cambridge Technologies, model 310 LR).
6.) Stimulate the muscle to contract using the stimulator (A-M Systems, model 2100) by placing electrodes on the tibial nerve.
7.) Keep the muscle warm and moist using 37.5 C mineral oil and a radiant heat lamp.
8.) Determine optimal length by finding maximum twitch force using a stimulation of 0.5 Hz.
9.) Stimulate muscle at 150 Hz to obtain maximum peak tetanic contraction. Allow muscle to rest for 2 minutes following each contraction. Save data to computer.

XII. Tissue Sectioning

1.) Set the cryostat specimen head temperature at -20 degrees Celsius.

2.) Frozen tissue was transported from the -80°C freezer placed within the cryostat chamber.
3.) Using single-edge razor blades, the portion of the tissue that is important for analysis is cut off before mounting onto specimen disks for sectioning.
4.) Mount tissue onto specimen disks using optimal cutting temperature compound (OCT).
5.) Insert specimen disk into specimen head and orient specimen head if necessary.

6.) Initially adjust base of the blade holder to bring blade close to tissue using coarse feed settings and handwheel.
7.) Begin sectioning tissue; ensuring sections are sliding under the anti-roll plate.
8.) Gently place sectioned tissue from blade holder using a microscope slide; two tissue sections are placed on each microscope slide.
9.) Appropriately label microscope slide and place in slide holder for future use.

XIII. H&E Staining

1) Place the slide in Harris Hematoxylin for 5 minutes.
2) Perform a gentle tap water rinse until the water runs clear.
3) Place the slide in Eosin for 2 minutes.
4) Perform a gentle tap water rinse until the water runs clear.
5) Rinse slide in 70% ethanol for several seconds.
6) Rinse in 100% ethanol for several seconds.
7) Rinse in xylene for several seconds.
8) Allow slide to dry, then mount a coverslip with Permount.

XIV. Immunohistochemistry

1.) Fix slides with cold acetone (stored in the -4°C chest freezer) for 7 to 8 mins at room temperature
    a. Wash with 1X PBS, 3 times (each 5 mins)
    b. Let it dry until there are no droplets left for ~10 mins
    c. Blot off excess droplets on the sides with Kimwipe
2.) Put slides in humid box (wet paper towel at the bottom of the box).
3.) Circle the specimens with the barrier pen and allow ~ 5 mins to dry
4.) With a dropper add, 5% donkey serum diluted with 1X PBS & 1% BSA

a. Cover the humid box and leave at room temperature for 2 hours

b. Let sections dry for ~10 mins (slant slides against the wall)

c. Blot off excess droplets on the sides w/Kimwipe.

5.) 1º Antibody

a. For all other primary antibodies, namely Desmin, MyoD, Myogenin and Neonatal myosin a 1:200 dilution is used. All antibodies are diluted in 1X PBS & 1% BSA & 5% donkey serum.

b. Leave overnight in the humid box in 4ºC fridge (~12 hours)

c. Wash with 1X PBS 3 times (each 5 mins)

d. Let sections dry until there are no droplets left for ~10 mins

e. Blot off excess droplets on the sides w/Kimwipe

6.) 2º Antibody → DO THIS IN THE DARK

a. 1% of 2º Antibody is diluted in 1% BSA & 5% donkey serum and applied to the tissue sections before incubation in the humid boxes.

b. Put foil over the top of the humid boxes.

c. Leave slides in the dark in the 4ºC fridge for 1.5 hours

d. Thaw the DAPI for 45 mins for the counterstain at room temperature. DAPI is stored in the -20ºC freezer when not in use.

e. Wash slides with 1X PBS 3 times (each 5 mins)

f. Let sections dry for ~10 mins (slant slides against the wall)

g. Blot off excess droplets on the sides w/Kimwipe

7.) DAPI (counterstain) → DO THIS IN THE DARK

a. Apply 1μL of DAPI + 1mL of 1X PBS to the sections for ~12 to 15 mins
b. Wash with 1X PBS 3 times (each 5 mins)
c. Let it dry for ~30 mins to an hour (slant slides against the wall)
d. Mount the slides w/Permount and let dry for ~30 mins to an hour.

XV. Collagenase Preparation

1.) Prepare a 2% collagenase II (Invitrogen) solution in DMEM.
2.) Filter sterilize the solution (0.2 um filter) and dilute to 1% collagenase with DMEM.
3.) You will need ~1 mL of collagenase solution for every 100 mg of muscle tissue. Aliquot proper amount into sterile 5 mL tube, and freeze the rest in properly labeled 15 mL tube.
4.) Preheat oven with rotator to 37 C.

XVI. Cell Isolation from Whole Muscle

1.) Before muscle isolation, prepare a properly labeled 35 mm dish with 3 mL sterile PBS for each group. Keep dishes on ice.
2.) Isolate muscle, weigh muscle on sterile weigh-boat, and place muscle in proper 35 mm dish. Keep muscles on ice.
3.) Finely mince muscle with curved scissors on the sterile lid of a 35 mm dish. After mincing is complete, add some collagenase solution to lid in order to aid in the transfer to the 5 mL tube. Transfer as much of the minced muscle to the tube as possible
4.) Once all muscles are minced and transferred into proper tubes, securely snap lids on tubes, and rotate tubes at 37 C for 20 minutes.

5.) After 20 minutes, removes tubes from rotator, and triturate solution with a sterile pipette until homogenous mixture is achieved. Rotate in oven for 20 minutes.
6.) Prepare 15 mL tubes with 5 mL of control media. Filter each 5 mL tube of homogenate into the correct 15 mL tube using either a 40 or 100 um filter. Make sure to wash filter with control media after all of the solution is transferred to prevent loss of cells stuck to filter.
7.) Spin tubes at 300g for 6 minutes.
8.) Decant supernatant and resuspend pellet in proper amount of control media (typically 1 – 3 mL, based on size of pellet). Keep cells on ice until plating.

XVII. Cell Counting with Hemacytometer

1.) Carefully prepare hemacytometer by placing cover slip in place.
2.) Prepare counting solutions by mixing 10 uL of cell suspension with 10uL of trypan blue. Transfer 10 uL of mix to hemacytometer.
3.) Count 4 quadrants on hemacytometer using brightfield microscope on 20X objective lens.
4.) Calculate cell numbers by: #cells/4 x ($2x10^4$) = cells per mL. Multiply by total mLs to get total cell count.

XVIII. Preparation of Cells for Flow Cytometry

1.) Prepare three 5 mL tubes for each sample: unstained, isotype control, and antibody tubes. Add 3 mL of FACS wash buffer (1% BSA in PBS + 0.05% sodium azide) to each tube.
2.) Aliquot ~ $1.5x10^5$ cells per tube and spin at 300g for 6 minutes.
3.) Decant supernatant and add 200 uL FACS blocking buffer (2% BSA in PBS + 0.05% sodium azide). Rotate on ice for 1 hour.

4.) While blocking, prepare antibody solutions. Add 1 uL of each antibody or isotype controls per 100 uL (100 uL per sample) of FACS blocking buffer into the proper tube.
5.) After blocking is complete, add 3 mL of FACS wash buffer and spin at 300g for 6 minutes
6.) Decant supernatant and add 100 uL of blocking buffer into unstained tubes, 100 uL of isotype solution into isotype tubes, and 100 uL of antibody solution into antibody tubes. Rotate for 1 hour on ice.
7.) Add 3 mL FACS wash buffer per tube and spin at 300g for 6 minutes.
8.) Decant supernatant and resuspend in 200 uL FACS wash buffer.
9.) Transport prepared cells in ice to the facility.

Appendix B: Raw Data

Maximum Tetanic Force (N)

Young		Old	
Control	TK	Control	TK
3.15	1	1.5	0.13
3.85	1.2	2.45	0.55
3.8	1.26	1.5	0.43
3.25	0.71	1.75	0.88
4.1	0.98	1.25	0.23
2.2	0.78	2.2	0.25
2.95	1.34	1.02	0.34
3.3	1.43	2.45	0.64
3.18		2.61	
3.3		2.75	
3.31		1.96	
3.2		2.32	
4.2		1.98	
2.85		1.7	
2.75		1.85	
4.03		2.03	
3.23		2.31	
2.5			

Gastrocnemius Mass (mg)

Young					Old				
Control	1 Day	3 Days	5 Days	7 Days	Control	1 Day	3 Days	5 Days	7 Days
160	172	173	128	163	134	173	145	186	103
139	188	236	158	116	136	188	151	136	92
184	223	171	180	153	122	149	133	159	120
179	206	161	138	164	163	191	177	124	81
154	208	254	157	143	146	188	199	122	115
157	219	190	174	126	132	207	189	155	64
171	203		178	133	137	206		89	100
159	221		173	149	125	182		111	125
175	219		176	150	106	186		96	114
176	193		186	138	143	224		116	112
194	229		165	139	135	204		148	134
133			173	138	148	174		124	61
165			185	165	153				94
190			133	152	131				104
153			203	153	153				102
164			176	171	138				92
162			203	167	145				119
172			191		154				106
155					141				111
169					125				
179					130				
166					134				
158					138				
156					123				
168					110				
171					135				
172					141				
185					133				
166					168				
158					137				
162					134				
162					159				
168					132				
161					96				
148					145				
165					88				
169					119				
159					113				
162					132				
166					126				
156					128				
185					121				
169					152				
169					113				
181					125				
185					117				
178					91				
					105				
					115				
					115				

F2-Isoprostane Levels (ng/g tissue)

Young				Old		
Control	2 Hour	1 Day	5 Day	Control	1 Day	5 Days
1.67	1.88	1.70	2.61	1.53	1.78	2.93
1.41	1.74	3.51	2.68	1.44	2.32	3.02
1.52	2.94	1.75	2.21	1.77	2.44	2.77
1.09	2.60	1.76	2.84	1.28	1.86	2.80
1.55	2.06	2.13	1.92	1.19	2.41	2.95
1.33	2.31	2.29	2.53	1.66	2.92	2.84
1.33				1.81		
1.74				1.56		
1.51				1.89		
1.09				1.70		
1.17				1.74		
0.93				2.01		
0.89						
1.22						
1.88						
1.34						
0.99						
1.76						

Relative IGF-I mRNA (AU)

Young							
Day 1		Day 3		Day 5		Day 7	
Control	TK	Control	TK	Control	TK	Control	TK
1.00	2.74	0.74	19.27	5.31	6.25	0.85	6.77
1.00	2.93	0.78	23.18	5.27	6.78	0.89	5.98
1.00	2.33	0.76	22.14	3.7	6.61	0.92	5.66
Old							
Day 1		Day 3		Day 5		Day 7	
Control	TK	Control	TK	Control	TK	Control	TK
0.53	0.71	0.56	5.33	0.47	8.67	0.46	5.56
0.52	0.68	0.59	5.39	0.46	7.5	0.53	5.35
0.42	0.11	0.45	6.43	0.49	8.17	0.55	4.8

IGF-I Content (ng/mg tissue)

Young		Old	
Control	TK	Control	TK
32.19	307.90	40.29	71.71
56.48	102.67	45.52	33.14
22.67	124.57	111.71	10.76
32.67		82.67	17.90

Relative Protein Abundance (AU)

pAkt (5 Day)				Total Akt (5 Day)			
Young		Old		Young		Old	
Control	TK	Control	TK	Control	TK	Control	TK
1.40	0.63	1.29	0.00	1.22	3.16	1.08	1.45
0.63	0.46	1.17	0.00	1.11	2.42	0.73	1.41
0.96	0.46	1.23	0.12	0.67	2.02	0.66	1.61
1.00	0.43	0.44	0.04	1.00	4.54	0.76	1.56
pAkt (7 Day)				**Total Akt (7 Day)**			
Young		Old		Young		Old	
Control	TK	Control	TK	Control	TK	Control	TK
1.05	0.70	0.73	0.56	1.01	3.93	1.14	4.98
1.09	0.80	0.67	0.41	1.09	6.08	1.38	4.58
0.86	0.74	0.96	0.71	0.90	5.12	1.53	4.24
1.00	0.80	0.45	0.21	1.00	7.68	1.07	5.76
pmTOR (7 Day)				**Total mTOR (7 Day)**			
Young		Old		Young		Old	
Control	TK	Control	TK	Control	TK	Control	TK
0.92	7.88	1.30	3.51	1.09	5.06	1.71	2.42
1.08	9.49	1.96	3.35	0.78	5.59	1.03	2.60
0.56	8.14	1.61	3.46	1.13	4.34	1.59	3.79
0.84		1.54		0.81		1.23	
1.60		1.01		1.02		1.39	
				1.17		0.86	
pFoxO3 (7 Day)				**Total FoxO3 (7 Day)**			
Young		Old		Young		Old	
Control	TK	Control	TK	Control	TK	Control	TK
1.00	3.00	1.51	1.31	1.00	2.16	0.93	1.87
1.49	2.38	0.20	1.04	1.15	1.37	0.65	2.64
0.51	2.06	0.77	0.91	0.85	0.63	0.64	2.26

IGF-I Release from PEGylated Fibrin Gel

2 hours		6 hours	
[IGF] (ng/mL)	Cumulative %	[IGF] (ng/mL)	Cumulative %
1230	41.75	675	64.66
1059	45.41	514	67.46
1453	37.81	986	63.47
24 hours		**48 hours**	
[IGF] (ng/mL)	Cumulative %	[IGF] (ng/mL)	Cumulative %
691	88.10	275	97.45
514	89.51	172	96.87
1147	93.31	182	98.05
72 hours		**96 hours**	
[IGF] (ng/mL)	Cumulative %	[IGF] (ng/mL)	Cumulative %
58.16	99.43	14.06	99.90
58.68	99.39	9.91	99.82
58.68	99.57	13.02	99.91

144 hours	
[IGF] (ng/mL)	Cumulative %
2.81	100.00
4.31	100.00
3.33	100.00

Maximum Force Production (N)

Control	Saline	bIGF	PEG-Fib	PEG-Fib-IGF
26.7	9.8	16.3	15.3	20.3
31	12.6	9.4	11.4	18.2
26.8	15.7	11.6	12	22.3
31	12.9	12.5	13.1	20.1
29.6	10.9		14.9	15.4
22.4	12.1		18.3	18.9
25.1	12			
26	13.4			
24.8				
23				
28.3				
28				
22				
24				

Muscle Fiber Size Distribution

Fiber	Control		Saline		Bolus IGF-I		PEG-Fib		PEG-Fib-IGF	
Size (mm^2)	Frequency	%	Frequency	%	Frequency	%	Frequency	%	Frequency	%
500	0	0.00	40	9.03	16	6.25	2	0.54	0	0.00
1000	0	0.00	88	19.86	40	15.63	15	4.02	2	0.32
1500	2	0.48	69	15.58	21	8.20	29	7.77	18	2.84
2000	7	1.67	43	9.71	41	16.02	40	10.72	39	6.15
2500	21	5.00	48	10.84	34	13.28	56	15.01	66	10.41
3000	37	8.81	35	7.90	30	11.72	57	15.28	85	13.41
3500	59	14.05	29	6.55	20	7.81	34	9.12	110	17.35
4000	68	16.19	16	3.61	9	3.52	38	10.19	77	12.15
4500	74	17.62	21	4.74	4	1.56	20	5.36	73	11.51
5000	72	17.14	9	2.03	5	1.95	28	7.51	45	7.10
5500	32	7.62	12	2.71	2	0.78	10	2.68	47	7.41
6000	24	5.71	10	2.26	7	2.73	4	1.07	34	5.36
6500	14	3.33	5	1.13	8	3.13	13	3.49	21	3.31
7000	3	0.71	3	0.68	9	3.52	8	2.14	3	0.47
More	6	1.43	15	3.39	10	3.91	19	5.09	13	2.05

Muscle Fibers <2000 mm^2 (%)

Control	Saline	bIGF	PEG-Fib	PEG-Fib-IGF
3.18	47.83	24.59	25.00	13.19
0.00	52.79	59.29	27.08	5.71
3.67	69.41	36.36	15.38	6.79

Immunohistochemisty Analysis

Desmin+ Fibers (%)			nMHC+ Fibers (%)			Myogenin+ Nuclei (%)		
Saline	PEG-Fib	PEG-Fib-IGF	Saline	PEG-Fib	PEG-Fib-IGF	Saline	PEG-Fib	PEG-Fib-IGF
42.42	13.79	76.92	25.00	57.14	13.51	55.23	13.19	1.16
38.71	48.00	78.00	29.41	45.31	4.08	58.82	6.72	2.22
30.43	65.12	94.74	24.24	53.70	0.00	52.94	37.00	7.48
3.23	56.60	94.12	51.06	28.26	6.00	32.04	1.48	0.19
29.17	18.52	98.08	20.45	16.98	16.67	17.76	2.06	2.20
40.54	56.90	95.00	30.77	26.00	16.07	56.58	1.57	2.06
25.00	47.62	100.00	30.19	18.42	1.61	65.61	29.32	0.00
45.45	44.74	64.15	60.00	27.78	3.51	31.28	27.06	1.18
46.00	50.00	97.92	44.90	23.08	7.69	26.59	46.51	1.18

Relative Protein Abundance (AU)

PEG-Fib				
pERK	pAkt	pmTOR	pp70S6K	MuRF-1
1.24	0.94	0.53	0.92	1.86
0.83	1.10	1.30	1.32	1.20
0.25	0.85	1.02	1.07	0.64
1.68	1.10	1.16	0.68	0.30
PEG-Fib-IGF				
pERK	pAkt	pmTOR	pp70S6K	MuRF-1
1.12	1.89	1.31	1.22	0.09
0.52	1.15	1.93	3.35	0.21
0.62	1.39	1.66	1.78	0.07
0.30	2.07	1.94	3.40	0.21

Relative Cell Numbers - Day 3					
Lateral Gastrocnemius			Tibialis Anterior		
CD 11b	Q2	Q4	CD 11b	Q2	Q4
0.97	0.63	0.22	1.80	1.18	0.54
0.80	0.40	0.19	2.56	1.44	0.80
0.94	0.52	0.27	0.91	0.51	0.22
1.20	0.68	0.45	0.99	0.56	0.36
1.09	0.62	0.31	1.65	0.96	0.51
Relative Cell Numbers - Day 5					
Lateral Gastrocnemius			Tibialis Anterior		
CD 11b	Q2	Q4	CD 11b	Q2	Q4
0.50	0.41	0.06	0.75	0.65	0.07
0.56	0.42	0.11	0.97	0.77	0.14
1.43	1.21	0.11	0.50	0.41	0.05
1.25	0.72	0.36	0.69	0.57	0.10

Lateral Gastrocnemius (Relative Cell Numbers)								
Day 3								
Saline			PEG-Fib			PEG-Fib-IGF		
CD 11b	Q2	Q4	CD 11b	Q2	Q4	CD 11b	Q2	Q4
0.99	0.65	0.23	1.40	1.08	0.19	1.37	0.88	0.23
0.81	0.41	0.19	1.16	0.63	0.32	0.97	0.52	0.23
0.97	0.53	0.27	2.34	1.41	0.78	2.03	1.25	0.60
1.23	0.70	0.46	1.39	0.83	0.46	1.48	0.91	0.51
Day 5								
Saline			PEG-Fib			PEG-Fib-IGF		
CD 11b	Q2	Q4	CD 11b	Q2	Q4	CD 11b	Q2	Q4
0.52	0.42	0.06	0.51	0.41	0.08	0.34	0.29	0.04
0.58	0.43	0.11	1.31	0.99	0.23	0.74	0.55	0.13
1.46	1.24	0.11	1.16	0.95	0.12	0.44	0.37	0.05
1.28	0.74	0.37	0.57	0.48	0.06			

Tibialis Anterior (Relative Cell Numbers)								
Day 3								
Saline			PEG-Fib			PEG-Fib-IGF		
CD 11b	Q2	Q4	CD 11b	Q2	Q4	CD 11b	Q2	Q4
1.84	1.20	0.55	2.53	1.80	0.63	1.47	0.88	0.43
2.62	1.47	0.82	2.64	1.39	1.00	3.62	2.31	0.95
0.93	0.52	0.23	3.74	2.47	0.97	2.54	1.60	0.72
1.02	0.57	0.37	0.84	0.57	0.24	0.79	0.46	0.30
Day 5								
Saline			PEG-Fib			PEG-Fib-IGF		
CD 11b	Q2	Q4	CD 11b	Q2	Q4	CD 11b	Q2	Q4
0.77	0.67	0.07	0.16	0.12	0.02	0.22	0.18	0.03
0.99	0.79	0.15	1.14	0.95	0.13	0.42	0.37	0.04
0.51	0.42	0.05	0.58	0.50	0.05	0.19	0.15	0.02
0.71	0.58	0.10	0.31	0.24	0.05			

Percent Recovery of Gastrocnemius- 14 Days					
Saline			Macrophage Treatment		
Force	Mass	Force : Mass	Force	Mass	Force : Mass
45.4	66.9	67.8	72.1	88.7	81.4
69.1	82.4	83.8	90.1	86.5	104.1
55.9	74.7	74.9	81.9	95.5	85.7
63.3	73.7	86.0	85.2	97.0	87.9

REFERENCES

1. **Adams, G.R., *Invited Review: Autocrine/paracrine IGF-I and skeletal muscle adaptation.* J Appl Physiol, 2002. 93(3): p. 1159-67.**

2. **Heron-Milhavet, L., et al., *Impaired muscle regeneration and myoblast differentiation in mice with a muscle-specific KO of IGF-IR.* J Cell Physiol, 2010. 225(1): p. 1-6.**

3. **Musaro, A., et al., *Localized Igf-1 transgene expression sustains hypertrophy and regeneration in senescent skeletal muscle.* Nat Genet, 2001. 27(2): p. 195-200.**

4. **Pelosi, L., et al., *Local expression of IGF-1 accelerates muscle regeneration by rapidly modulating inflammatory cytokines and chemokines.* FASEB J, 2007. 21(7): p. 1393-402.**

5. **Tidball, J.G., *Inflammatory processes in muscle injury and repair.* Am J Physiol Regul Integr Comp Physiol, 2005. 288(2): p. R345-53.**

6. **Tidball, J.G., E. Berchenko, and J. Frenette, *Macrophage invasion does not contribute to muscle membrane injury during inflammation.* J Leukoc Biol, 1999. 65(4): p. 492-8.**

7. **Nguyen, H.X. and J.G. Tidball, *Interactions between neutrophils and macrophages promote macrophage killing of rat muscle cells in vitro.* J Physiol, 2003. 547(Pt 1): p. 125-32.**

8. **St Pierre, B.A. and J.G. Tidball, *Differential response of macrophage subpopulations to soleus muscle reloading after rat hindlimb suspension.* J Appl Physiol, 1994. 77(1): p. 290-7.**

9. **McLennan, I.S., *Resident macrophages (ED2- and ED3-positive) do not phagocytose degenerating rat skeletal muscle fibres.* Cell Tissue Res, 1993. 272(1): p. 193-6.**

10. **Honda, H., H. Kimura, and A. Rostami, *Demonstration and phenotypic characterization of resident macrophages in rat skeletal muscle.* Immunology, 1990. 70(2): p. 272-7.**

11. **Cantini, M., et al., *Macrophage-secreted myogenic factors: a promising tool for greatly enhancing the proliferative capacity of myoblasts in vitro and in vivo.* Neurol Sci, 2002. 23(4): p. 189-94.**

12. **Massimino, M.L., et al., *ED2+ macrophages increase selectively myoblast proliferation in muscle cultures.* Biochem Biophys Res Commun, 1997. 235(3): p. 754-9.**

13. **Geissmann, F., S. Jung, and D.R. Littman, *Blood monocytes consist of two principal subsets with distinct migratory properties.* Immunity, 2003. 19(1): p. 71-82.**

14. **Arnold, L., et al., *Inflammatory monocytes recruited after skeletal muscle injury switch into antiinflammatory macrophages to support myogenesis.* J Exp Med, 2007. 204(5): p. 1057-69.**

15. **Hawke, T.J. and D.J. Garry, *Myogenic satellite cells: physiology to molecular biology.* J Appl Physiol, 2001. 91(2): p. 534-51.**

16. **Sherwood, R.I., et al., *Determinants of skeletal muscle contributions from circulating cells, bone marrow cells, and hematopoietic stem cells.* Stem Cells, 2004. 22(7): p. 1292-304.**

17. **Asakura, A., et al., *Myogenic specification of side population cells in skeletal muscle.* J Cell Biol, 2002. 159(1): p. 123-34.**

18. **Mauro, A., *Satellite cell of skeletal muscle fibers.* J Biophys Biochem Cytol, 1961. 9: p. 493-5.**

19. **Seale, P., et al., *Pax7 is required for the specification of myogenic satellite cells.* Cell, 2000. 102(6): p. 777-86.**

20. **Olguin, H.C. and B.B. Olwin, *Pax-7 up-regulation inhibits myogenesis and cell cycle progression in satellite cells: a potential mechanism for self-renewal.* Dev Biol, 2004. 275(2): p. 375-88.**

21. **Jones, N.C., et al., *The p38alpha/beta MAPK functions as a molecular switch to activate the quiescent satellite cell.* J Cell Biol, 2005. 169(1): p. 105-16.**

22. **Megeney, L.A., et al., *MyoD is required for myogenic stem cell function in adult skeletal muscle.* Genes Dev, 1996. 10(10): p. 1173-83.**

23. **Cornelison, D.D. and B.J. Wold, *Single-cell analysis of regulatory gene expression in quiescent and activated mouse skeletal muscle satellite cells.* Dev Biol, 1997. 191(2): p. 270-83.**

24. **Adamo, M.L. and R.P. Farrar, *Resistance training, and IGF involvement in the maintenance of muscle mass during the aging process.* Ageing Res Rev, 2006. 5(3): p. 310-31.**

25. **Conboy, I.M. and T.A. Rando, *Aging, stem cells and tissue regeneration: lessons from muscle.* Cell Cycle, 2005. 4(3): p. 407-10.**

26. **Hammers, D.W., et al., *Functional deficits and insulin-like growth factor-I gene expression following tourniquet-induced injury of skeletal muscle in young and old rats.* J Appl Physiol, 2008. 105(4): p. 1274-81.**

27. **Carlson, B.M. and J.A. Faulkner, *Muscle transplantation between young and old rats: age of host determines recovery.* Am J Physiol, 1989. 256(6 Pt 1): p. C1262-6.**

28. **Conboy, I.M., et al., *Rejuvenation of aged progenitor cells by exposure to a young systemic environment.* Nature, 2005. 433(7027): p. 760-4.**

29. **Florini, J.R., D.Z. Ewton, and S.A. Coolican, *Growth hormone and the insulin-like growth factor system in myogenesis.* Endocr Rev, 1996. 17(5): p. 481-517.**

30. **Adams, G.R. and S.A. McCue, *Localized infusion of IGF-I results in skeletal muscle hypertrophy in rats.* J Appl Physiol, 1998. 84(5): p. 1716-22.**

31. **Coleman, M.E., et al., *Myogenic vector expression of insulin-like growth factor I stimulates muscle cell differentiation and myofiber hypertrophy in transgenic mice.* J Biol Chem, 1995. 270(20): p. 12109-16.**

32. **Lee, S., et al., *Viral expression of insulin-like growth factor-I enhances muscle hypertrophy in resistance-trained rats.* J Appl Physiol, 2004. 96(3): p. 1097-104.**

33. **Rommel, C., et al., *Mediation of IGF-1-induced skeletal myotube hypertrophy by PI(3)K/Akt/mTOR and PI(3)K/Akt/GSK3 pathways.* Nat Cell Biol, 2001. 3(11): p. 1009-13.**

34. **Stitt, T.N., et al., *The IGF-1/PI3K/Akt pathway prevents expression of muscle atrophy-induced ubiquitin ligases by inhibiting FOXO transcription factors.* Mol Cell, 2004. 14(3): p. 395-403.**

35. **Song, Y.H., et al., *Muscle-specific expression of IGF-1 blocks angiotensin II-induced skeletal muscle wasting.* J Clin Invest, 2005. 115(2): p. 451-8.**

36. **Sacheck, J.M., et al.,** ***IGF-I stimulates muscle growth by suppressing protein breakdown and expression of atrophy-related ubiquitin ligases, atrogin-1 and MuRF1.*** **Am J Physiol Endocrinol Metab, 2004. 287(4): p. E591-601.**

37. **Sandri, M., et al.,** ***Foxo transcription factors induce the atrophy-related ubiquitin ligase atrogin-1 and cause skeletal muscle atrophy.*** **Cell, 2004. 117(3): p. 399-412.**

38. **Kooijman, R.,** ***Regulation of apoptosis by insulin-like growth factor (IGF)-I.*** **Cytokine Growth Factor Rev, 2006. 17(4): p. 305-23.**

39. **Charge, S.B. and M.A. Rudnicki,** ***Cellular and molecular regulation of muscle regeneration.*** **Physiol Rev, 2004. 84(1): p. 209-38.**

40. **Coolican, S.A., et al.,** ***The mitogenic and myogenic actions of insulin-like growth factors utilize distinct signaling pathways.*** **J Biol Chem, 1997. 272(10): p. 6653-62.**

41. **Edwall, D., et al.,** ***Induction of insulin-like growth factor I messenger ribonucleic acid during regeneration of rat skeletal muscle.*** **Endocrinology, 1989. 124(2): p. 820-5.**

42. **Jennische, E., A. Skottner, and H.A. Hansson,** ***Satellite cells express the trophic factor IGF-I in regenerating skeletal muscle.*** **Acta Physiol Scand, 1987. 129(1): p. 9-15.**

43. **Jennische, E. and H.A. Hansson,** ***Regenerating skeletal muscle cells express insulin-like growth factor I.*** **Acta Physiol Scand, 1987. 130(2): p. 327-32.**

44. **Hayashi, S., et al.,** ***Sequence of IGF-I, IGF-II, and HGF expression in regenerating skeletal muscle.*** **Histochem Cell Biol, 2004. 122(5): p. 427-34.**

45. **Keller, H.L., et al.,** ***Association of IGF-I and IGF-II with myofiber regeneration in vivo.*** **Muscle Nerve, 1999. 22(3): p. 347-54.**

46. **Yang, S., et al.,** ***Cloning and characterization of an IGF-1 isoform expressed in skeletal muscle subjected to stretch.*** **J Muscle Res Cell Motil, 1996. 17(4): p. 487-95.**

47. **Welle, S., et al.,** ***Insulin-like growth factor-1 and myostatin mRNA expression in muscle: comparison between 62-77 and 21-31 yr old men.*** **Exp Gerontol, 2002. 37(6): p. 833-9.**

48. **Owino, V., S.Y. Yang, and G. Goldspink,** ***Age-related loss of skeletal muscle function and the inability to express the autocrine form of insulin-like growth factor-1 (MGF) in response to mechanical overload.*** **FEBS Lett, 2001. 505(2): p. 259-63.**

49. **Barton-Davis, E.R., et al.,** ***Viral mediated expression of insulin-like growth factor I blocks the aging-related loss of skeletal muscle function.*** **Proc Natl Acad Sci U S A, 1998. 95(26): p. 15603-7.**

50. **Hammers, D.W., et al.,** ***Impairment of IGF-I expression and anabolic signaling following ischemia/reperfusion in skeletal muscle of old mice.*** **Experimental Gerontology, 2011. 46(4): p. 265-72.**

51. **Bondesen, B.A., et al.,** ***The COX-2 pathway is essential during early stages of skeletal muscle regeneration.*** **Am J Physiol Cell Physiol, 2004. 287(2): p. C475-83.**

52. **Lescaudron, L., et al.,** ***Blood borne macrophages are essential for the triggering of muscle regeneration following muscle transplant.*** **Neuromuscul Disord, 1999. 9(2): p. 72-80.**

53. **Shireman, P.K., et al.,** ***MCP-1 deficiency causes altered inflammation with impaired skeletal muscle regeneration.*** **J Leukoc Biol, 2006.**

54. **Summan, M., et al.,** ***Macrophages and skeletal muscle regeneration: a clodronate-containing liposome depletion study.*** **Am J Physiol Regul Integr Comp Physiol, 2006. 290(6): p. R1488-95.**

55. **Tidball, J.G. and M. Wehling-Henricks,** ***Macrophages promote muscle membrane repair and muscle fibre growth and regeneration during modified muscle loading in mice in vivo.*** **J Physiol, 2007. 578(Pt 1): p. 327-36.**

56. **DiPasquale, D.M., et al.,** ***Urokinase-type plasminogen activator and macrophages are required for skeletal muscle hypertrophy in mice.*** **Am J Physiol Cell Physiol, 2007. 293(4): p. C1278-85.**

57. **Arkins, S., et al.,** ***Murine macrophages express abundant insulin-like growth factor-I class I Ea and Eb transcripts.*** **Endocrinology, 1993. 133(5): p. 2334-43.**

58. **Bryer, S.C., et al.,** ***Urokinase-type plasminogen activator plays essential roles in macrophage chemotaxis and skeletal muscle regeneration.*** **J Immunol, 2008. 180(2): p. 1179-88.**

59. **Lu, H., et al.,** ***Macrophages recruited via CCR2 produce insulin-like growth factor-1 to repair acute skeletal muscle injury.*** **FASEB journal : official publication of the Federation of American Societies for Experimental Biology, 2011. 25(1): p. 358-69.**

60. **Brooks, S.V. and J.A. Faulkner,** ***The magnitude of the initial injury induced by stretches of maximally activated muscle fibres of mice and rats increases in old age.*** **J Physiol, 1996. 497 (Pt 2): p. 573-80.**

61. **Zerba, E., T.E. Komorowski, and J.A. Faulkner,** ***Free radical injury to skeletal muscles of young, adult, and old mice.*** **Am J Physiol, 1990. 258(3 Pt 1): p. C429-35.**

62. **Brooks, S.V. and J.A. Faulkner,** ***Contraction-induced injury: recovery of skeletal muscles in young and old mice.*** **Am J Physiol, 1990. 258(3 Pt 1): p. C436-42.**

63. **Sadeh, M.,** ***Effects of aging on skeletal muscle regeneration.*** **J Neurol Sci, 1988. 87(1): p. 67-74.**

64. **McEwen, J.A. and K. Inkpen,** ***Surgical Tourniquet Technology Adapted for Military and Prehospital Use.*** **RTO-MP-HFM, 2004. 109: p. 1-12.**

65. **Blaisdell, F.W.,** ***The pathophysiology of skeletal muscle ischemia and the reperfusion syndrome: a review.*** **Cardiovasc Surg, 2002. 10(6): p. 620-30.**

66. **Hill, M. and G. Goldspink,** ***Expression and splicing of the insulin-like growth factor gene in rodent muscle is associated with muscle satellite (stem) cell activation following local tissue damage.*** **J Physiol, 2003. 549(Pt 2): p. 409-18.**

67. **Hill, M., A. Wernig, and G. Goldspink,** ***Muscle satellite (stem) cell activation during local tissue injury and repair.*** **J Anat, 2003. 203(1): p. 89-99.**

68. **Adams, G.R.,** ***Autocrine and/or paracrine insulin-like growth factor-I activity in skeletal muscle.*** **Clin Orthop Relat Res, 2002(403 Suppl): p. S188-96.**

69. **Walters, T.J., et al.,** ***The combined influence of hemorrhage and tourniquet application on the recovery of muscle function in rats.*** **J Orthop Trauma, 2008. 22(1): p. 47-51.**

70. **Thaveau, F., et al.,** ***Contralateral leg as a control during skeletal muscle ischemia-reperfusion.*** **J Surg Res, 2009. 155(1): p. 65-9.**

71. **Walters, T.J., J.F. Kragh, and D.G. Baer,** ***Influence of fiber-type composition on recovery from tourniquet-induced skeletal muscle ischemia-reperfusion injury.*** **Appl Physiol Nutr Metab, 2008. 33(2): p. 272-81.**

72. **Ward, W.F., et al.,** ***Effects of age and caloric restriction on lipid peroxidation: measurement of oxidative stress by F2-isoprostane levels.*** **J Gerontol A Biol Sci Med Sci, 2005. 60(7): p. 847-51.**

73. **D'Ercole, A.J., A.D. Stiles, and L.E. Underwood,** ***Tissue concentrations of somatomedin C: further evidence for multiple sites of synthesis and paracrine or autocrine mechanisms of action.*** **Proc Natl Acad Sci U S A, 1984. 81(3): p. 935-9.**

74. **Bradford, M.M.,** ***A rapid and sensitive method for the quantitation of microgram quantities of protein utilizing the principle of protein-dye binding.*** **Anal Biochem, 1976. 72: p. 248-54.**

75. **Roberts, L.J. and J.D. Morrow,** ***Measurement of F(2)-isoprostanes as an index of oxidative stress in vivo.*** **Free Radic Biol Med, 2000. 28(4): p. 505-13.**

76. **Bodine, S.C.,** ***mTOR signaling and the molecular adaptation to resistance exercise.*** **Med Sci Sports Exerc, 2006. 38(11): p. 1950-7.**

77. **Huang, H. and D.J. Tindall,** ***Dynamic FoxO transcription factors.*** **J Cell Sci, 2007. 120(Pt 15): p. 2479-87.**

78. **Rantanen, T.,** ***Muscle strength, disability and mortality.*** **Scand J Med Sci Sports, 2003. 13(1): p. 3-8.**

79. **Latres, E., et al.,** ***Insulin-like growth factor-1 (IGF-1) inversely regulates atrophy-induced genes via the phosphatidylinositol 3-kinase/Akt/mammalian target of rapamycin (PI3K/Akt/mTOR) pathway.*** **J Biol Chem, 2005. 280(4): p. 2737-44.**

80. **Musaro, A., et al.,** ***Stem cell-mediated muscle regeneration is enhanced by local isoform of insulin-like growth factor 1.*** **Proc Natl Acad Sci U S A, 2004. 101(5): p. 1206-10.**

81. **Sacco, A., et al.,** ***IGF-I increases bone marrow contribution to adult skeletal muscle and enhances the fusion of myelomonocytic precursors.*** **J Cell Biol, 2005. 171(3): p. 483-92.**

82. **Garcia-Fernandez, M., et al.,** ***Antioxidant effects of insulin-like growth factor-I (IGF-I) in rats with advanced liver cirrhosis.*** **BMC Gastroenterol, 2005. 5: p. 7.**

83. **Jallali, N., et al.,** ***Modulation of intracellular reactive oxygen species level in chondrocytes by IGF-1, FGF, and TGF-beta1.*** **Connect Tissue Res, 2007. 48(3): p. 149-58.**

84. **Puche, J.E., et al.,** ***Low doses of insulin-like growth factor-I induce mitochondrial protection in aging rats.*** **Endocrinology, 2008. 149(5): p. 2620-7.**

85. **Chakravarthy, M.V., B.S. Davis, and F.W. Booth,** ***IGF-I restores satellite cell proliferative potential in immobilized old skeletal muscle.*** **J Appl Physiol, 2000. 89(4): p. 1365-79.**

86. **Bodine, S.C., et al.,** ***Akt/mTOR pathway is a crucial regulator of skeletal muscle hypertrophy and can prevent muscle atrophy in vivo.*** **Nat Cell Biol, 2001. 3(11): p. 1014-9.**

87. **Burnett, P.E., et al.,** ***RAFT1 phosphorylation of the translational regulators p70 S6 kinase and 4E-BP1.*** **Proc Natl Acad Sci U S A, 1998. 95(4): p. 1432-7.**

88. **Hwee, D.T. and S.C. Bodine,** ***Age-related deficit in load-induced skeletal muscle growth.*** **J Gerontol A Biol Sci Med Sci, 2009. 64(6): p. 618-28.**

89. **Senf, S.M., et al.,** ***Hsp70 overexpression inhibits NF-kappaB and Foxo3a transcriptional activities and prevents skeletal muscle atrophy.*** **Faseb J, 2008. 22(11): p. 3836-45.**

90. **Mammucari, C., et al.,** ***FoxO3 controls autophagy in skeletal muscle in vivo.*** **Cell Metab, 2007. 6(6): p. 458-71.**

91. **Sengupta, A., J.D. Molkentin, and K.E. Yutzey,** ***FoxO transcription factors promote autophagy in cardiomyocytes.*** **J Biol Chem, 2009. 284(41): p. 28319-31.**

92. **Zhao, J., et al.,** ***FoxO3 coordinately activates protein degradation by the autophagic/lysosomal and proteasomal pathways in atrophying muscle cells.*** **Cell Metab, 2007. 6(6): p. 472-83.**

93. **Machida, S., E.E. Spangenburg, and F.W. Booth,** ***Forkhead transcription factor FoxO1 transduces insulin-like growth factor's signal to p27Kip1 in primary skeletal muscle satellite cells.*** **J Cell Physiol, 2003. 196(3): p. 523-31.**

94. **Rathbone, C.R., F.W. Booth, and S.J. Lees, *FoxO3a preferentially induces p27Kip1 expression while impairing muscle precursor cell-cycle progression.* Muscle Nerve, 2008. 37(1): p. 84-9.**

95. **Matheny, R.W., Jr. and M.L. Adamo, *Role of Akt isoforms in IGF-I-mediated signaling and survival in myoblasts.* Biochem Biophys Res Commun, 2009. 389(1): p. 117-21.**

96. **McLoughlin, T.J., et al., *FoxO1 induces apoptosis in skeletal myotubes in a DNA-binding-dependent manner.* Am J Physiol Cell Physiol, 2009. 297(3): p. C548-55.**

97. **Walsh, S.R., et al., *Remote ischemic preconditioning in major vascular surgery.* J Vasc Surg, 2009. 49(1): p. 240-3.**

98. **Honda, H.M., P. Korge, and J.N. Weiss, *Mitochondria and ischemia/reperfusion injury.* Ann N Y Acad Sci, 2005. 1047: p. 248-58.**

99. **Zhang, G., et al., *Enhancing efficacy of stem cell transplantation to the heart with a PEGylated fibrin biomatrix.* Tissue Eng Part A, 2008. 14(6): p. 1025-36.**

100. **Zhang, G., et al., *Controlled release of stromal cell-derived factor-1 alpha in situ increases c-kit+ cell homing to infarcted heart.* Tissue Eng, 2007. 13(8): p. 2063-71.**

101. **Drinnan, C.T., et al., *Multimodal release of transforming growth factor-beta1 and the BB isoform of platelet derived growth factor from PEGylated fibrin gels.* Journal of controlled release : official journal of the Controlled Release Society, 2010. 147(2): p. 180-6.**

102. **Merritt, E.K., et al., *Functional assessment of skeletal muscle regeneration utilizing homologous extracellular matrix as scaffolding.* Tissue Eng Part A, 2010. 16(4): p. 1395-405.**

103. **Coolican, S.A., et al., *The mitogenic and myogenic actions of insulin-like growth factors utilize distinct signaling pathways.* The Journal of biological chemistry, 1997. 272(10): p. 6653-62.**

104. **Davani, E.Y., et al., *Insulin-like growth factor-1 protects ischemic murine myocardium from ischemia/reperfusion associated injury.* Critical care, 2003. 7(6): p. R176-83.**

105. **Friden, J. and R.L. Lieber, *Segmental muscle fiber lesions after repetitive eccentric contractions.* Cell and tissue research, 1998. 293(1): p. 165-71.**

106. Borselli, C., et al., *Functional muscle regeneration with combined delivery of angiogenesis and myogenesis factors.* Proc Natl Acad Sci U S A, 2010. 107(8): p. 3287-92.

107. Catelas, I., J.F. Dwyer, and S. Helgerson, *Controlled release of bioactive transforming growth factor beta-1 from fibrin gels in vitro.* Tissue engineering. Part C, Methods, 2008. 14(2): p. 119-28.

108. Giannoni, P. and E.B. Hunziker, *Release kinetics of transforming growth factor-beta1 from fibrin clots.* Biotechnology and bioengineering, 2003. 83(1): p. 121-3.

109. Grainger, D.J., et al., *Release and activation of platelet latent TGF-beta in blood clots during dissolution with plasmin.* Nature medicine, 1995. 1(9): p. 932-7.

110. Ishii, I., et al., *Healing of full-thickness defects of the articular cartilage in rabbits using fibroblast growth factor-2 and a fibrin sealant.* The Journal of bone and joint surgery. British volume, 2007. 89(5): p. 693-700.

111. Sahni, A., T. Odrljin, and C.W. Francis, *Binding of basic fibroblast growth factor to fibrinogen and fibrin.* The Journal of biological chemistry, 1998. 273(13): p. 7554-9.

112. Sahni, A. and C.W. Francis, *Vascular endothelial growth factor binds to fibrinogen and fibrin and stimulates endothelial cell proliferation.* Blood, 2000. 96(12): p. 3772-8.

113. Bandman, E., *Continued expression of neonatal myosin heavy chain in adult dystrophic skeletal muscle.* Science, 1985. 227(4688): p. 780-2.

114. Conboy, I.M. and T.A. Rando, *The regulation of Notch signaling controls satellite cell activation and cell fate determination in postnatal myogenesis.* Dev Cell, 2002. 3(3): p. 397-409.

115. Frost, R.A. and C.H. Lang, *Protein kinase B/Akt: a nexus of growth factor and cytokine signaling in determining muscle mass.* J Appl Physiol, 2007. 103(1): p. 378-87.

116. Bodine, S.C., et al., *Akt/mTOR pathway is a crucial regulator of skeletal muscle hypertrophy and can prevent muscle atrophy in vivo.* Nature cell biology, 2001. 3(11): p. 1014-9.

117. Sacheck, J.M., et al., ***IGF-I stimulates muscle growth by suppressing protein breakdown and expression of atrophy-related ubiquitin ligases, atrogin-1 and MuRF1.*** **American journal of physiology. Endocrinology and metabolism, 2004. 287(4): p. E591-601.**

118. Stitt, T.N., et al., ***The IGF-1/PI3K/Akt pathway prevents expression of muscle atrophy-induced ubiquitin ligases by inhibiting FOXO transcription factors.*** **Molecular cell, 2004. 14(3): p. 395-403.**

119. Clarke, B.A., et al., ***The E3 Ligase MuRF1 degrades myosin heavy chain protein in dexamethasone-treated skeletal muscle.*** **Cell metabolism, 2007. 6(5): p. 376-85.**

120. Cohen, S., et al., ***During muscle atrophy, thick, but not thin, filament components are degraded by MuRF1-dependent ubiquitylation.*** **The Journal of cell biology, 2009. 185(6): p. 1083-95.**

121. Mocanu, M.M., R.M. Bell, and D.M. Yellon, ***PI3 kinase and not p42/p44 appears to be implicated in the protection conferred by ischemic preconditioning.*** **Journal of molecular and cellular cardiology, 2002. 34(6): p. 661-8.**

122. Li, L., et al., ***Glucagon-like peptide-1 protects beta cells from cytokine-induced apoptosis and necrosis: role of protein kinase B.*** **Diabetologia, 2005. 48(7): p. 1339-49.**

123. Harada, N., et al., ***Akt activation protects rat liver from ischemia/reperfusion injury.*** **The Journal of surgical research, 2004. 121(2): p. 159-70.**

124. Richardson, T.P., et al., ***Polymeric system for dual growth factor delivery.*** **Nature biotechnology, 2001. 19(11): p. 1029-34.**

125. Lu, H., et al., ***Acute skeletal muscle injury: CCL2 expression by both monocytes and injured muscle is required for repair.*** **FASEB journal : official publication of the Federation of American Societies for Experimental Biology, 2011. 25(10): p. 3344-55.**

126. Ruffell, D., et al., ***A CREB-C/EBPbeta cascade induces M2 macrophage-specific gene expression and promotes muscle injury repair.*** **Proceedings of the National Academy of Sciences of the United States of America, 2009. 106(41): p. 17475-80.**

127. Otsuka, M., S. Tsuchiya, and Y. Aramaki, ***Involvement of ERK, a MAP kinase, in the production of TGF-beta by macrophages treated with liposomes***

composed of phosphatidylserine. **Biochemical and biophysical research communications, 2004. 324(4): p. 1400-5.**

128. Dumont, N. and J. Frenette, *Macrophages protect against muscle atrophy and promote muscle recovery in vivo and in vitro: a mechanism partly dependent on the insulin-like growth factor-1 signaling molecule.* The American journal of pathology, 2010. 176(5): p. 2228-35.

129. Przybyla, B., et al., *Aging alters macrophage properties in human skeletal muscle both at rest and in response to acute resistance exercise.* Exp Gerontol, 2006. 41(3): p. 320-7.

130. Liu, P., et al., *Attenuation of antioxidative capacity enhances reperfusion injury in aged rat myocardium after MI/R.* American journal of physiology. Heart and circulatory physiology, 2004. 287(6): p. H2719-27.

131. Liu, P., et al., *Age-related difference in myocardial function and inflammation in a rat model of myocardial ischemia-reperfusion.* Cardiovascular research, 2002. 56(3): p. 443-53.

132. Nguyen, M.H., M. Cheng, and T.J. Koh, *Impaired muscle regeneration in ob/ob and db/db mice.* TheScientificWorldJournal, 2011. 11: p. 1525-35.

133. Hammers, D.W., et al., *Controlled release of IGF-I from a biodegradable matrix improves functional recovery of skeletal muscle from ischemia/reperfusion.* Biotechnology and bioengineering, 2012. 109(4): p. 1051-9.

134. Flick, M.J., X. Du, and J.L. Degen, *Fibrin(ogen)-alpha M beta 2 interactions regulate leukocyte function and innate immunity in vivo.* Experimental biology and medicine, 2004. 229(11): p. 1105-10.

135. Chazaud, B., et al., *Satellite cells attract monocytes and use macrophages as a support to escape apoptosis and enhance muscle growth.* J Cell Biol, 2003. 163(5): p. 1133-43.

136. Sonnet, C., et al., *Human macrophages rescue myoblasts and myotubes from apoptosis through a set of adhesion molecular systems.* J Cell Sci, 2006. 119(Pt 12): p. 2497-507.

137. Leor, J., et al., *Ex vivo activated human macrophages improve healing, remodeling, and function of the infarcted heart.* Circulation, 2006. 114(1 Suppl): p. I94-100.

138. Orenstein, A., et al., *Treatment of deep sternal wound infections post-open heart surgery by application of activated macrophage suspension.* Wound repair and regeneration : official publication of the Wound Healing Society [and] the European Tissue Repair Society, 2005. 13(3): p. 237-42.

139. Zuloff-Shani, A., et al., *Macrophage suspensions prepared from a blood unit for treatment of refractory human ulcers.* Transfusion and apheresis science : official journal of the World Apheresis Association : official journal of the European Society for Haemapheresis, 2004. 30(2): p. 163-7.

140. Frenkel, O., et al., *Activated macrophages for treating skin ulceration: gene expression in human monocytes after hypo-osmotic shock.* Clinical and experimental immunology, 2002. 128(1): p. 59-66.

141. Danon, D., et al., *Treatment of human ulcers by application of macrophages prepared from a blood unit.* Experimental gerontology, 1997. 32(6): p. 633-41.

142. Danon, D., et al., *Macrophage treatment of pressure sores in paraplegia.* Journal of wound care, 1998. 7(6): p. 281-3.

143. Danon, D., M.A. Kowatch, and G.S. Roth, *Promotion of wound repair in old mice by local injection of macrophages.* Proceedings of the National Academy of Sciences of the United States of America, 1989. 86(6): p. 2018-20.

VITA

David Wayne Hammers is still alive. He can be reached via email at dhammers@utexas.edu. This work was typed by the author.